INTERNATIONAL UNIVERSITY LIAISON INDONESIA (IULI)

BACHELOR'S THESIS

CONCEPTUAL DESIGN OF A GLIDING BOMB

By

Muhammad Bimo Adjie Athallah
11202101003

Presented to the Faculty of Engineering and Life Sciences
In Partial Fulfilment Of the Requirements for the Degree of

SARJANA TEKNIK
In
AVIATION ENGINEERING

FACULTY OF ENGINEERING AND LIFE SCIENCES

BSD City 15345
Indonesia
January 2025

APPROVAL PAGE

CONCEPTUAL DESIGN OF A GLIDING BOMB

MUHAMMAD BIMO ADJIE ATHALLAH
11202101003
Presented to the Faculty of Engineering
In Partial Fulfillment of the Requirements for the Degree of

SARJANA TEKNIK
In
AVIATION ENGINEERING

FACULTY OF ENGINEERING AND LIFE SCIENCES

Triwanto Simanjuntak, PhD	____________________
Thesis Advisor	Date (MM/DD/YYY)
Dr. Eng. Ressa Octavianty	____________________
Thesis Co-Advisor	Date (MM/DD/YYY)
Dipl.-Ing. Sentot Wahjoe Georitno, M.Si.	____________________
Dean of Faculty of Engineering and Life Sciences	Date (MM/DD/YYY)

EXAMINERS APPROVAL PAGE

Dewi Habsari Budiarti, PhD
Examiner 1

Date (MM/DD/YYY)

Dr. Jemie Muliadi
Examiner 2

Date (MM/DD/YYY)

STATEMENT BY THE AUTHOR

I hereby declare that this submission is my own work and to the best of my knowledge, it contains no material previously published or written by another person, nor material which to a substantial extent has been accepted for the award of any other degree or diploma at any educational institution, except where due acknowledgment is made in the thesis.

Muhammad Bimo Adjie Athallah	
Student	Date (MM/DD/YYY)

ABSTRACT

Conceptual Design of a Gliding Bomb

by

Muhammad Bimo Adjie Athallah

Triwanto Simanjuntak, PhD, Advisor

Dr. Eng. Ressa Octavianty, Co-Advisor

This study explores the conceptual design process of a gliding bomb which addresses the issue of re-purposing old dumb bombs and utilizing their capabilities for destruction in a much more effective manner. This design takes these munitions and modifies their aerodynamic characteristics, which result in said munition being able to travel much further distances than originally designed. The utilization of a "wing kit" allows this to happen and is configured with a High wing design. A $2\,\mathrm{m}$ meter wingspan and $0.15\,\mathrm{m}$ chord length enables the wing to be stowed during transport and is able to provide sufficient lift for the bomb it is carrying to glide distances of over $300\,\mathrm{km}$. The entirety of the kit plus bomb comes in at just over $235\,\mathrm{kg}$ and an estimated range and endurance of $431\,\mathrm{km}$ distance or $167\,\mathrm{min}$ minutes of airtime.

Keyword: *Conceptual Design, Gliding Bomb, Wing kit*

ACKNOWLEDGEMENTS

First and foremost, I would like to express my heartfelt gratitude to Allah SWT who has graciously given me the health, strength and blessings to complete this thesis in its entirety.

I would then like to express my sincerest appreciation to my two thesis advisors, Triwanto Simanjuntak, PhD and Dr. Eng. Ressa Octavianty, for their continued assistance, motivation, mentorship, expertise and valuable time in helping me to refine both my thesis and, most importantly, myself into a better version than when I started. Their extremely valuable insights, suggestions, guidance and expertise have only helped me grow, not only as a student, but as a person as well. Despite the times I felt very demoralized and lazy, they consistently pushed me to regain focus and helped me to complete this thesis.

Next, I would love to thank my family who have always supported me unconditionally from back home. Without their love, support and encouragement, I do not think that I would have been able to complete this thesis. Their faith in me has been the most important factor in motivating me to complete this thesis.

Next, I would like to thank my friends and colleagues for their support and encouragement during the tough times and help whenever I had a problem with certain software issues. Their constant late night noise also helped me stay up at night and complete my thesis.

Finally, I would also like to express my gratitude to Dr. Dewi Habsari Budiarti and Dr. Jemie Muliadi for their invaluable contributions as examiners for my thesis.

I will forever be grateful to everyone who has contributed in one way or another towards the completion of this thesis. This accomplishment would not have been possible without all your help and encouragement from everyone who had faith in me. Again, thank you all, I hope I did not let you down.

Contents

Approval Page i

EXAMINERS APPROVAL PAGE ii

Statement by The Author iii

Abstract iv

Acknowledgements v

Contents vi

List of Figures x

List of Tables xiv

1 Introduction 1

1.1 Background 1
1.2 Problem Statement 4
1.3 The Objectives of this Study 5
1.4 The Scope and Limitations of this Study 5
1.4.1 The Scope of the Study 5
1.4.2 The Limitations of this Study 5
1.5 The Significance of this Study 5

2 Literature Review 7

2.1 Glide Bomb 7
2.1.1 Introduction to Glide Bombs 7

2.1.2 What is a Glide Bomb? 7
2.1.3 Guided Munition and Glide Bomb history and Recent Developments 8
2.1.4 Glide Bomb terminologies 17
2.2 The True Cost of War 18
2.3 Aerodynamic Basis 19
2.3.1 Wing and Tail Geometrical Characteristics 19
2.3.2 Aerodynamic Forces and Moments 19
2.4 Equations of Motion (EOM) for Gliding Flight 22
2.4.1 Symmetric Flight 22
2.4.2 Altitude Effects 27
2.4.3 Wind Effects 29
2.4.4 Turning Flight 31
2.5 Gliding Stability 36
2.5.1 The Modes of Aircraft Motion 36
2.5.2 Axes of Reference 36
2.5.3 Static and Dynamic Stability 38
2.6 Design Approach 39
2.7 Aircraft Structure Components 40
2.7.1 Fuselage/Wing Kit Body 40
2.7.2 Wing 41
2.7.3 Tail/Stabilizer(s) 42
2.8 Previous/Similar Iterations of Glide Bombs 43
2.9 Future Developments 44

3 Research Methodology **47**
3.1 Conceptual Design Process Flowchart 47
3.2 Benchmark Study 47
3.3 Mission Profile and Design Requirements 48
3.3.1 Design Requirements 49
3.3.2 Mission Profile 49
3.4 V-n Diagram 52
3.5 Avionics Component Selection 54

3.5.1 Bomb Selection 54
3.6 XFLR5 Modeling 56
3.6.1 Introduction to XFLR5 56
3.6.2 Wing and Tail modeling 57
3.6.3 Mass and Inertia Input 61
3.7 Structural Design: Wing 61
3.8 Structural Design: Fuselage 62
3.9 Structural Design: Tail/Fins 63
3.10 Structural Assembly 65
3.11 Final Concept Options 66
3.11.1 High Wing, X-Tail 66
3.11.2 High Wing, Inverted Y-Tail 68
3.11.3 High Oblique-Style Wing, X-Tail 69
3.11.4 Fully Integrated Winged Explosive Munition 69

4 Results and Discussions **71**
4.1 Benchmark Study 71
4.2 Mission Profile 72
4.3 Avionics Component Selection 74
4.3.1 Final Selection 74
4.3.2 Commercial-Off-The-Shelf components 74
4.3.3 Bomb selection 75
4.4 V-n Diagram 76
4.5 Aerodynamic Analysis 78
4.5.1 Configuration Selection 78
4.5.2 Body 79
4.5.3 Airfoil 79
4.5.4 Wing 82
4.5.5 Tail 83
4.6 Structure Design: Kit Body/Fuselage 85
4.7 Structure Design: Wing 88
4.8 Structure Design: Tail/Fin 91
4.8.1 V1: Standard X-Tail 91

4.8.2 V2: JDAM Tail . . . 91
4.8.3 V3: JDAM-Style X-tail and system (re-engineered system) . 92
4.8.4 V4: Inverted Y-tail . . . 92
4.9 Structural Assembly and Analysis . . . 92
4.9.1 AA1 Gliding Shark . . . 93
4.9.2 AA2 Sky Shark . . . 94
4.10 Final Decided Version . . . 95
4.10.1 Performance Characteristics and Specifications . . . 95

5 Summary, Conclusion, Recommendation **101**
5.1 Summary . . . 101
5.2 Conclusion . . . 102
5.3 Recommendations . . . 102

Bibliography **104**

Appendices **110**

Turnitin Report **124**

Curriculum Vitae **134**

List of Figures

1.1 Indonesia Air Force, 1st Wing Operations fleet [1] 2
1.2 Korean Aerospace Industry T-50 Golden Eagle [2] 2
1.3 Royal Air Force Airbus A400M [3] 3

2.1 Herschel Hs-293 [8] 9
2.2 Fritz X [9] 10
2.3 XM-108 GB-1 AZON [10] 10
2.4 AGM-62 Walleye [11] 11
2.5 AGM-65 Maverick [12] 11
2.6 HOBOS [13] 11
2.7 Paveway-1 [16] 12
2.8 Bolt-117 [16] 12
2.9 Paveway Series [16] 12
2.10 JDAM series [17] 13
2.11 Paveway-4 [18] 14
2.12 HGK [19] 14
2.13 JDAM-ER [20] 15
2.14 KGGB [21] 15
2.15 KGK [22] 15
2.16 Umbani [23] 16
2.17 UMPK [24] 16
2.18 Wing Parameters 20
2.19 Force Balance Coordinates [26] 20
2.20 Steady Symmetric Gliding Conditions [28] 23
2.21 Example Calculations of Glide Performance [28] 24

2.22 Hodograph of Gliding Performance, with assumption of $\cos \gamma_d = 1$ [28] . . . 26
2.23 Altitude's effects on Gliding Performance [28] . . . 28
2.24 Hodograph with and without the effects of wind [28] . . . 30
2.25 Wind's effects on the hodograph [28] . . . 30
2.26 Banking Angle effects on the curve of the Hodograph [28] . . . 34
2.27 Descent rate against Turning radius for various Bank angles [28] . 35
2.28 Aircraft Motion [30] . . . 37
2.29 Aircraft Reference Axes [31] . . . 38
2.30 The Structure of a Fuselage [34] . . . 41
2.31 The structure of a wing [35] . . . 42
2.32 Iranian Defense Industry YASIN [36] . . . 43
2.33 LOTDC LS PGB [37] . . . 44
2.34 Rafael SPICE [38] . . . 44
2.35 Raytheon AGM-154 [39] . . . 44
2.36 NESCOM H-4 SOW [40] . . . 45
2.37 Diehl BGT HOSBO [41] . . . 45
2.38 DRDO Gaurav [42] . . . 45

3.1 Conceptual Design Flowchart . . . 47
3.2 Mission Profile Side view . . . 49
3.3 Mission Profile Dynamic view . . . 50
3.4 Bomb drop . . . 50
3.5 Bomb approaching target . . . 51
3.6 Abbott V-n Diagram [44] . . . 52
3.7 General Dynamics Mark 82 [46] . . . 55
3.8 Soviet era FAB-500 [47] . . . 55
3.9 Dahana P-250L [48] . . . 56
3.10 XFLR5 Airfoil Generator . . . 57
3.11 XFLR5 Direct Foil Analysis . . . 58
3.12 XFLR5 Direct Foil Analysis Module . . . 59
3.13 XFLR5 Wing Generator . . . 59
3.14 XFLR5 Tailfin Generator . . . 60

3.15 XFLR5 Plane Generator 60
3.16 XFLR5 Mass Inertia 61
3.17 X-Tail 64
3.18 Inverted Y-tail 64
3.19 Ring Tail 65
3.20 High Wing, X-Tail configuration 67
3.21 High Wing, Inverted Y-Tail configuration 68
3.22 High Oblique-style Wing, X-Tail configuration 69
3.23 Fully Integrated Winged Explosive Munition V1 70
3.24 Fully Integrated Winged Explosive Munition V2 70

4.1 Table of Performance Characteristics 73
4.2 Mission Profile 73
4.3 Mark 82 dimensions in Inches [50] 75
4.4 Mark 82 remodeled on Onshape 76
4.5 Vn Diagram of AA1 Concept 78
4.6 Vn Diagram of AA2 Concept 78
4.7 AA1 Wing Kit Body design 80
4.8 AA2 Wing Kit Body design 80
4.9 Clark Y Airfoil [51] 81
4.10 Sokolov Airfoil [54] 81
4.11 Eppler 393 Airfoil [52] 81
4.12 NACA 4412 Airfoil **4412** 81
4.13 NACA 4415 Airfoil **4415** 81
4.14 Aerodynamic data of Clark Y-winged aircraft 83
4.15 Lateral Stability Analysis results 84
4.16 Longitudinal Stability Analysis results 85
4.17 Line up of Avionic Components for AA1 concept 86
4.18 Line up of Avionic Components for AA2 concept 87
4.19 I-beam cross section 88
4.20 C-beam cross section 88
4.21 Wing Spar Structure Shape 90
4.22 AA1 Sketch 93

4.23 AA1 Gliding Shark 93
4.24 AA2 Sketch 94
4.25 AA2 Sky Shark 94
4.26 AA1 3-View Sketch 95
4.27 AA1 Dynamic View 96
4.28 AA1 Structure Dynamic View 96
4.29 AA1 Front View 97
4.30 AA1 Structure Front View 97
4.31 AA1 Side View 97
4.32 AA1 Structure Side View 97
4.33 AA1 Performance Characteristics 98
4.34 AA1 Hodograph of Gliding Performance with the assumption of $\cos\gamma_d = 1$ 99

List of Tables

4.1 JDAM-ER and UMPK Comparison table 72
4.2 Table of Chosen components 74
4.3 Table of chosen COTS components 75
4.4 Table of Parameters 77
4.5 V-n Diagram Results 77
4.6 Airfoil comparison table in planned configuration 82
4.7 Wing Parameters 83
4.8 Frame cross-section dimensions 87
4.9 Wing Structure Parameters 91
4.10 AA1 materials list with characteristic data by [57] 99
4.11 AA1 mass components. 100

List of Abbreviations

UAV	**U**nmanned **A**erial **V**ehicle
CG	**C**enter of **G**ravity
CAD	**C**omputer **A**ided **D**esign
RPM	**R**otation **P**er **M**inute
ESC	**E**lectronic **S**peed **C**ontrol
MRTT	**M**ulti **R**ole **T**anker **T**ransport
MCLOS	**M**anual **C**ommand **L**ine **O**f **S**ight
EO	**E**lectro **O**ptical
IR	**I**nfrared **R**adiation
LGB	**L**aser **G**uided **B**omb
PGK	**P**recision **G**uided **K**it
GPS	**G**lobal **P**ositioning **S**ystem
INS	**I**nertial **N**avigation **S**ystem
RF	**R**adio **F**requency
JDAM	**J**oint **D**irect **A**ttack **M**unition
ER	**E**xtended **R**ange
SOW	**S**tand **O**ff **W**eapon

Dedicated to my family

CHAPTER 1
INTRODUCTION

1.1 Background

With several nations falling into war, the Indonesian government has been seen as a major power in negotiating potential peace talks between the battling parties. However, hesitation to intervene has forced those at war to stay in battle without stopping. Saying that, Indonesia still has a ways to go before it is considered prepared enough for a war offensive effort against any nation. With the nation's military still relying on older American-made Lockheed Martin F-16 Fighting Falcons, Russian-made Sukhoi Su-22s and Su-30s, Brazilian-made Embraer EMB-314s and British-made British Aerospace Hawk 200s. Supported by even older Lockheed Martin C-130 Hercules Transport aircraft (depicted in Figure 1.1).

Recently, Indonesia has expressed its intention to modernize and strengthen its air force fleet by introducing newer aircraft. The first being the South Korean-made KAI T-50 Golden Eagle (Figure 1.2), the French-made Airbus A400M MRTT (Multi Role Tanker Transport) type (Figure 1.3) and the Dassault Rafale multirole fighter, also originating from France. With the first A400M expected to arrive in 2025 and the first Rafale in 2026 at the earliest. While the Air Force have already received several T-50s, with a few more still on order.

With the modernizing of their aircraft fleet underway, the Air Force would also be considering a modernization project towards their military munitions inventory. Currently, their armament inventory is occupied by mainly American and Russian munitions, mainly in their air-to-surface munitions arsenal.

FIGURE 1.1: Indonesia Air Force, 1st Wing Operations fleet [1]

FIGURE 1.2: Korean Aerospace Industry T-50 Golden Eagle [2]

For now, the armaments owned by the Indonesian Air Force were first introduced in the early 1950s. Russian FAB- series and American Mark 8- series unguided bombs make up most of the arsenal, with very little modifications made to it from its original design. The only way to develop these weapons without compromising its effectiveness in battle, is to develop a means to increase its targeting accuracy when dropped on strategic military targets.

However, due to a very limited fleet in the Indonesian Air Force's inventory, a direct bombing run onto enemy territory may cause a large casualty count due

FIGURE 1.3: Royal Air Force Airbus A400M [3]

to anti-air firepower of the enemy and their defense forces. So the only safer method is to launch the munitions from a further away distance and still be able to hit its target accurately. To achieve this, the use of Glide Bombs are necessary.

Gliding bombs are not new technology. They have been utilized as far back as the 11th century. But the more refined first generation of the technology would not be used until 1914, by the German Navy in World War 1, where they introduced the Siemens Torpedo Glider. Per its name, the design was a flying missile that utilized a wiring-guiding system to guide a naval torpedo that was strapped onto an airframe. There were no intentions for it to be flown directly onto into its target, rather it would be flown and dropped from a certain height and point, then a transmitted signal would be order the airframe to detach from the 'missile.' What would follow was, the torpedo would dive into the waves and carry on its course until it reaches its intended destination.

The next generation of glide bomb development, also spearheaded by Nazi Germany, would be in the form of the Henschel HS 293 and the Fritz X. Both were much more refined than its predecessor, with a better integrated airframe and a much more aerodynamic platform. The HS 293 sported a more conventional straight wing design, while the Fritz X lived up to its name by incorporating an X wing configuration. Both had the similar mission as its predecessor, which was to destroy/cripple naval vessels. The first air-to-surface glide bomb, intended for ground targets would be introduced around the same time as the HS 293 and Fritz X, but by American firm Aeronca Aircraft, with their XM-108, also known as the GB-1 Grapefruit Bomb. World War 2 would see the debut of such a weapon and the beginning of modern bomb technology.

Modern iterations of glide bombs are significantly different to the ones in World War 2. With development being spearheaded by American and Australian technology firms, they have introduced the Joint Direct Attack Munition-Extended Range, or JDAM-ER. Which is a wing kit attached to a standard bomb that has also been equipped with a JDAM tailcone. Further developments have also included an integrated Inertial and GPS guiding system as well as a laser guidance system for enhanced accuracy.

Returning to Indonesia, the Air Force has recently acquired one hundred JDAM kits. However, these have arrived without wing kits. This conceptual design of gliding air-dropped aircraft is designed to provide an initial sketch to how Indonesia can develop its armory of munitions up to a higher standard of accuracy and modernization.

1.2 Problem Statement

In the current time that we live in, wars have been breaking out everywhere. War is a costly matter and takes a significant toll on a nation's resources, both human and non-human. However, those losses have come up as a result of failed missions and constant losses. Unguided bombs sent as care packages towards the enemy usually do not reach their target due to either poor navigation or their courier being shot down, hence an increase in weapons and humans. One solution is to modify these unguided munitions and turn them into smart bombs. However, smart bombs still need to be dropped from above its target and that risks the lives of pilots who fly large bombers that are easy targets without protection. One solution to this is to develop our very own Gliding Bomb kit which allows the munition to be launched from a further away distance and not risking direct warfare between the enemy and our own pilots. This kit allows for enhancements in bomb performance, accuracy and is a much more efficient method to accomplish its missions rather than direct over-the-target bombing runs.

1.3 The Objectives of this Study

The objectives of this conceptual design research are to investigate:

- To produce a conceptual design of a gliding bomb.
- Enable the dumb bomb to travel a maximum distance of over 150 km.
- Design a glide gomb that is statically and dynamically stable.

1.4 The Scope and Limitations of this Study

1.4.1 The Scope of the Study

- This conceptual design has been limited to the types of munitions that are available in Indonesia. Specifically, those that are in the possession of the Indonesian Air Force explosives inventory.
- Any mention of cost in this study are to be considered as qualitative.

1.4.2 The Limitations of this Study

- No optimization has been done.
- Avionics used are not custom, but utilize commercially available components and systems.
- No cost analysis is to be carried out in this conceptual design.

1.5 The Significance of this Study

The expectations of this study are to result in:

- This conceptual design can be used by Indonesia defense firms or other entities as a base design to develop the technology further.

- Create comparisons to other designs and/or kits that are readily available on the market of similar specification.
- The study can be used to estimate the operational budget when utilizing it in warfare.

CHAPTER 2
LITERATURE REVIEW

2.1 Glide Bomb

2.1.1 Introduction to Glide Bombs

The Glide Bomb, also known as a Stand-off Bomb, is a weapon used to destroy strategic targets by military forces by explosive means. However, how it differs from an unguided Bomb is that Glide Bombs are aided with flight control surfaces that allows it to have a much flatter and more gliding flight path rather than a straight down path that would usually be experienced by a conventional Bomb.

With the control surfaces, such bombs are able to ’fly’ for much further distances and protect its dropping aircraft from territories that may be guarding the target and could cause damage to the aircraft carrying the bomb.

2.1.2 What is a Glide Bomb?

Merriam-Webster defines the glide bomb as,"A bomb fitted with airfoils so that it glides towards its target with or without a guidance system." In our case, a glide bomb is any explosive munition that is directed towards its intended target by using a wing kit and guidance system in order to increase its range and accuracy [4].

This means that any kind of explosive munition that uses the principles of glide flight in order to deliver its payload, can be defined as a glide bomb.

So the main parts that differentiate a glide bomb from a unguided dumb bomb are:

- A wing (kit) attached.
- An INS navigation system.

- A GPS navigation system.
- A means to adjust course/flight path.

2.1.3 Guided Munition and Glide Bomb history and Recent Developments

Guidance kits have been used as far back as the 1920s. Although the first to develop the technology was the British, by introducing the first Radio-controlled glide Bomb, dubbed the Larynx, it unfortunately didn't make the headlines as a future piece of warfare technology. During those days, major targets for aerial bombings were mainly enemy trench areas on the front lines, railroads, factories, military facilities or other strategic points on a map that may benefit the bombing party. All targets would be stationary and do not, necessarily, require a munition equipped with a guidance system. With that being said, the British drew to the conclusion that larger manned bombers would be better rather than investing heavily on the development of a guided weapon. Meanwhile, on the other side of the North Sea, the Germans , who understood the difficulty of using manned bombers for aerial bombings, from their past war experience in Spain during the 1930s, realized the need for a guided munition, especially in Naval theaters of combat. What they learned was that it was extremely difficult for Naval bombers to hit enemy ships using the conventional free-falling bombs. Hence they started the research and development of a radio-guided munition [5].

The development of the first radio-controlled bombs were spearheaded by Nazi Germany and 2 examples were unleashed upon the ground of war. The first being the Fritz X and the other, the Henschel Hs-298. The Fritz X, named for its X-wing configuration, had all of its control surfaces on its tail. Roll, pitch and yaw were all controlled from the rear. The control surfaces were controlled via a radio control link, in this case the Kehl-Strasbourg MCLOS Radio Control System [6]. The MCLOS system would be used to send signals to the control surfaces and would adjust the bomb's course as it glides from an altitude out of a bomber aircraft. Interestingly, the Fritz X would be controlled by the bombardier from inside of the bomber aircraft. However, to allow the bombardier to effectively control the flight of the Fritz X, the bomber aircraft had to slow down its airspeed near instantly, to allow the controller to be able to see the bombs heading. This made the bomber an open target to Anti-Aircraft Gunfire and to facilitate this issue, a new design would be needed. Enter, the Hs-293 glide bomb. This 2nd iteration of radio-controlled bomb resembled a small aircraft and was controlled the same way, but was controllable from a much further away distance. Given an added 10 second boost by a rocket, it was able to fly slightly further and faster than the Fritz X. On top of the rocket, it sported a conventional wing which aided in its range expansion. Both saw action and success in battles of World War II, mainly in Naval theaters of action and were highly effective against Italian and British battleships. The first non-German guided bomb is believed to be the AZON, short for AZimuth ONly. It was developed by the allies in an attempt to reverse engineer a Fritz X that they can use to possibly turn the tide of war in their favor. However, unlike the Fritz X, the AZON could only have its Yaw controlled, not its pitch or roll. Overall, Radio-controlled systems have a very limited operating range and accuracy. Not to mention that radio signals come with a significant risk factor, where they were easily disturbed/jammed by enemies and are a main reason why the technology is no longer used today [5], [7].

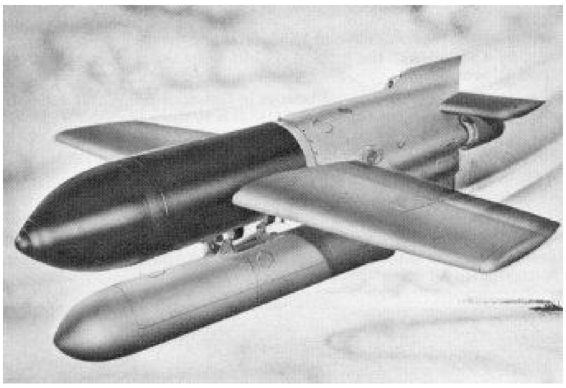

FIGURE 2.1: Herschel Hs-293 [8]

As development efforts were carried on, a new guidance system was invented and is a major step up from the use of Radio waves. This new system uses Electro Optics and Infrared Radiation (EO/IR) is able to follow targets automatically and possesses the ability to analyze contrasting variations via a live video stream onto a computer screen [7]. The variations that are seen come in the form of heat signatures, such as body or motor engine heat. They are easily detected and

FIGURE 2.2: Fritz X [9]

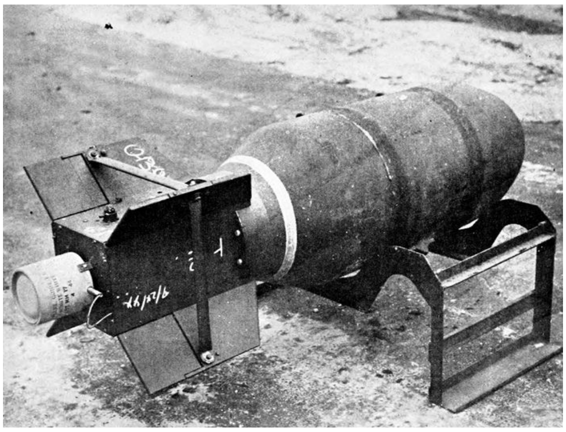

FIGURE 2.3: XM-108 GB-1 AZON [10]

therefore make it a Heat-seeking missile, in a way. The most popular example of an EO/IR bomb is the AGM-62 Walleye, introduced in 1967. Although it was a TV wave-guided gliding munition, it was inaccurately branded as an air-to-ground missile. When in reality, it would also be considered a real fire-and-forget system. Other examples of glide bombs that utilize the same guidance system include the Rockwell HOBOS and the AGM-65 Maverick.

Another alternate guiding system that is efficient and effective against targets would be the laser guidance. This involves the use of laser beams as a means to project a path towards a target [14], [15]. Laser guidance also ensures that the target could be accurately struck, even if friendly soldiers are nearby and reduces the chances of damage to your own teammates. In early adaptations of this technology, the lasers were hand-controlled and guidance was manually

FIGURE 2.4: AGM-62 Walleye [11]

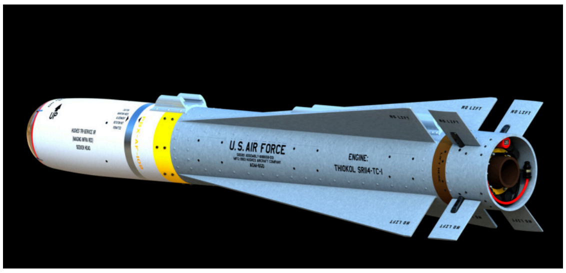

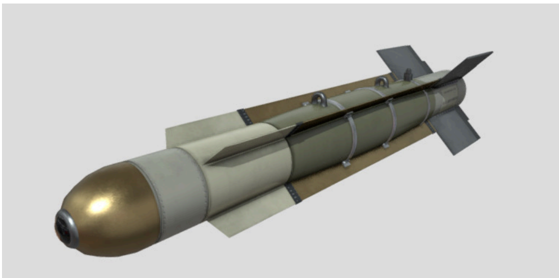

FIGURE 2.6: HOBOS [13]

inputted by an operator from either on board the aircraft, or a laser operator on the ground. The first Laser Guided Bomb (LGB) to be introduced is the BOLT-117. Developed by Texas Instruments in 1967, it utilizes a KMU-342 laser guidance control kit, connected to a standard M117 General purpose bomb. Another LGB is the Paveway-1, which utilizes the KMU-388, KMU-421 and KMU-351 guidance kits and were paired with the Mk- series of General purpose bomb, rather than the older M117.

A major drawback of the LGB guidance system was the use of a laser itself. The laser must mark the target accurately, so the target must be within the line of sight of the laser operator. This might give away the position of the operator

FIGURE 2.7: Paveway-1 [16]

FIGURE 2.8: Bolt-117 [16]

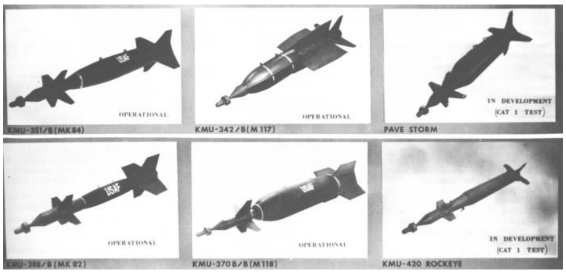

FIGURE 2.9: Paveway Series [16]

and put their team at risk of retaliating gunfire. Another drawback was the incapability to use the LGB in the events of horrendous weather conditions because the laser needs to be clearly visible by the munition to ensure it hit the target effectively. The factor of weather did not become a concern until the reduced effectiveness of the LGB in unclear conditions. New solutions were needed and what arrived was the Precision Guidance Kit (PGK). These kits were designed and developed to increase the accuracy of munitions, reduce collateral damage and increase its lethal effects. These kits, also called satellite-guided munitions, house 2 main navigating systems, a Global Positioning System (GPS) and an Inertial Navigation System (INS). Both work in unison and are able to operate in all-weather conditions, hence why they are very much sought after in the military market, even today. What makes it different from the previous iterations of guidance systems, is that this system is not reliant on light. No infrared, laser nor visual light is needed to mark its target. As previously mentioned, these PGKs work better in any weather condition, unlike its predecessors that did not work in weather with heavy cloud cover, rain or fog. The GPS and INS satellites send signals to adjust the course of descent of the bomb. The two systems need to work as one because GPS signals can be disrupted and distorted via the use of Radio Frequency (RF) signals from the enemy. So this GPS/INS system will correct each other and adjust the drop path of the munition. In the event of a loss in GPS signals, the munition moves into Inertial Navigation mode as a fail safe, results will still be the same. The biggest example of the PGK is the US-made JDAM or Joint Direct Attack Munition. The JDAM is the result of research and development to produce a guided bomb that is capable of operating in the worst meteorological conditions imaginable. Introduced in 1997, it first saw active combat in the Kosovo war where B-2 bombers dropped a total of 651 JDAM munitions that saw 87 percent of which hit its target accurately. On the other side of the Atlantic, Raytheon UK introduced the Paveway IV, also a guidance kit which too saw great success.

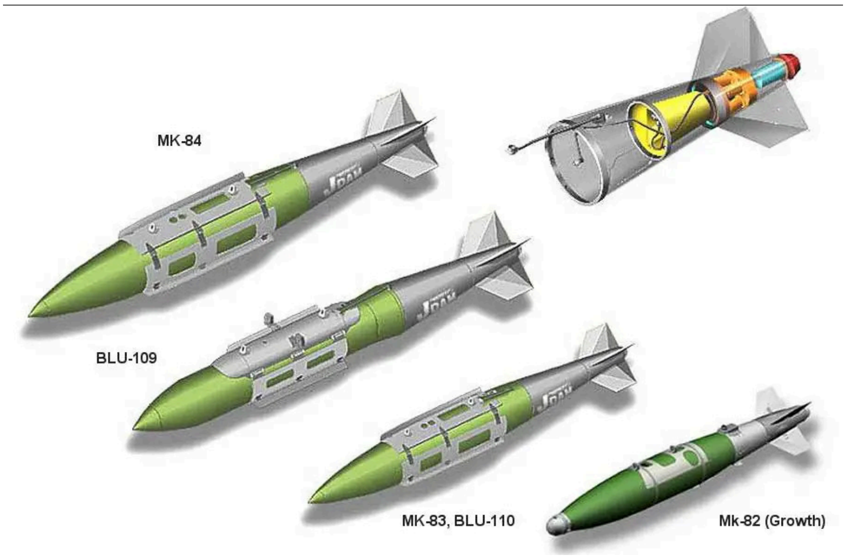

FIGURE 2.10: JDAM series [17]

In recent years, there have been an increased number of nations who have invested in the development and production of PGKs. One example is the one

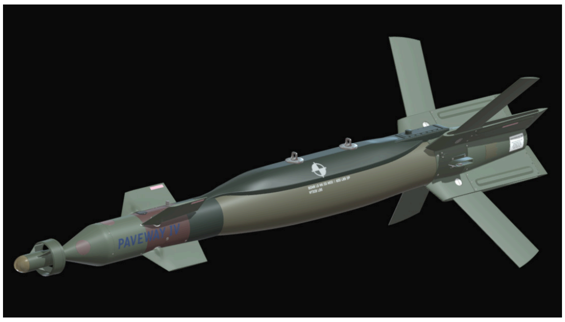

FIGURE 2.11: Paveway-4 [18]

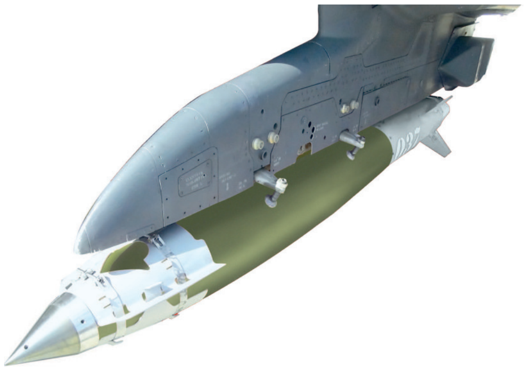

FIGURE 2.12: HGK [19]

made by the Turkish defense company, TUBITAK SAGE. Their product, the Hassas Güdüm Kiti, or HGK for short, is similar to the JDAM in many ways, including its utilization of Mk-series bombs as a baseline as well as its course adjusting system installed in the tail. Although the PGKs are revolutionary and clever, they still need to be dropped from directly above the target, or at least from a close range to the target. They possess fins to aid in accurate drop, but it does not aid in adding range in any way. Hence why the next iteration of guided munitions are further enhanced by the use of wings/wing kits.

The use of wing kit-equipped bombs and glide bombs are not very different in terms of effectiveness, just in the way it is configured. Where pure glide bombs such as the Fritz X, HOSBO and GBU-39 are developed as a Gliding Bomb with a completely integrated guidance system, explosive and wing. Wing kits are separate from the main bomb and are installed as a sort of modification to the munition. They usually use market-available bombs such as the Russian FAB and

American Mk-series bombs, then produce an aerodynamically efficient wing kit around the munition. Usually they also feature a GPS/INS guidance system, but some iterations have also featured a laser guidance system. Some examples of wing kit-equipped bombs include the JDAM-ER (United States), KGGB (South Korea), KGK (Turkiye) and Umbani/Al Tariq (South Africa), that utilize the Mk-series bomb, and the UMPK (Russia) that utilize the FAB series bomb.

FIGURE 2.13: JDAM-ER [20]

FIGURE 2.14: KGGB [21]

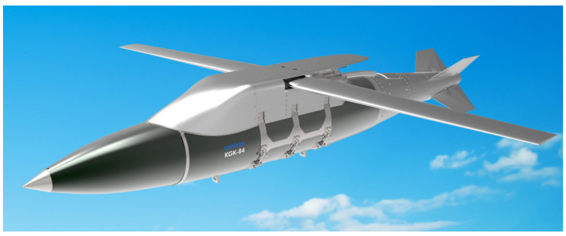

FIGURE 2.15: KGK [22]

FIGURE 2.16: Umbani [23]

FIGURE 2.17: UMPK [24]

2.1.4 Glide Bomb terminologies

Term		Definition
INS	:⇔	The INS, or Inertial Navigation System, is a self-contained navigation technique which obtains its data and measurements from devices such as accelerometers and gyroscopes. These devices are used to track position and orientation of any object that is relative to a known point of origin orientation and velocity.
GPS	:⇔	GPS, or Global Positioning System, is a space-based radio-navigation system that broadcasts navigational pulses to users on/near Earth with high accuracy.
SOW	:⇔	Stand-Off Weapons are those that are launched from a distance in order to avoid opposition.
Glide Range	:⇔	Glide range refers to how far an aircraft/glider is able to travel along the ground during its glide descent.
Gliding Flight	:⇔	Gliding flight is the means of flying objects that are heavier than air and without the use of thrust or propulsion.
Glide Bombing	:⇔	Glide bombing is the act of launching a bomb via the means of gliding flight. Here, bombs do not follow a ballistic trajectory, but rather they 'fly' towards their target from a distance further away.
Unguided Bomb	:⇔	Unguided, or sometimes referred to as dumb, bombs are conventional aircraft-delivered bombs that do not possess any sort of guiding system and therefore follow a basic ballistic trajectory.

Term		Definition
Smart Bomb	:⇔	A smart bomb is a type of bomb that possesses a means for it to be controlled, such as radio or laser-beam control, in order for it to more accurately hit its target.
Warhead	:⇔	A warhead is the front part if a bomb or missile that contains the explosive aspect of a bomb. Similar terms include payload.
Elevon	:⇔	A type of hybrid control surface that acts as the aircraft aileron and elevator. Prominently seen on aircraft with a delta (Triangular) or flying wing configuration, such as the Concorde and F-117 Nighthawk.
Flaperon	:⇔	A type of hybrid control surface that acts as the aircraft flap and aileron. Prominently seen on small aircraft whose wing is too small to include both an aileron and flap.

2.2 The True Cost of War

The cost of war is not one that is usually measurable in currency. However, long term battles will cost a military force into the millions in used armaments, the highest cost being in heavy munitions and ammunition. Procuring and/or producing new munitions do not come at a cheap cost, especially when it comes to explosive devices. It will cost even more if they are unable to hit their assigned targets and are deemed written off. It is important to note that military expenditure in 2023, has increased in certain regions and a sizable chunk of that can be considered as "wasted" as much of that budget has gone on munitions and armaments. The "wasted" bits are those that aren't able to accomplish their mission due to factors such as opposition or even just missing the target completely [25].

The use of glide bomb kits provide a solution to this problem. Military forces that have a large supply of unguided bombs from the past, such as Russia, are able to turn those "dumb" bombs into smarter guided munitions. The kits the Russians use, the UMPK, are the efficient solution to their costly ongoing conflict. These wing kits enable the bombs to be launched from the safety of Russian airspace and will hit targets in their rival's own land. This protects their fighter aircraft from enemy retaliating gunfire and reduces the number of lost aircraft in battle.

These kits, similar to the ones being conceptualized here, are cheap to produce and will increase the performance of dumb bombs much more significantly.

2.3 Aerodynamic Basis

2.3.1 Wing and Tail Geometrical Characteristics

The most crucial part of the glide bomb is, of course, the wing. It is what generates lift to the munition and so must be designed carefully in order to achieve peak performance when in service. The list below shows all of the main parameters of the wing and its tail geometry as well as a depiction in Figure 2.18.

- C_T = Tip chord of the wing
- C_0 = Root chord of the wing
- S = Wing plan area
- λ = Wing taper ratio, C_T/C_0
- b = Wing span
- A or $AR = b^2/S$
- $\frac{t}{c}$ = The wing's thickness chord ratio. The maximum local thickness, divided by the chord length
- α = Geometric angle of attack
- MAC = Mean aerodynamic chord

2.3.2 Aerodynamic Forces and Moments

The aerodynamic forces and moments are attributed solely towards two primary sources. The pressure distribution p and the shear stress distribution τ. The combined outcome of these factors will be a Resultant Force, denoted by R While

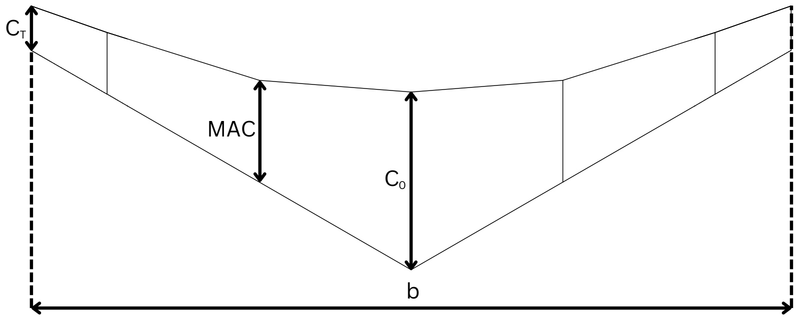

FIGURE 2.18: Wing Parameters

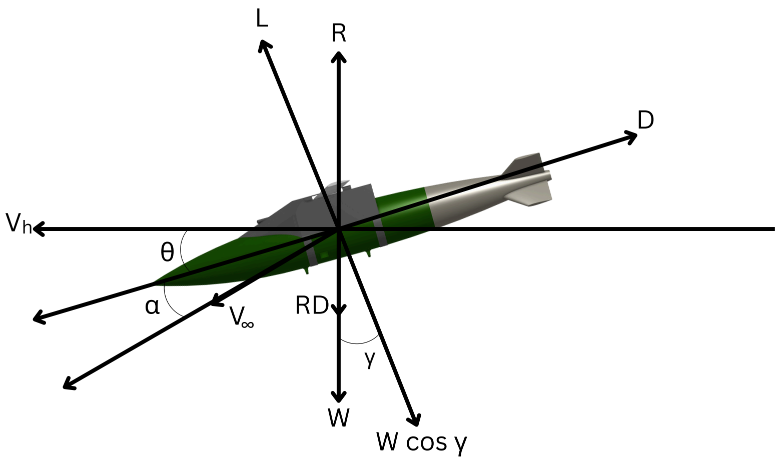

FIGURE 2.19: Force Balance Coordinates [26]

acting on the body, it is the moment, denoted by M. According to Figure 2.19, the resultant force is divided into several components,namely:

- V_∞ = Free-stream Velocity
- $L \equiv$ Lift $\equiv$ A component of R and is perpendicular to V_∞
- $D \equiv$ Drag $\equiv$ A component of R and is parallel to V_∞
- $N \equiv$ Normal Force $\equiv$ A component of R and is perpendicular to c
- $A \equiv$ Axial Force $\equiv$ A component of R and is parallel to c

with the angle of attack α, located between c and $V\infty$. This means that α is defined as the angle between L and N as well as between D and A [27] .

- $L = N\cos\alpha - A\sin\alpha$
- $D = N\sin\alpha + A\cos\alpha$

The lift and drag forces are expressed more commonly as coefficients without dimensions as stated in the Equations below. The wing's reference area, often known as S_{ref} or simply as S. This refers to the area of the region that extends up to the aircraft's center-line. The dynamic pressure of free-stream air is referred to as q [27] .

$$L = qSC_L \tag{2.1}$$

$$D = qSC_D \tag{2.2}$$

Where,

$$q = \frac{1}{2}\rho V^2 \tag{2.3}$$

C_L with the uppercase subscripts mean that the wing is of a Three-Dimensional shape. On the flip-side, lower case subscripts mean that the C_L has the characteristics of a 2-dimensional Airfoil [27] .

Uncambered:

$$C_D = C_{D_0} + KC_L^2 \tag{2.4}$$

Cambered:

$$C_D = C_{D_{\text{min}}} + K(C_L - C_{L_{\text{min drag}}})^2 \tag{2.5}$$

With C_{D_0} being the Zero-lift drag, $C_{D_{\text{min}}}$ the minimum drag coefficient, and $C_{L_{\text{min drag}}}$ the lift coefficient when an aircraft is experiencing minimum drag.

2.4 Equations of Motion (EOM) for Gliding Flight

2.4.1 Symmetric Flight

By definition, gliding flight is defined as the flight with no thrust. So it is natural to see that it is the case for gliders and/or sailplane aircraft. Setting the thrust, T, to zero, we get two Equations as follows;

$$-D - W \sin \gamma = 0 \tag{2.6}$$

$$L - W \cos \gamma = 0 \tag{2.7}$$

The Equations 2.6 and 2.7 provide a description on the forces for a symmetric and unpowered flight and proves that the weight of the aircraft must be balanced by the other forces that act on it, such as lift and drag. As drag acts on the negative X_a-axis, a state of equilibrium can exist if the weight is able to furnish a component of force in the flight's direction. Or to summarize, the aircraft must travel downwards, so that the value of γ is less than zero, $\gamma < 0$, as seen in Figure 2.20. To achieve this, the flight-path angle must also be negative and the aircraft can be said to be in a dive or descending flight. In order to use the formula for negative flight-path angles, it can be defined as;

$$\gamma_d = -\gamma \tag{2.8}$$

Hence the value of γ_d is said to be a positive downward angle, also known as the angle of descent or gliding angle. Similarly speaking, it can be said that a negative rate of climb ($-RC$) is equal to a positive rate of descent (RD). This can be expressed as;

$$RD = -RC \tag{2.9}$$

Now, we substitute $\gamma_d = -\gamma$ into the first 2 Equations, 2.6 and 2.7, and then by using the familiar expressions for the Equations of lift and drag, $L = \frac{1}{2}\rho V^2 C_L S$ and $D = \frac{1}{2}\rho V^2 C_D S$, respectively, we get;

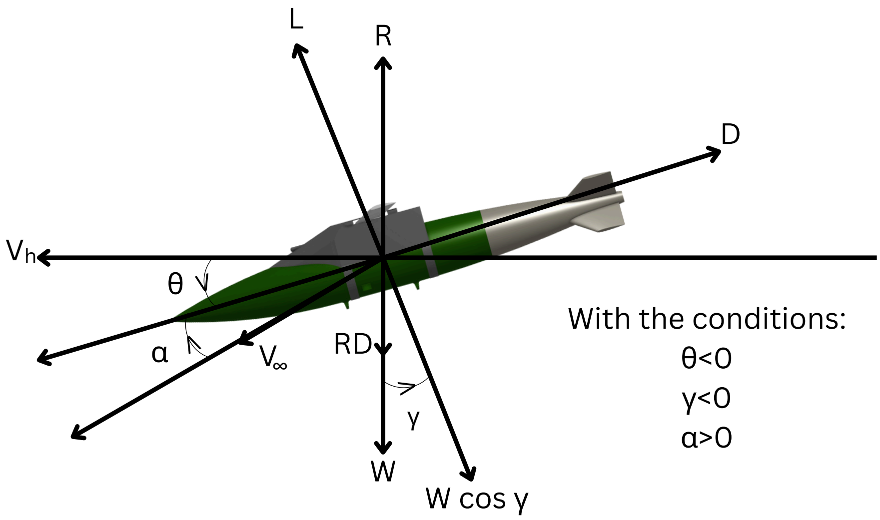

FIGURE 2.20: Steady Symmetric Gliding Conditions [28]

$$D = \frac{1}{2}\rho V^2 C_D S = W \sin\gamma_d \tag{2.10}$$

and

$$L = \frac{1}{2}\rho V^2 C_L S = W \cos\gamma_d. \tag{2.11}$$

With Equation 2.11 able to be re-written as:

$$V = \sqrt{\frac{W}{S}\frac{2}{\rho}\frac{1}{C_L}\cos\gamma_d} \tag{2.12}$$

Then, when we divide the Equation 2.10 by Equation 2.11, we obtain;

$$\tan\gamma_d = \frac{C_D}{C_L} \tag{2.13}$$

Now, from the Equations 2.12 and 2.13, we can obtain the rate of descent, or RD in the gliding flight. The Equation is as follows;

$$RD = V \sin \gamma_d = V \frac{C_D}{C_L} \cos \gamma_d = \sqrt{\frac{W}{S} \frac{2}{\rho} \frac{C_D^2}{C_L^3}} \cos^3 \gamma_d. \tag{2.14}$$

From the Equations 2.12 and 2.14, it is important to note that, at speeds that are low subsonic levels, and while neglecting the effects of the Reynolds number, the quantities involved, V, γ_d and RD, are determined by the aircraft's angle of attack where, its single control variable is able to be augmented by the aircraft's elevator control surface.

Below, we have an example of a table of calculations, in Table 2.21 done on an aircraft with its specifications mentioned as well. There, you are able to see the set of numbers that are expected when calculations are to be done and include the values for rate of descent, airspeed, and etc.

	airplane weight			W = 4,000 N			
	wing area			$S = 10\,\text{m}^2$			
	altitude			H = 2,000 m (I.S.A.)			
	configuration			clean			
C_L	C_D	C_L/C_D	C_L^3/C_D^2	γ_d deg.	V, km/h	RD, m/s	V_h km/h
1.50	0.0570	26.3	1038.8	2.176	82.8	0.874	82.8
1.40	0.0512	27.3	1046.8	2.094	85.7	0.871	85.7
1.30	0.0458	28.4	1047.4	2.018	89.0	0.870	88.9
1.20	0.0408	29.4	1038.1	1.947	92.6	0.874	92.6
1.10	0.0362	30.4	1015.7	1.885	96.7	0.884	96.7
1.00	0.0320	31.3	976.6	1.833	101.5	0.901	101.4
0.90	0.0282	31.9	916.7	1.795	107.0	0.930	106.9
0.80	0.0248	32.3	832.5	1.776	113.4	0.976	113.4
0.70	0.0218	32.1	721.7	1.784	121.3	1.049	121.2
0.60	0.0192	31.3	585.9	1.833	131.0	1.164	130.9
0.50	0.0170	29.4	432.5	1.947	143.5	1.354	143.4
0.40	0.0152	26.3	277.0	2.176	160.4	1.692	160.3
0.30	0.0138	21.7	141.8	2.634	185.2	2.364	185.0
0.20	0.0128	15.6	48.8	3.662	226.7	4.022	226.3

FIGURE 2.21: Example Calculations of Glide Performance [28]

There is another expression that is used to calculate the terminal-speed when in vertical dive and this is obtained by subbing out C_D for C_{D_0} and also taking

$\gamma_d = 1$ in Equation 2.10. This gives us;

$$V_{\text{max}} = \sqrt{\frac{W}{S}\frac{2}{\rho}\frac{1}{C_{D_0}}}. \tag{2.15}$$

To many, a minimized rate of descent is considered most ideal for maximizing endurance, or in other words, getting the most time in the air as possible. This is calculated using the Equation 2.16 below;

$$t_{\text{max}} = \int_H^0 \frac{-dH}{RD_{\text{min}}} = \int_H^0 \frac{dH}{RD_{\text{min}}} \tag{2.16}$$

With this, there is a need for a minimized angle of descent.

$$s_{\text{max}} = \int_H^0 \frac{dH}{\tan \gamma_{d_{\text{min}}}} = \frac{H}{\tan \gamma_{d_{\text{min}}}} \tag{2.17}$$

As we can see from Equation 2.13, that is the Equation for the smallest angle of descent and so the maximum horizontal distance traveled by the aircraft is obtainable when the value of the angle of attack, α, is at the point where the lift-to-drag ratio is at its maximum. So we get the expression;

$$s_{\text{max}} = H \left[\frac{C_L}{C_D}\right]_{\text{max}} \tag{2.18}$$

Do note that there is no variable for weight. That is because weight has no effect on the minimum angle of descent, nor does it affect the maximum range of the gliding aircraft. However, weight does, in fact, affect the aircraft's endurance when it is at a certain height and coefficient of lift, C_L.

From Table 2.21, we can see that, when making observations that regard the gliding performance in a normal range of airspeeds, the descent angle remains small in order to keep the assumption that $\gamma_d = 1$. So, using the approximations in Equations 2.12, 2.13 and 2.14, we get the following Equations for gliding flight;

$$V = \sqrt{\frac{W}{S}\frac{2}{\rho}\frac{1}{C_L}} \tag{2.19}$$

$$\gamma_d = \tan^{-1}\frac{C_D}{C_L} = \sin^{-1}\frac{C_D}{C_L} \tag{2.20}$$

$$RD = \sqrt{\frac{W}{S}\frac{2}{\rho}\frac{C_D^2}{C_L^3}} \tag{2.21}$$

The Equation 2.21 shows that, with the assumption of $\cos\gamma_d = 1$, the minimum descent rate is acquired when the value of the climb factor, $\frac{C_L^3}{C_D^2}$ is then maximized. We are also able to observe that, when at speed for the ideal glide angle, the aircraft's drag is also kept at a minimum.

$$D_{\text{min}} = W \sin\gamma_{d_{\text{min}}} = \frac{W}{\left(\frac{C_L}{C_D}\right)_{\text{max}}} \tag{2.22}$$

Also, when at the speed that is ideal for the minimum descent rate, the required power is too, minimum.

$$P_{\text{r min}} = (DV)_{\text{min}} = (WV\sin\gamma_d)_{\text{min}} = W(RD_{\text{min}}). \tag{2.23}$$

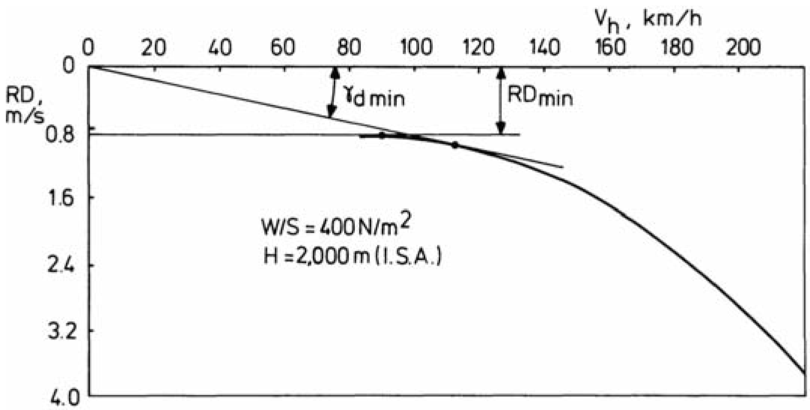

FIGURE 2.22: Hodograph of Gliding Performance, with assumption of $\cos\gamma_d = 1$ [28]

The Figure 2.22 illustrates the glider's performance, when $\cos\gamma_d$ is assumed to be equal to 1. Now we get to adopt the concept of Parabolic lift-drag polar, $C_D = C_{D0} + \frac{C_L^2}{\pi Ae}$, the speed for the best value of gliding angle and for the lowest possible descent rate can be expressed from Equation 2.19 as;

$$V_{\gamma_{d_{\min}}} = \sqrt{\frac{W}{S}\frac{2}{\rho}\frac{1}{\sqrt{C_{D0}\pi Ae}}} \tag{2.24}$$

and

$$V_{\gamma_{d_{\min}}} = \sqrt{\frac{W}{S}\frac{2}{\rho}\frac{1}{\sqrt{3C_{D0}\pi Ae}}} \tag{2.25}$$

Where A represents the aspect ratio of the wing and e is known as the Oswald's efficiency factor whose value varies between $0.6 - 0.9$ [28].

2.4.2 Altitude Effects

Gliding involves launching the aircraft from high altitude in order to get a long range of flight. However, it is important to look into what effects the higher altitude has on and how it affects the performance of a gliding aircraft during its flight. To help in investigating, two conditions have been taken, two different altitudes will be used as comparison, but the same angle of attack, α, will be used. The constant value of α is used as it would keep other factors such as C_L and C_D also constant, even as the altitude differs. This assumption is used provided that the slight effects of Reynolds number on the lift-drag polar is neglected. Since Equation 2.13 provides the gliding angle, γ_d, and it is purely determined by the lift-to-drag ratio, we can see that the value of γ_d is also kept unchanged. By designating the first and second flight conditions using 1 and 2, so $h1$ and $h2$, respectively, we can obtain the Equation for the ratio of horizontal velocities as follows;

$$\frac{V_{h2}}{V_{h1}} = \frac{\sqrt{\frac{W}{S}\frac{2}{\rho_2}\frac{1}{C_L}\cos\gamma_d}\cos\gamma_d}{\sqrt{\frac{W}{S}\frac{2}{\rho_1}\frac{1}{C_L}\cos\gamma_d}\cos\gamma_d} = \sqrt{\frac{\rho_1}{\rho_2}} \tag{2.26}$$

Similarly, the Equation for the ratio of vertical velocities is expressed as;

$$\frac{RD_2}{RD_1} = \frac{\sqrt{\frac{W}{S}\frac{2}{\rho_2}\frac{1}{C_L}\cos\gamma_d}\sin\gamma_d}{\sqrt{\frac{W}{S}\frac{2}{\rho_1}\frac{1}{C_L}\cos\gamma_d}\sin\gamma_d} = \sqrt{\frac{\rho_1}{\rho_2}} \tag{2.27}$$

From the previous 2 Equations, 2.26 and 2.27, we can combine them to obtain the expression;

$$\frac{V_{h2}}{V_1} = \frac{RD_{h2}}{RD_1} \tag{2.28}$$

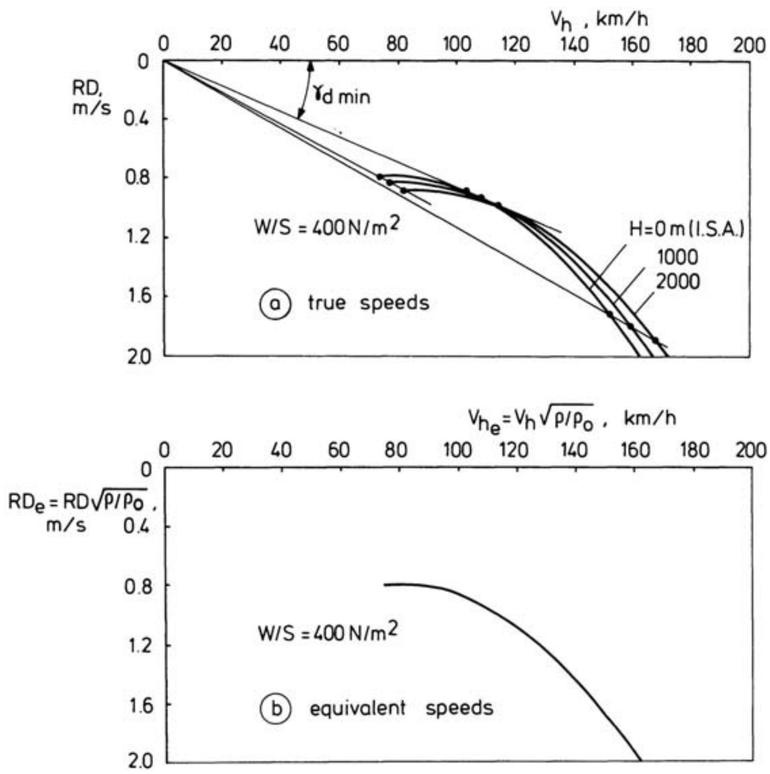

FIGURE 2.23: Altitude's effects on Gliding Performance [28]

Now, look at Figure 2.23 . We have a hodograph that shows the effects of three values of altitudes on a glider. From the Equation 2.28, we are able to view the corresponding points on the curve that move from left and up along a straight line right through the point of origin when the altitude starts to drop, which means an increase in air density, ρ. All curves have a joint tangent that gives the value for the minimum angle of glide. Do take note that, at a given value of α, the airspeed as well as the rate of descent begin to decrease as the altitude reaches ever closer to the ground.

Now when we see Equations 2.16 and 2.21 , we can observe that, if the flight is to achieve maximum performance in both range and endurance, it will require augmentation from either a pilot or an automated system. The aircraft needs to perform flight adjustments in such a way that, throughout its time in the air in a glide, it must be able to keep a constant dynamic pressure. Or in another sense, the equivalent airspeed must be constant as the aircraft executes a quasi-steady flight. This is when the actual/true airspeed increases as the glider continues its gliding descent.

It will be evident that, when plotting the hodograph curves using a base of the equivalent airspeeds, will lead to a single curve that applies to all altitudes. This can be seen in the lower graph of Figure 2.23

In that sense, we can take down that, in our case, the system needs to go against two types of airspeed data, the equivalent and true airspeed, which are viewed on the data as airspeed and vertical-speed, respectively.

2.4.3 Wind Effects

It is important to remember that wind will always have a part to play in the performance of an aircraft. Whether it is doing unpowered gliding or powered flight, wind will always be a key player that affects performance and is usually a oddball factor due to its random nature in some cases. Per [28], the velocity of the aircraft is relative to the velocity on the ground, or in other words, ground speed, or V_g. Its value is acquired from the sum of the airspeed V and the velocity of the wind V_W.

When putting wind and its effects into consideration for gliding performance, we will have to assume that the wind that the glider will encounter is steady, and not random as I previously warned. Another made assumption is that, the wind is blowing in a parallel direction to the aircraft's plane of symmetry. Now, using these conditions, the velocity of wind can be added to the velocities of flight that can be found on the hodograph curve that was calculated in still air in order to obtain the value of ground speed.

As we can see in Figure 2.24 , it is a re-plotted hodograph from Figure 2.22. Figure 2.24 now shows the hodograph with the added effect of steady wind. It is

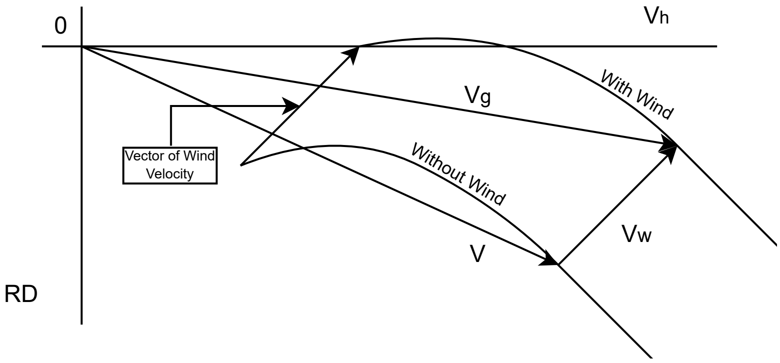

FIGURE 2.24: Hodograph with and without the effects of wind [28]

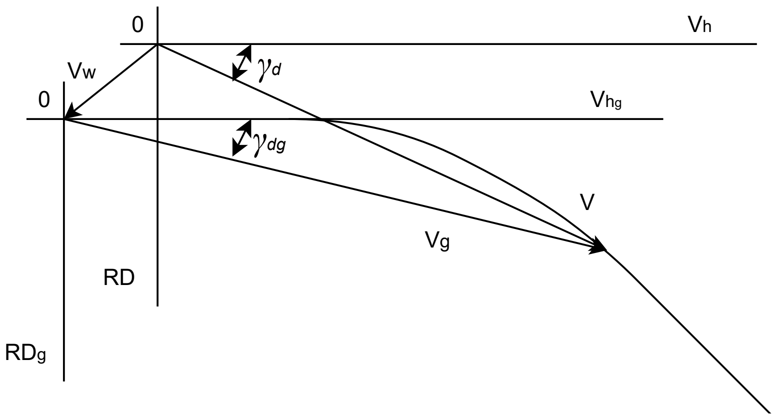

FIGURE 2.25: Wind's effects on the hodograph [28]

important to not that, wind has no effect on the glider's rate of descent or climb, but does have the ability to disrupt the glide angle of the glider. Hence why both curves, with and without wind, have the exact same gradient.

The resultant upward component of the wind's velocity produces a positive rate of climb. These upwind streams make it possible for gliders to increase altitude without the need for thrust to push the aircraft forward.

2.4.4 Turning Flight

As aforementioned in the previous subchapter, the wind will play a key role in the performance of the glider. Saying that, it does also have the power to disrupt the main mission of the gliding bomb, which could happen by pushing the munition off of its trajectory.

To fix this, the glider must be able to turn and a glider's most appropriate turning radius as well as its associated bank angle and airspeed for optimum performance will be heavily dependent on the manner of the vertical speed that varies with radius.

With that being said, the relationship between the minimum descent rate and turning radius is of utmost importance. To look into this correlation, we must consider the Equations that govern the translational motion of the aircraft during a steady and coordinated turn, Equations 2.29, 2.30 and 2.31. Then by changing the values of Thrust, T to zero and the angle $\gamma = -\gamma_d$ into the following Equations;

$$T - D - W \sin \gamma = 0 \tag{2.29}$$

$$L \sin \mu - C = 0 \tag{2.30}$$

$$-L \cos \mu + W \cos \gamma = 0 \tag{2.31}$$

After changing values, we obtain;

$$-D + \sin \gamma_d = 0 \tag{2.32}$$

$$L \sin \mu - C = 0 \tag{2.33}$$

$$-L \cos \mu + W \cos \gamma_d = 0 \tag{2.34}$$

Then we can see that, from the Equation $C = \frac{W}{8} V \Omega cos\gamma = \frac{W}{g} \frac{V^2}{R} \cos^2 \gamma$, we can exchange certain values and obtain the Equation, 2.35, for centrifugal force

C for our case as;

$$C = \frac{W}{8} V\Omega cos\gamma_d = \frac{W}{g}\frac{V^2}{R}\cos^2\gamma_d \tag{2.35}$$

With the exchanging of the Equation 2.35 with the Equations for drag and lift, $D = C_D\frac{1}{2}\rho V^2 S$ and $L = C_L\frac{1}{2}\rho V^2 S$, the Equations for turning will therefore turn to;

$$C_D\frac{1}{2}\rho V^2 S = W\sin\gamma_d \tag{2.36}$$

$$C_L\frac{1}{2}\rho V^2 S\sin\mu = \frac{W}{g}V\Omega\cos\gamma_d = \frac{W}{g}\frac{V^2}{R}\cos^2\gamma_d \tag{2.37}$$

$$C_L\frac{1}{2}\rho V^2 S\cos\mu = W\sin\gamma_d \tag{2.38}$$

For a given value of weight as well as the conditions in the atmosphere, the Equations, 2.36, 2.37, 2.38, contain five key variables. Mainly, α, V, γ_d, μ and R in order to fulfill instantaneous flight conditions that are definable via the selection of two control variables. Where R is defined as the radius of the curvature of the turn.

We are able to express these performance factors in terms of angle of attack, α, and the aerodynamic roll angle, μ, which is the angle at which an aircraft turns, or "banks", in order to alter its flight direction. From which we are able to obtain;

$$V = \sqrt{\frac{W}{S}\frac{2}{\rho}\frac{1}{C_L}\frac{\cos\gamma_d}{\cos\mu}} \tag{2.39}$$

$$\tan\gamma_d = \frac{C_D}{C_L}\frac{1}{\cos\mu} \tag{2.40}$$

$$RD = \sqrt{\frac{W}{S}\frac{2}{\rho}\frac{C_D^2}{C_L^3}\frac{\cos^3\gamma_d}{\cos^3\mu}} \tag{2.41}$$

$$n = \frac{L}{W} = \frac{\cos\gamma_d}{\cos\mu} = \frac{C_L}{C_D}\sin\gamma_d \tag{2.42}$$

$$R = \frac{V^2 \cos\gamma_d}{g\tan\mu} = \frac{W}{S}\frac{2}{\rho}\frac{1}{g}\frac{1}{C_L}\frac{\cos^2\gamma_d}{\sin\mu} \tag{2.43}$$

$$\Omega = \frac{V\cos\gamma_d}{R} = \frac{g\tan\mu}{V} \tag{2.44}$$

$$T_\pi = \frac{\pi}{\Omega} = \frac{\pi R}{V\cos\gamma_d} \tag{2.45}$$

With the angle of descent normally being small, it is safe to assume that $\cos\gamma_d$ can be approximated to be equal to unity in the Equations above. However, since we are considering coordinated turns being made, from Equation 2.29 that $\cos\gamma_d = 1$ and the aerodynamic roll angle is equal to the bank angle, or banking angle, ϕ. Hence why we are able to re-write the Equations, 2.35-2.49, above as;

$$V = \sqrt{\frac{W}{S}\frac{2}{\rho}\frac{1}{C_L}\frac{1}{\cos\phi}} \tag{2.46}$$

$$\tan\gamma_d = \frac{C_D}{C_L}\frac{1}{\cos\phi} \tag{2.47}$$

$$RD = \sqrt{\frac{W}{S}\frac{2}{\rho}\frac{C_D^2}{C_L^3}\frac{1}{\cos^3\phi}} \tag{2.48}$$

$$n = \frac{L}{W} = \frac{1}{\cos\phi} = \frac{C_L}{C_D}\sin\gamma_d \tag{2.49}$$

$$R = \frac{V^2\cos\gamma_d}{g\tan\mu} = \frac{W}{S}\frac{2}{\rho}\frac{1}{g}\frac{1}{C_L}\frac{1}{\sin\phi} \tag{2.50}$$

$$\Omega = \frac{V}{R} = \frac{g\tan\phi}{V} \tag{2.51}$$

$$T_\pi = \frac{\pi}{\Omega} = \frac{\pi R}{V} \tag{2.52}$$

The effect of banking towards the curve of the hodograph can be looked into by looking back at the two conditions of flight at different banking angles, but at the same angle of attack. Now, assuming that at a constant value of α, both C_L and C_D also remain constant. Hence we are able to obtain;

$$\frac{V_{h2}}{V_{h1}} = \left[\frac{\cos\phi_1}{\cos\phi_2}\right]^{\frac{1}{2}} = \left[\frac{n_2}{n_1}\right]^{\frac{1}{2}} \tag{2.53}$$

$$\frac{RD_2}{RD_1} = \left[\frac{\cos\phi_1}{\cos\phi_2}\right]^{\frac{3}{2}} = \left[\frac{n_2}{n_1}\right]^{\frac{3}{2}} \tag{2.54}$$

$$\frac{RD_2}{RD_1} = \left[\frac{V_{h2}}{V_{h1}}\right]^{3} \tag{2.55}$$

Note: The notations "1" and "2" regard to the conditions of bank angles ϕ_1 and ϕ_2.

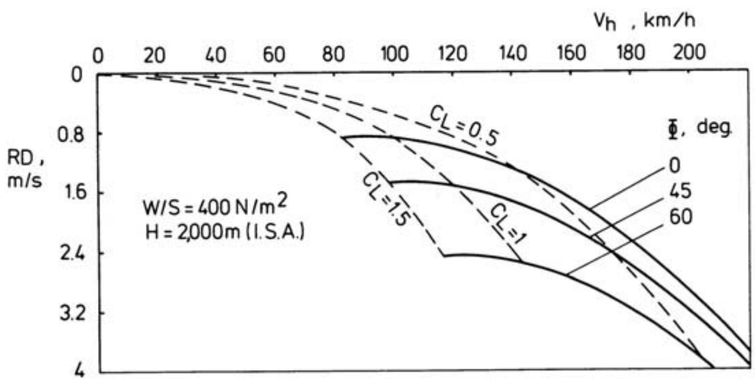

FIGURE 2.26: Banking Angle effects on the curve of the Hodograph [28]

As you can see from the hodograph in Figure 2.26, we can see a representation of the glider's performance during a turn at a fixed bank angle. The curves have been deduced from the hodograph curve of a straight flight, in the exact same manner we previously discussed. The points on the curve are corresponding to the same C_L value throughout the flight and are conjoined to dashed lines. Figure 2.27 shows the descent rate as a function of the turn radius for various values of bank angle, as calculated using the Equations 2.41, 2.42 and 2.43. It can be seen that all the points are connected and correspond to the exact same value of speed, or V. The upper dashed line is representing the minimum descent

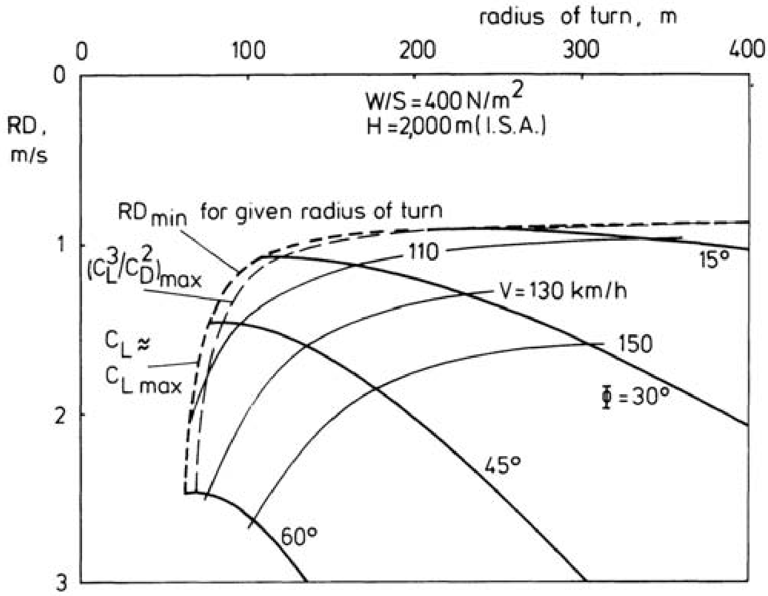

FIGURE 2.27: Descent rate against Turning radius for various Bank angles [28]

rate which is obtainable at each turn radius. On this line, the airspeed and bank angle will continue to increase as the turning radius decreases. The relationship between RD and R can be formulated by the elimination of the bank angle from Equations 2.41, 2.42 and 2.43, and yields;

$$RD = \sqrt{\frac{W}{S}\frac{2}{\rho}\frac{C_D^2}{\left[C_L^2 - \left[\frac{W}{S}\frac{2}{\rho}\frac{1}{g}\frac{1}{R}\right]^2\right]^{\frac{3}{2}}}} \tag{2.56}$$

Also, it will be apparent when values are given to aircraft weight, air density and turning radius, the minimum descent rate will be acquired when the term between the brackets in the Equation above, 2.56 ,is kept at a minimum. Another expression for the lift coefficient that corresponds to the Equation, 2.56, can be derived by taking in the derivation of the terms with respect to C_L and must equate to zero. Using the Equation for parabolic drag, $C_D = C_{D0} + \frac{C_L^2}{\pi A e}$, so the optimum lift coefficient for a minimum descent rate can be expressed as;

$$C_L = \sqrt{3C_{D0}\pi Ae + 4\left[\frac{W}{S}\frac{2}{\rho}\frac{1}{g}\frac{1}{R}\right]^2} \tag{2.57}$$

This Equation, 2.57, proves that, for a minimized descent rate, the glider will fly at a large C_L whose value varies when the climbing factor is at maximum (when the radius of turn is infinite, $R = \infty$) and when it reaches close to the maximum C_L (when radius of turn is at its lowest possible value, $R = R_{\text{min}}$) [28].

2.5 Gliding Stability

According to [29], stability is defined as a system that has started in a state of static equilibrium and so it is said to be stable. If a disturbance occurs, of a finite amplitude and during a finite amount of time, the resultant response is one that becomes vanishingly tiny as time continues on. Hence it is why stability is concerned with the nature of free motion in a system that follows a disturbance.

2.5.1 The Modes of Aircraft Motion

The motion of an aircraft in a 3-dimensional space are classified into 2 modes:

- Longitudinal mode: Which moves the aircraft along Xb and Zb axes and rotates around the Yb axis,and
- Lateral-directional mode: Which moves the aircraft within 2 lateral planes, Yb and Zb, as well as its directional planes, Xb and Yb.

For a better representation, Figure 2.28 and Figure 2.29 shows the parameters of motion in a 3-dimensional space, which includes the:

- Translation: X, Y, Z
- Rotations: ϕ, θ, ψ

2.5.2 Axes of Reference

Figure 2.29 shows an aircraft with wind, relative to its side, and the standard right-hand set of body-fixed reference frames. That fixed reference frame is frame

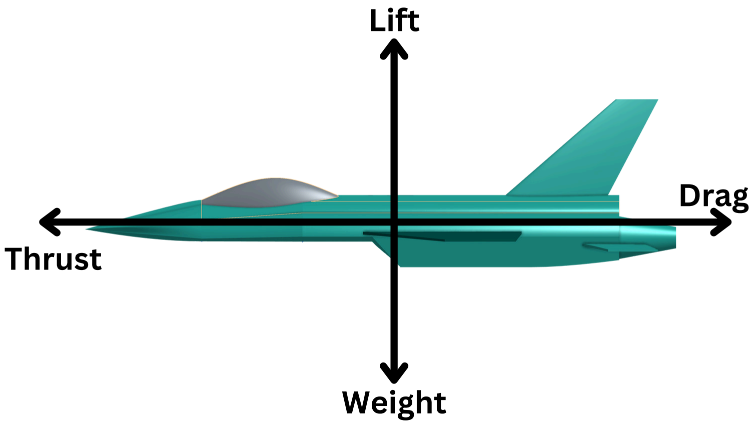

FIGURE 2.28: Aircraft Motion [30]

B, which is connected to the aircraft's center of gravity and has axes that are aligned with the line of reference of the fuselage. Two more reference frames are to be added, both are also tied to the center of gravity:

- The stability reference frame S, which is utilized for analysis on the potential impacts that come from the deviations of a steady-state flight, and
- The wind reference frame W,

The angle of attack, α, as well as the sideslip angle, β, are both defined by the revolution of the plane around the body's y-axis and is followed by a rotation of the plane about the z-axis. This leaves the last axis, the x-axis, to be aligned with the relative wind. The initial rotation (Rotation 1) produces the stability reference frame S, while the next one after it (Rotation 2) produces wind reference frame W. It is important to note that a positive angle of attack, α, will result in a negative rotation along the y-axis (shown as positive in Figure 2.29). If the rotation about the z-axis (Stability Axis), the sideslip angle, β, will too be positive (Shown as positive in Figure 2.29).

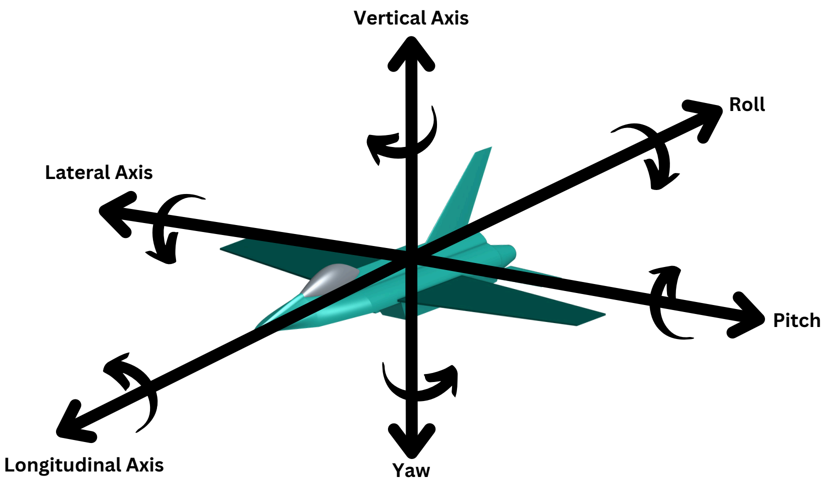

FIGURE 2.29: Aircraft Reference Axes [31]

2.5.3 Static and Dynamic Stability

With stability being the ability of an aircraft to be able to correct its flight for conditions that are acting on it, these include turbulence or inputs made to control surfaces. In aircraft, there are two main types of stability that are generally known: Static and Dynamic.

While most aircraft are designed with stability kept in mind, others are not. Small aircraft, such as trainers, are designed and built to be very stable. While aircraft such as fighter jets are designed to be unstable in order for them to perform high speed maneuvers. However, they become not flyable without the aid of a computer-assisted fly-by-wire system.

Static stability is an aircraft's initial tendency to return to its original position after it has been disrupted [32].

2.6 Design Approach

As we can see in Appendix A, researching similar glide bombs and glide kits and/or the potential market will set the foundation for a comprehensive comparison. Gathering critical data is crucial for the initial calculations. Some market research not only assesses the economic feasibility for a glide bomb wing kit for military purposes, but also evaluates the readiness of the technology for integration into future designs. We then proceed to the next step which involves compiling a "Design Proposal." This is a crucial step that precedes the design process and includes the considerations regarding the potential of the kit itself and future applications it may possess. At the same time, defining the mission creates crucial limits for the new wing kit, which includes endurance, gliding range, and optimum operating altitude.

Once the mission has been clearly defined, the process moves into the conceptual design stage. Here, preliminary estimations for the weights involved in the kit, such as the weights of avionic components, wing, tail, etc, and aerodynamic characteristics are aligned with the design proposal. The conceptual design further determines the load affecting crucial components such as the wing, kit body and tail. This is also where adjustments to weight placements can be made in order to meet the requirements for static stability. Here, the size of certain aspects, such as control surfaces, to achieve the desired level of maneuverability. The conceptual design is then adapted into the mission specifications stated in the design proposal.

The next step is to perform the preliminary stage where the focus starts to shift towards fine-tuning the design. Further calculations are conducted with a focus on stability, controllability, structural stress and flight mechanics. By now, extra confirmation may be needed via actually building a test bed and testing proposed structural components in a wind tunnel to ensure that calculations match up with any data gathered from the tests. This step is a continuation of the design assessment and is to ensure the practicality and economic feasibility of the project. Once a review is complete, the design has essentially been fixed and frozen, where no more revisions are possible without another visit to the preliminary design.

The proceeding stage is the fun part, designing all the necessary components to build the wing kit. This stage relies on mainly structural design, control surfaces, components and subsystems. Testing and integration procedures will ensure that all components work in unison effectively.

2.7 Aircraft Structure Components

2.7.1 Fuselage/Wing Kit Body

The body of the wing kit are carefully designed and engineered structures that are made up of thin sheets of material as its outer skin, reinforced by a network of longitudinal stringer, strengthened by transverse frames and integrated with the bulkhead in a way that gives it a more aerodynamic surface in order to reduce or eliminate unnecessary drag forces. Other support structures such as the Longeron usually extend across a number of the frame members in order to enhance the structural integrity by supporting the skin from bending loads. Another support structure that can be used are Stringers. They too provide additional support, as well as being used to attach the skin to the frame(s). Altogether, these parts will almost guarantee the structural stability and aerodynamic effectiveness of the fuselage. The main defense for the structural frames is the skin, which protects the supports and frames from the outside air pressure. Stringers provide the critical reinforcement by increasing the skin's rigidity and resistance against bending and compressive stresses.

By crossing stringers around, the transverse frames are able to aid in distributing the loads and stresses, keep the fuselage's shape and increase the strength of the structure overall. In order to keep the glide bomb's performance during gliding flight consistent, this complex mixture of skin, stringers and frames must be able to withstand a number of stresses, such as induced aerodynamic forces, pressure differentials, and dynamic loads of takeoff and descent. An example of what a fuselage frame can look like is shown in Figure 2.30 [33].

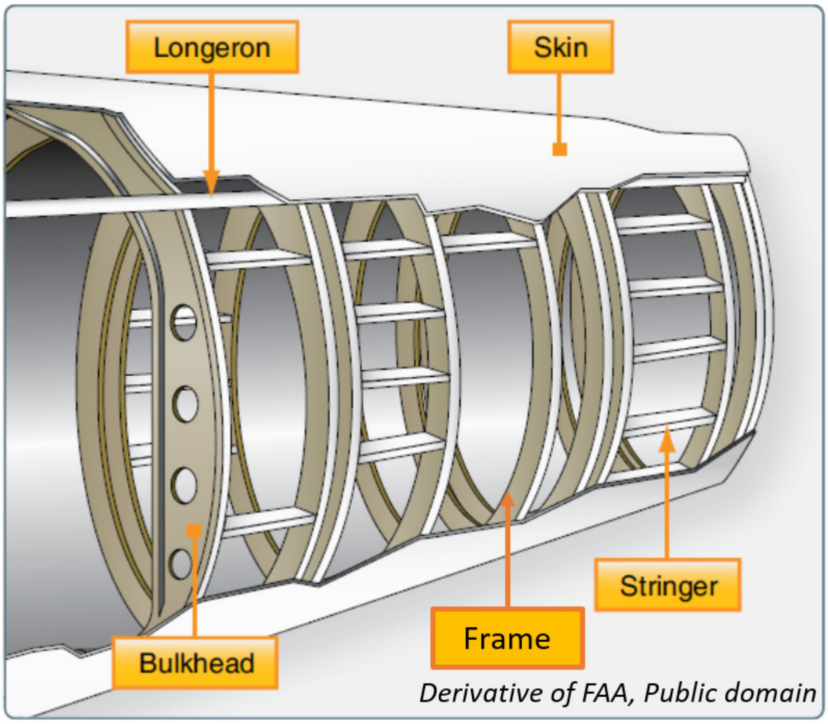

FIGURE 2.30: The Structure of a Fuselage [34]

2.7.2 Wing

The most important part of an aircraft is its wing because it is the main component that produces lift for the entire aircraft. The wing is separated into sections and consists of thin, reinforced skin that covers an entire assembly of stringers, spars and ribs. Figure 2.31 depicts what a conventional wing structure looks like. As a whole, all the elements maintain the structural integrity of the wing and retain its aerodynamic performance and efficiency. Similar to the fuselage, the skin is what protects the structures from the outside forces of air. The skin, or the outer layer, has to be both strong and lightweight, and at the same time be able to withstand the stresses of aerodynamic forces that apply during a flight. Stringers are longitudinally run structures that are attached along the wing and increase the wing's resistance against the bending and torsion loading that comes from forces that are induced during flight.

The part of the structure that takes most of the grunt are the spars. They run lengthwise across the wing and supports it against bending loads. Another part, the ribs, are spaced periodically and aids in maintaining the airfoil's shape as well as to distribute the aerodynamic forces across the entire surface of the wing. The relationship between these parts are a complex one, to say the least. But they do aid in guaranteeing that the wing remains sturdy enough to endure the stress and strain of flight, but also light enough that it does not hinder the aircraft's efficiency and performance. All these components are crucial in maintaining the wing's structure and retaining its efficiency during operations due to their critical function in helping to determine the aircraft's lift, stability and control.

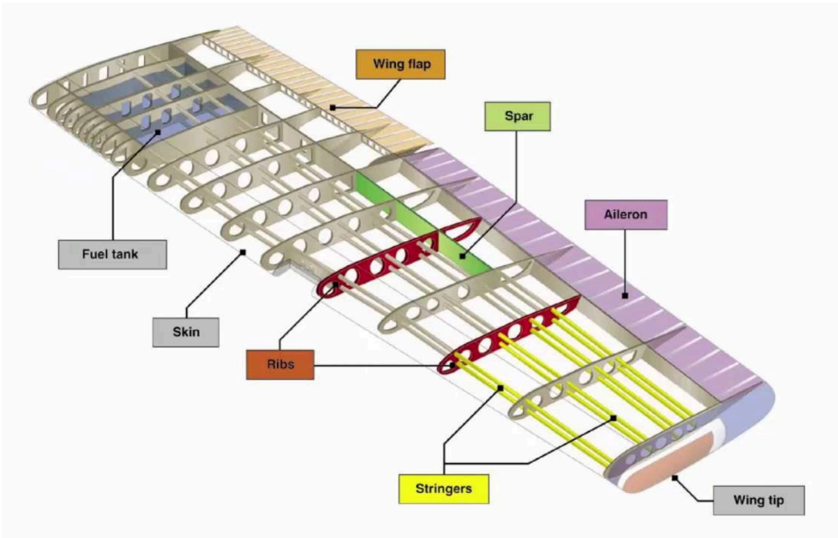

FIGURE 2.31: The structure of a wing [35]

2.7.3 Tail/Stabilizer(s)

Sometimes called the empennage, the tail section of the aircraft is a crucial part of the overall design because it aids in stabilizing the aircraft's rear end. It consists of a tail cone as well as both, a stationary and moving aerodynamic feature, such as stabilizers or fins. The structures of these stabilizers, consists of structural parts similar to that of the wing, where it has a combination of skin, spars, stringers and ribs. These structures play a critical role in stabilizing the aircraft and to reinforce the stabilizer against the stresses applied from the forces of shear, twist and bending that are all experienced during a flight. They also aid in efficiently distributing the extra loads endured by the fuselage and transfers the dynamic stresses to the empennage.

2.8 Previous/Similar Iterations of Glide Bombs

Some examples of past iterations of glide bomb kits include:

- Bazalt Design Bureau UMPK (Russia)
- Boeing/Mcdonnell Douglas JDAM-ER (United States)
- Iranian Defense Industry Yasin (Iran)
- LOTDC LS PGB (P.R. China)
- LiG Nex1 KGGB (South Korea)
- TUBITAK-SAGE KGK (Turkiye)
- Rafael SPICE (Israel)
- Denel Dynamics Umbani (South Africa)

and some examples of pure glide bombs include:

- Raytheon AGM-154 (United States)
- NESCOM H-4 SOW (Pakistan)
- Diehl BGT HOPE and HOSBO (Germany)
- DRDO Gaurav (India)

FIGURE 2.32: Iranian Defense Industry YASIN [36]

FIGURE 2.33: LOTDC LS PGB [37]

FIGURE 2.34: Rafael SPICE [38]

FIGURE 2.35: Raytheon AGM-154 [39]

2.9 Future Developments

Since this study is based on a gliding aerial vehicle system (no propulsion), future developments may include a powered or propulsion system in order to increase the level of impacted damage, accuracy and range of flight. Proof of this can be seen in the utilization of fixed wing Unmanned Aerial Vehicles (UAVs) around the

FIGURE 2.36: NESCOM H-4 SOW [40]

FIGURE 2.37: Diehl BGT HOSBO [41]

FIGURE 2.38: DRDO Gaurav [42]

world.

Small fixed wing UAVs have several advantages compared to its rotary wing (Rotorcraft UAV) counterpart. Where they mainly focus on efficiency in 3 sectors:

- More efficient on fuel/power
- Increased endurance (Time in air)
- and Increased range (Distance traveled)

Since the base gliding munition already possesses a wing, it would be wise for its continued development to go through a phase of powering the aircraft in order to gain all the advantages previously mentioned.

CHAPTER 3
RESEARCH METHODOLOGY

3.1 Conceptual Design Process Flowchart

Here in Chapter 3, we will discuss the methodology behind this thesis. Figure 3.1 represents the steps taken throughout the entire process of making this thesis.

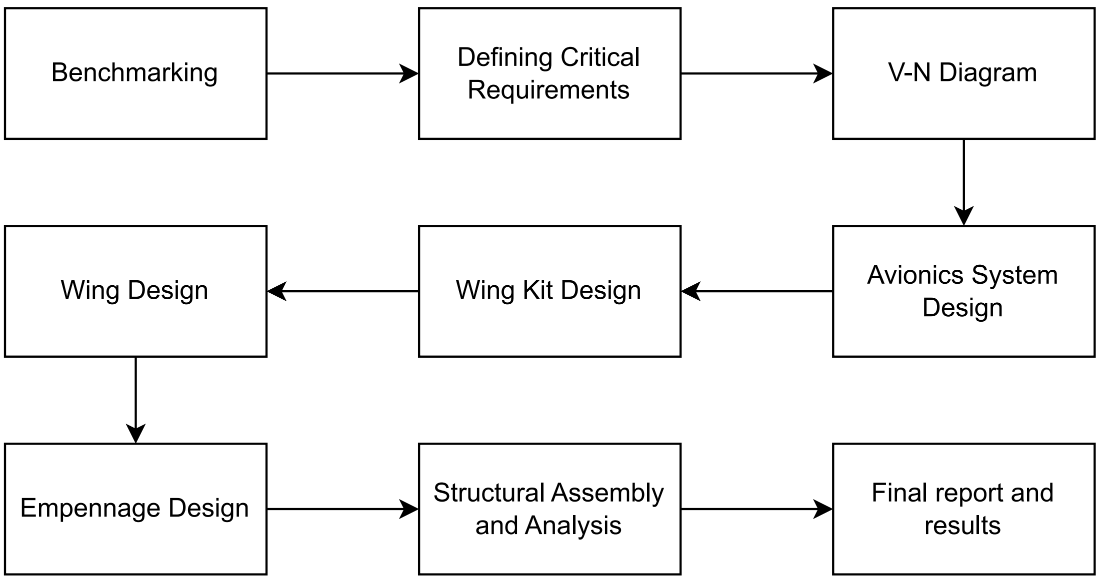

FIGURE 3.1: Conceptual Design Flowchart

3.2 Benchmark Study

The benchmarking process began with a literature study on 11 glide bombs and glide bomb kits from various manufacturers and nations around the world, as well as collecting and evaluating of available data on 3 potential warheads that are at the disposal of the Indonesian Armed Forces as well as the aircraft that are able to use said munitions that are owned, or to-be owned by the Indonesian Air Force.

The first stage was crucial for assessing the market for such a weapon and determines critical requirements and performance parameters, such as compatible aircraft and gliding range. The analysis focuses on a number of factors, including but not limited to the handling capabilities, technological features, compatibility to currently-owned equipment, and etc. That is why it is important to note that not all glide bombs and glide bomb kits have readily available data on the internet. But are coming back into light after the recent events in Europe and the Middle East. This provides a solid foundation on the current demand and urgency for glide bomb kits as a means of an effective type of weapon and highlights certain designs and characteristics that match the requirements of combat.

3.3 Mission Profile and Design Requirements

The mission profile is based on the user's requirements. With that in mind, as a result, different configurations may require the making of different mission profiles. For this conceptual design, we will use the mission profile that has been established after conducting a benchmark analysis based on market analysis on glide bombs and based on availability of certain crucial parts within the Indonesia Armed Forces. As a reference point, 2 glide bombs have been chosen from the benchmarking study and those two are the US-made JDAM-ER by Boeing and the Russian-made UMPK glide bomb kit. The list and Figure 3.3 below shows the design requirements and mission profile, respectively. Both were modeled after [43] with slight modifications, such as the removal of the propulsion system and a significant reduction in performance, but this was expected due to this being a gliding munition and the reference being a small, fast aircraft. Furthermore, numerous mission types were conceptualized and divided into two major categories; Explosive payload and Relief supply delivery. Each has similar design criteria and demands for their individual missions. Main difference is that one is for destruction and the other for aid. The development of the configurations has been led by an investigation into the availability of certain Military Commercial

Off The Shelf, or Mil-COTS, components and data. While extremely limited, it did provide crucial input in this stage of the designing process. As mentioned, both missions will have similar criteria and demands, the details of their weights, which is a crucial aspect in glide performance, have been capped at:

- Explosives: 230 kg (500 lbs) warhead
- Aid: Relief supplies, such as food, fresh water and medicine, weighing up to a maximum of 230 kg (Supplies will be stored in a makeshift 'warhead shell' in order to fit with the glide kit)

3.3.1 Design Requirements

- Total Payload = 230 kg or 500 lbs
- Maximum Range = >150 km
- Maximum Operating Altitude = 10.7 km or 35.000 ft

3.3.2 Mission Profile

The mission profile of this gliding bomb can be seen in Figures 3.2, 3.3, 3.4, and 3.5

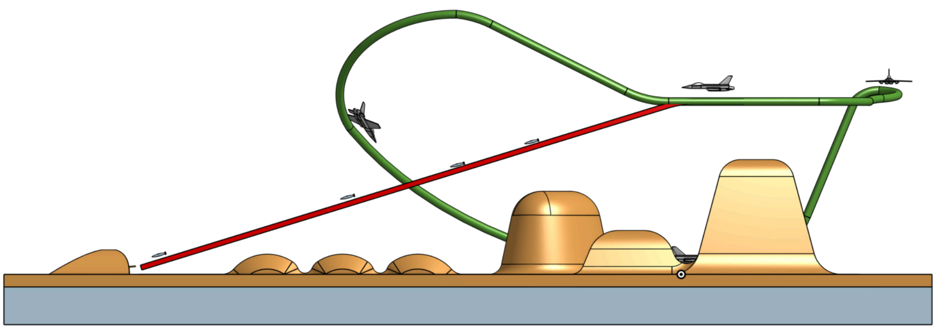

FIGURE 3.2: Mission Profile Side view

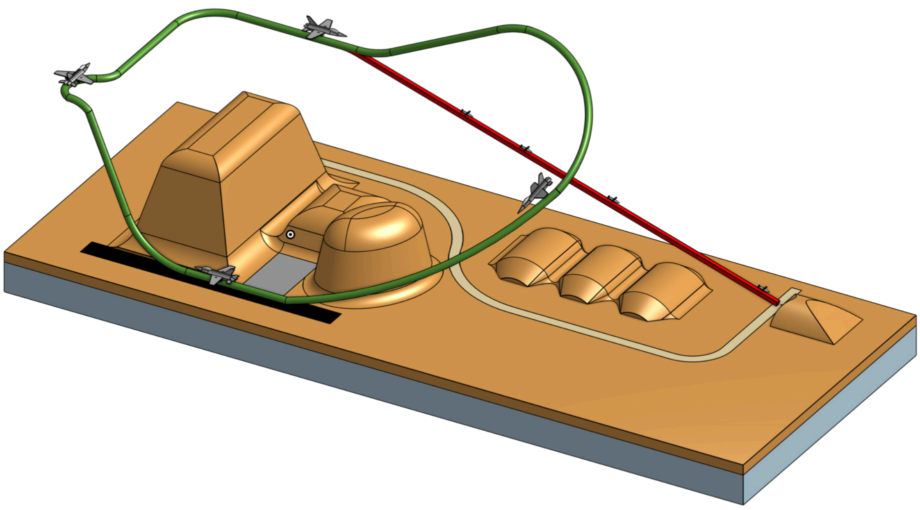

FIGURE 3.3: Mission Profile Dynamic view

FIGURE 3.4: Bomb drop

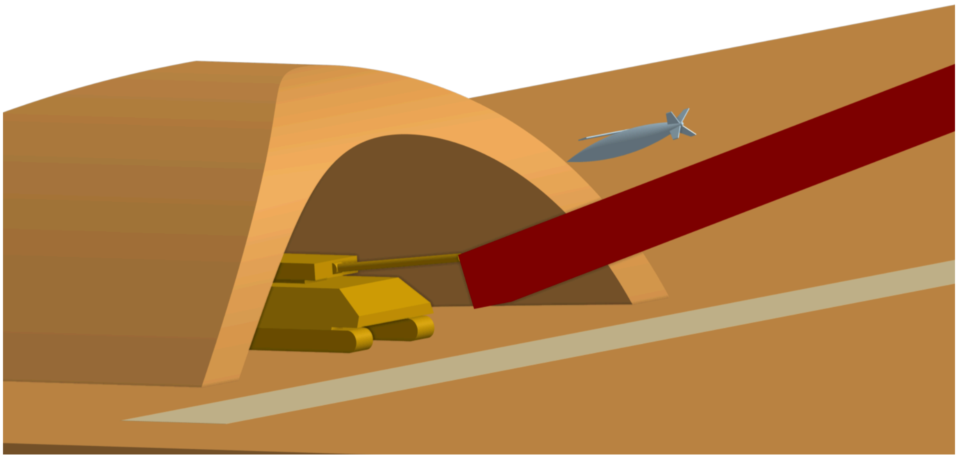

FIGURE 3.5: Bomb approaching target

3.4 V-n Diagram

Once the avionics design phase has been completed, we move on to creating the V-n diagram, also known as a Velocity-Load factor diagram. The very first step to make one is to gather detailed data on Aerodynamics and Performance of the aircraft, in this case, the Gliding Performance. The required data includes:

- Total weight of the bomb + glide bomb kit
- Area of the wing
- Air Density
- Maximum and Minimum lift coefficients
- C_{l_α}, which is the aircraft's lift curve slope/gradient.
- Speed of stall
- The mean geometric chord length
- Gliding speed
- Velocity of gust/wind

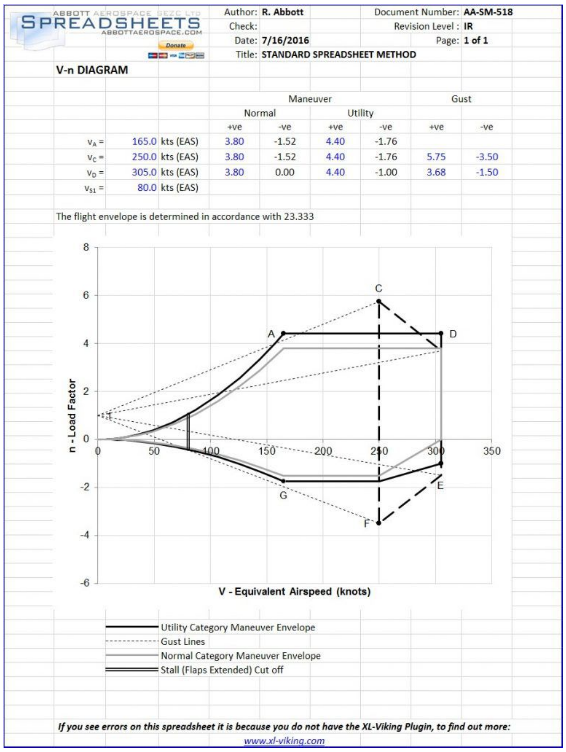

FIGURE 3.6: Abbott V-n Diagram [44]

Using the information, we can use the study from the Snorri General Aviation Aircraft Design Textbook [45] that uses formulas, that were developed from said book, to determine key components that are needed for producing a V-n diagram. These factors include:

- Positive Load Factor:
$$n_+ = 2.1 + \frac{24000}{W_0 + 10000} \tag{3.1}$$
- Negative Load Factor:
$$n_- = -0.4n_+ \tag{3.2}$$
- Dive Speed:
$$V_D > 1.40V_C \tag{3.3}$$
- Positive Maneuvering Speed:
$$V_A = V_S\sqrt{n_+} \tag{3.4}$$
- Negative Maneuvering Speed:
$$V_G = \sqrt{\frac{2|n_-|W}{\rho S C_{L_{\text{min}}}}} \tag{3.5}$$
- Gust Load factor:
$$n_g = 1 + \frac{K_g \times U_{\text{de}} \times V \times C_{L_\alpha}}{498\frac{W}{S}} \tag{3.6}$$

After identifying the crucial values of load factors and velocities, the researching methodology uses a specific application on Microsoft Excel, provided by Abbott aerospace. As shown in Figure 3.6, it shows a V-n diagram with several factors included such as the maneuvering, cruising, dive and stall speeds that all have been included into the spreadsheet. By this stage, the glide bomb's operational envelope can be seen and so can its performance capabilities, as well as its structural limitations under load. This is why the V-n diagram is a critical tool in ensuring that the design fits with the operational and performance requirements.

3.5 Avionics Component Selection

The next step of this research is to select the most suitable avionics components for the glide bomb. Main contributors of this process are that of the similar glide bombs and what components that are used in their architecture and systems. The main intention of the study is to determine the most suitable components by process of comparison. This means that the final concept will present itself with the best components that are available on the market and allow it to compete against it's competitors. Due to reasons of military secrecy, certain information and/or components that may be used in real-life examples may not be available for the general public, nor its information and specification. Availability concerns were kept in mind and when openly available data was unavailable, further investigation on comparisons were carried out. The compatibility of the selected components will improve the glide bomb's operational effectiveness, navigation and control whilst in gliding flight.

3.5.1 Bomb Selection

The selection process of the bombs were limited to those that were owned and used by the Indonesian Air Force. The 3 munitions that were available and of fitting weight for gliding were;

- General Dynamics Mark 82(Figure 3.7)
- Soviet era FAB-250(Figure 3.8)
- Dahana P-250L(Figure 3.9)

Another factor that affected the bomb selection was the type of aircraft that would be able to deliver the glide bomb to the launch area.

The aircraft that will be used to launch these munitions include but are not limited to;

- General Dynamics F-16 Fighting Falcon
- KAI T-50 Golden Eagle
- Embraer EMB-341 Super Tucano
- British Aerospace Hawk 200
- Dassault Rafale (Arriving in 2026)

- Boeing F-15EX (To be confirmed)
- Sukhoi Su-27
- Sukhoi Su-30

FIGURE 3.7: General Dynamics Mark 82 [46]

FIGURE 3.8: Soviet era FAB-500 [47]

FIGURE 3.9: Dahana P-250L [48]

3.6 XFLR5 Modeling

3.6.1 Introduction to XFLR5

XFLR5 is a user-friendly design and analysis tool for airfoils, wings, and planes operating at low Reynolds Number using X-FOIL codes for subsonic two-dimensional airfoil aerodynamic performance analysis. Although it does have the capabilities to conduct analysis of wings and even a full model aircraft in certain conditions, it is primarily used for the design and analysis of airfoils along with their performance in air. This provides the user with the capability to do calculations on the aerodynamic characteristic of airfoils as well as the possibility to analyze its behavior in two- or three-dimensional flow of air. This tool sees plenty of action in the aviation community of aircraft modeling and is plentifully used by students and educators alike under the Aerospace/Aeronautical Engineering umbrella as it is an ideal tool to be used for teaching purposes.

Users are able to analyze airfoil characteristics such as generated lift, drag and coefficients of moment and pressure. XFLR5 uses potential flow analysis with a boundary layer analysis method to conduct its calculations and production of results. Outside of airfoils, XFLR5 do bear the capability to perform 3D wing analysis as well as analysis on planes using Lifting Line Theory (LLT) and Vortex Lattice analysis Methods (VLM). Do note that these methods are assumed to be inviscid, incompressible and stagnant in flow. This is considered a limitation for more complex analyzing methods. XFLR5 also enables for the computation of polars, which are the plots of characteristics such as moment coefficients, Lift and Drag against the angle of attack the analysis is taking place at. This is important because it allows us to understand the aerodynamic performance of the airfoil and/or the wing in many different conditions. This program also includes tools that allow users to modify airfoil shapes and for designing conceptual aircraft wings. To sum up everything here, XFLR5 has proven to be a valuable software for those in the field of aerodynamics, especially those who focus their research on low Reynold numbers. It is easy to use and its interface makes it simple to learn and understand. The near-instant visual feedback it provides make it an ideal tool for education due to its impressive capabilities to perform wing and airfoil analysis which are sufficient for many preliminary research applications.

3.6.2 Wing and Tail modeling

Now, we are able to create a 3-Dimensional Wing and Tail shape on XFLR5. But before that, we must define the airfoil's design as well as its initial characteristics. In the module named "Direct Foil Design," we can define our own airfoil, either using the NACA airfoil generator already available in XFLR5, or by importing from the internet. Figure 3.10, shows what the module looks like and how it should look like with an airfoil defined in it. To use non-NACA airfoils, we need to import the airfoil's DAT file which are readily available on websites all over the internet such as Airfoil Tools and BigFoil.

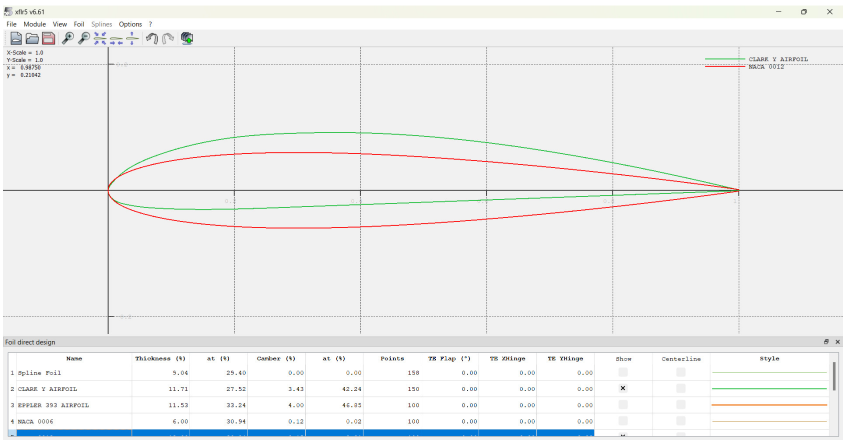

FIGURE 3.10: XFLR5 Airfoil Generator

After defining the airfoils, the next step is to analyze them in the "XFoil direct analysis" module. Shown in Figure 3.11 To save time, it is advised to use the

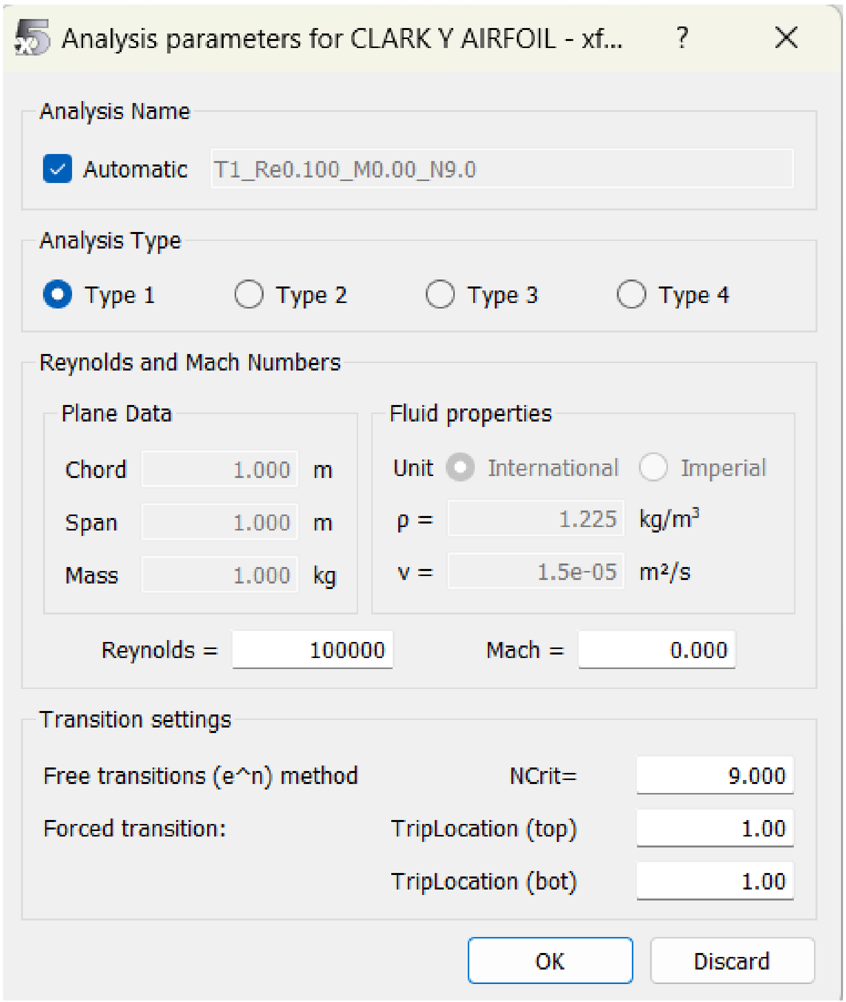

FIGURE 3.11: XFLR5 Direct Foil Analysis

batch analysis feature as it is able to conduct the needed analysis on a variety of values of Reynolds numbers at one time.

Next, to actually make the wing and tail, we need to complete the design. To accomplish this, we need to define certain measurements such as the chord lengths, wing span, dihedral angle (if any) and sweep distance between points. The design process can be seen in Figures 3.13, and 3.14. However, it has to be said that there is limited support for unconventional empennage configurations, and so with that in mind, the X tail configuration uses both elevators and double fins at a dihedral angle of -45 and 45 degrees, respectively. (As seen in Figure 3.14)

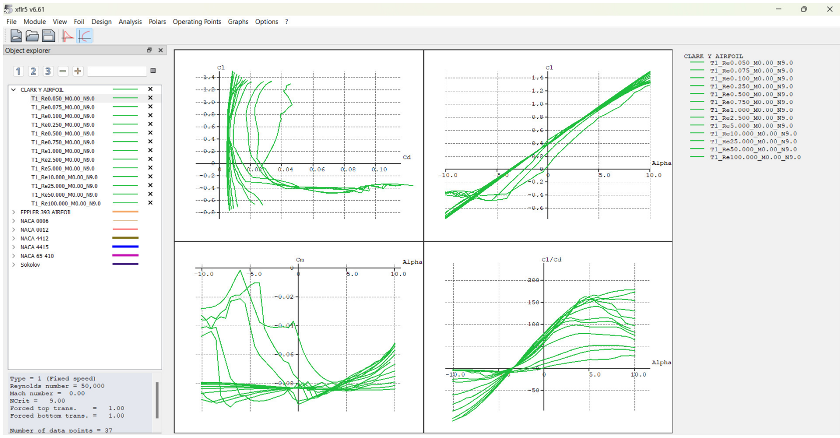

FIGURE 3.12: XFLR5 Direct Foil Analysis Module

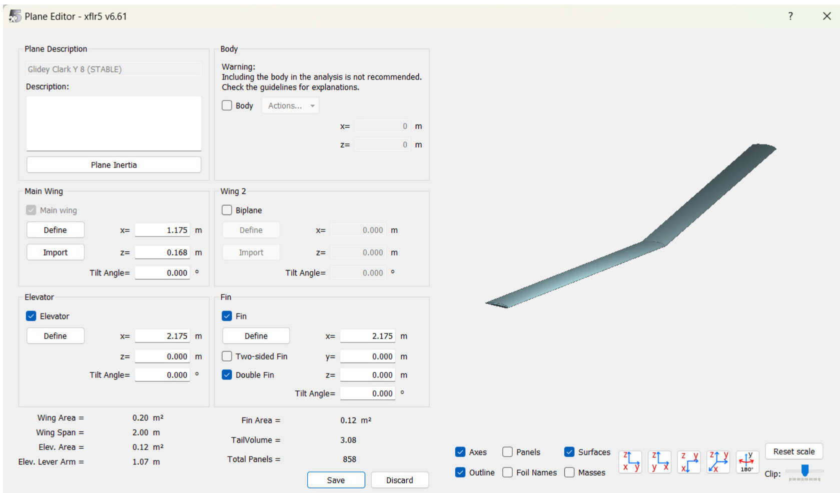

FIGURE 3.13: XFLR5 Wing Generator

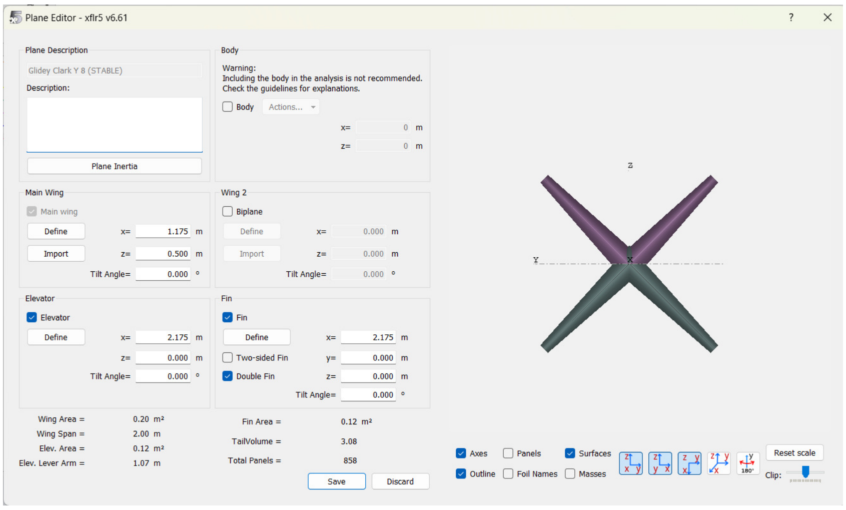

FIGURE 3.14: XFLR5 Tailfin Generator

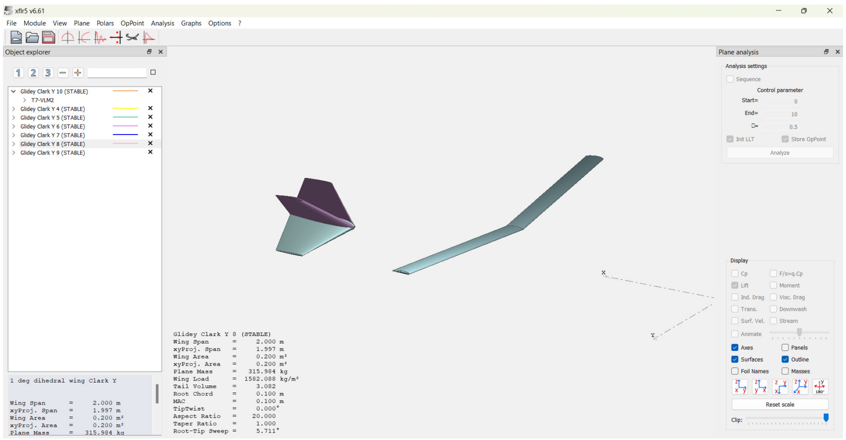

FIGURE 3.15: XFLR5 Plane Generator

3.6.3 Mass and Inertia Input

Now, as mentioned previously, the weight is crucial in an aircraft as it helps in defining its stability. Here, we will look into the stability analysis of the glider. In XFLR5, the masses are split into 5 sections, the main wing, secondary wing, elevator, fin and body, as seen in Figure 3.16. However, XFLR5 does not recommend the inputting of the body mass as it would require putting a fuselage shape into the analysis. Instead, as a substitute, a mass point will be added to represent the 500 lb bomb. The reason for not including a bomb shape/body into XFLR5 is that, if a fuselage/body were to be added into the analysis, it may result in inaccurate readings as it is an inherent limitation of the software. Same as the bomb, subsystems and component weights will be added as point masses.

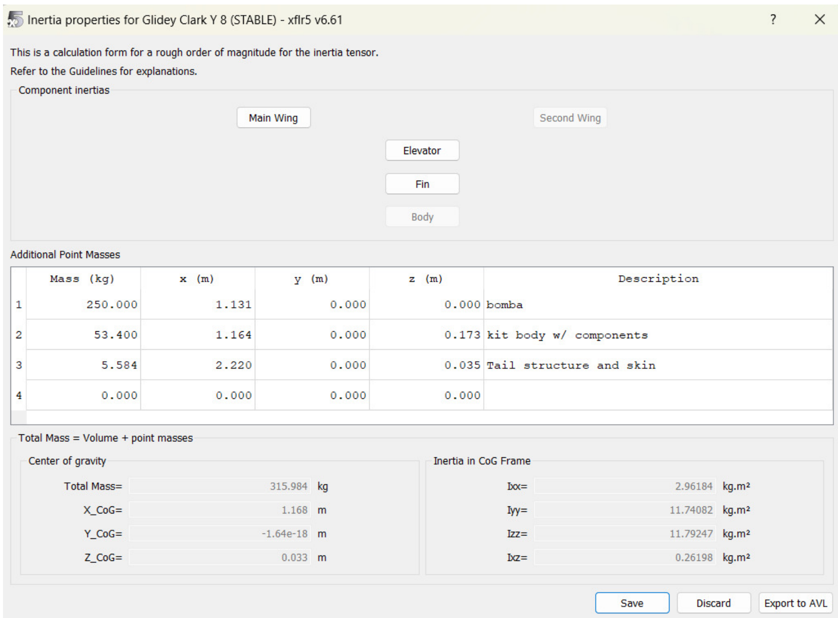

FIGURE 3.16: XFLR5 Mass Inertia

3.7 Structural Design: Wing

Before beginning this design phase, we must obtain data from aerodynamic analysis and comparisons on other kit examples to find the ideal measurements of the wing. Here, we require certain data such as the root chord, tip chord, dihedral angle, sweep distance and wing span, along with what airfoil will be used on the root and tip (only if it is assumed that there will be two different airfoils used on the wing). After obtaining all numbers, we are able to design a wing. The reason why we need the numbers first is to mainly get an aerodynamic profile and the dimensions of the wing, because this will directly affect the design process along the line. After a shape has been defined and finalized, we move to the 3D CAD Software to actually make the wing.

Using Onshape, a cloud-based 3D design software, we are able to accurately make the wing, as well as its structures and substructures. Once completed, we are able to get the weights of every component in, on and around the wing (if any) after applying the type of material to each part. This step is crucial as it will provide an overview of the weights that the wing itself will weigh and how much it will add to the final product. It will also help determine the performance characteristics of the gliding craft. I do have to point out the importance of material selection, because the material needs to be robust and strong to withstand the strain and stress of aerodynamic forces, but also light enough to not add unnecessary weight to the glide bomb.

3.8 Structural Design: Fuselage

After designing the wing, we continue to design its kit body/fuselage. However, prior to continuing the design of the fuselage/wing kit body, we need to consider numerous factors, including:

- Storage space for the wing
- Stowage space for avionic components
- Smooth shape that does not disrupt the aerodynamics of the warhead
- Provisions to attach the bomb to the aircraft

With taking all 4 into consideration, we then look at rival or similar designs that are already in operation and used in warfare by other nations. Here, we can get hints of inspiration on how to stow the wing, how to attach the kit to the munition, as well as how the configuration would be attached onto the bombing aircraft. We then get to see and analyze how the avionic components are laid out on/in the kit and how it is balanced with respect to the weight of the warhead and the tail. This step is known as initial sizing and is crucial at figuring out the potential dimensions and scale of certain structural parts and components, as well as gives a solid baseline for the following design stages.

Once the initial stage is complete, focus shifts to sketching out the design itself. Using Onshape again, we will use it to help provide a dynamic platform to design and develop concepts. This shape is important as it is the most efficient means to turn theory into real design schematics. With this, it allows me to give a more accurate representation of my ideas and illustrate a complete design/product. Once sketching is done, we assign materials to the parts and obtain the weights of said parts. This part is particularly important as it serves a reference point to how the munition will be balanced at the end, and balance is important during gliding flight as there is no propulsion system, hence why stability is a critical aspect in, not only gliding, but in flight as a whole.

3.9 Structural Design: Tail/Fins

After designing the glide kit's wing and body, we proceed to focus on the tail section. This area is critical to aid in correcting the gliding bombs trajectory, glide path and rear-end instability while in glide. Since the warhead/bomb itself is a fixed design and the tail section of the bomb itself is removable, there is some freedom to choose the configuration as well as what layout is able to be used for optimal stability and control. After analysis on XFLR5, 3 main configurations have been identified, analyzed and found to be the most stable.

- X-Tail (As seen in Figure 3.17)
- Inverted Y-Tail (As seen in Figure 3.18)
- Ring Tail (As seen in Figure 3.19)

It is important to note that all tail configurations are attached onto the warhead itself and are not directly connected to the wing kit.

The work done on XFLR5 helps in defining the fundamental requirements for the aerodynamic profile of the tail. Next, we design the tail using the help of Onshape yet again. Once the most ideal configuration has been chosen, the design

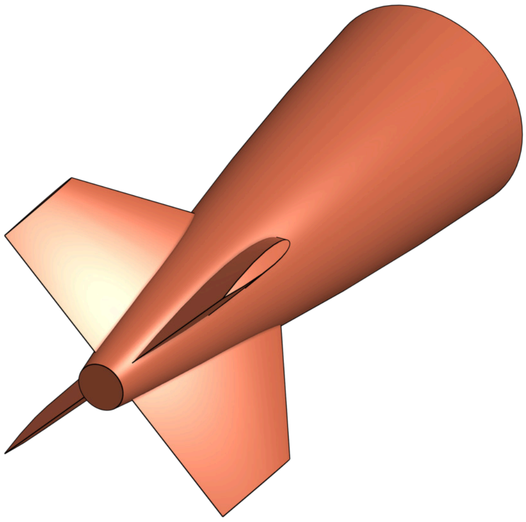

FIGURE 3.17: X-Tail

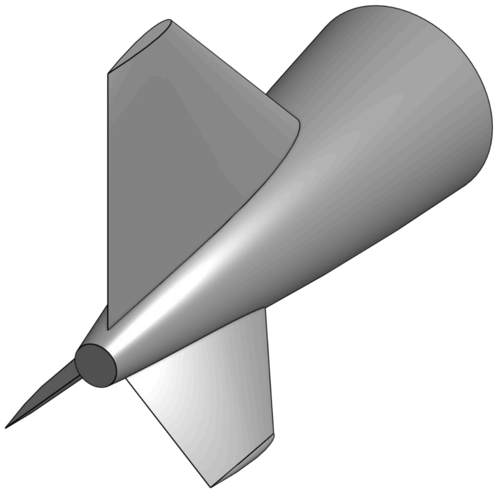

FIGURE 3.18: Inverted Y-tail

nears its end with the final sketches being made. This is an important step as it provides the end users a clear visual representation of what the concept(s) look like. The final part of the tail designing process is selecting the most appropriate material and constructing the frame of the tail. As previously mentioned, this is a critical part of the design as it defines not only the weight, but also the strength of the part. Ideally, the structure must be lightweight and durable.

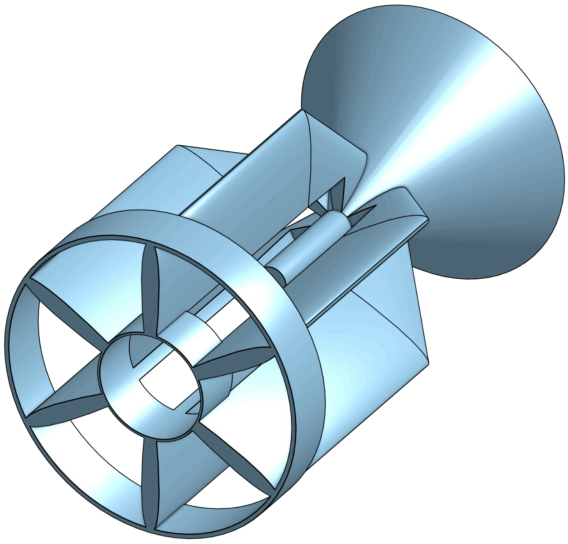

FIGURE 3.19: Ring Tail

3.10 Structural Assembly

As the project nears its completion, we move to the last but certainly not least phase, which is the assembly. This part will involve all designed parts and components mentioned above and previously. This time, we move away from the sketchpad and move to the assembly station. This area has to be carried out with the utmost precision. This is because the assembly will define the entire project as a whole and what end product we can present as a result.

The assembly of the structural components will make up the aircraft's structure, which will serve as base construction for everything else that will be put on and/or in. Once completed, the integration of avionics systems must be carried out due to it being an important part of the aircraft's system architecture and the means for it to carry out its missions. These systems need to be arranged in a careful and pre planned manner, in order to not disrupt the balance of the aircraft during flight. This is due to the importance of the location of an aircraft's Center of Gravity, hence why Weight distribution is crucial to any aircraft design. These avionic components must also, not interfere with the main structure of the aircraft in any way. This is to ensure structural stability throughout its mission.

After installation of avionics and assembly of structural components are complete, the project can finally see the light at the end of the tunnel and move into final stages, which is the phase of analysis. With all components and structures already assembled and weights defined, we can get a proper evaluation of the potential performance that can be expected in the field. These include gliding range, gliding endurance, airspeed while in glide and payload capacity.

3.11 Final Concept Options

After much deliberation, 3 concepts were drawn up and their visual representations are explained below. Although they are different in one way or another, they all share some of the same factors, such as:

- Wing configuration: High Wing
- Warhead: Mark 82
- Wingspan: $2.0\,\mathrm{m}$
- Chord length: $0.15\,\mathrm{m}$
- Dihedral angle: $3\,\mathrm{deg}$
- Sweep angle: $6.45\,\mathrm{deg}$
- Primary Control Surfaces: Elevator + Aileron (Elevon)
- Stability: Laterally and Longitudinally stable

3.11.1 High Wing, X-Tail

The first concept is very much a 'standard' among competitors and, at first glance, seems similar to the JDAM-ER model, however it is not the same technical wise. While the JDAM-ER utilizes a control surface-less wing and solely relies on the JDAM tail-fin module to adjust its heading and trajectory. This concept utilizes a fixed fin and a wing that uses a 2-in-1 control surface known as the elevon, which is a combination of elevators and ailerons.

The lack of a moving tail section will reduce the amount of weight that is put onto the tail cone and aids in the positioning of the center of gravity. The concept is very straightforward and has been utilized by many other competitors such as the South Korean KGGB and Russian UMPK.

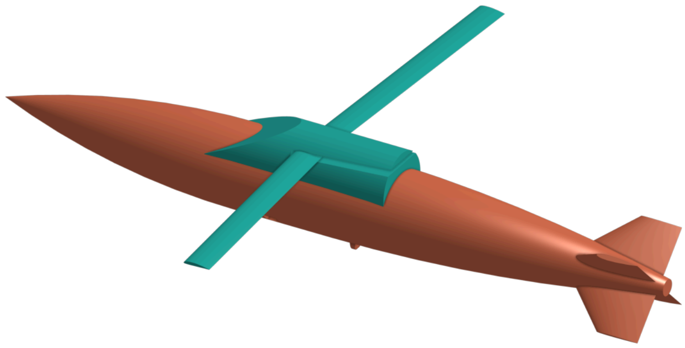

FIGURE 3.20: High Wing, X-Tail configuration

The high wing configuration offers many advantages compared to other configurations such as the low or mid-mounted wing. It allows for the bomb to be positioned low and below the wing, and allows for a lighter structure of the clamp around the bomb. I previously mentioned the center of gravity position and with the wing being above the center of gravity, it allows for better control of the glider. There is also an inherent increased dihedral effect (C_{l_β}) that makes the aircraft much more stable laterally. This is due to the higher contribution of the fuselage, or in this case payload, to the wing's dihedral effect ($C_{l_{\beta W}}$). The wing will also produce much more lift compared to its counterparts and allow for the glider to have a much lower stall speed since the value of ($C_{l_{\max}}$) will be higher. The drag of the wing will also produce a natural nose-pitching-up moment that makes it destabilize in the longitudinal plane. This effect is due to the wing's drag line being in a higher position relative to the center of gravity of the aircraft, or in mathematical terms, $M_{D_{cg}} > 0$ [49].

The tail, in our case, does not move and is stable throughout its glide. The tail is designed to keep the bomb stable during its drop. Those same principles are used here, but in a gliding medium rather than straight down. The X-tail will keep the aircraft directionally stable.

A disadvantage of this configuration is that the aircraft will have to utilize rolling and pitch alterations to change directions, since there is an obvious lack of a direction altering device, such as a rudder.

3.11.2 High Wing, Inverted Y-Tail

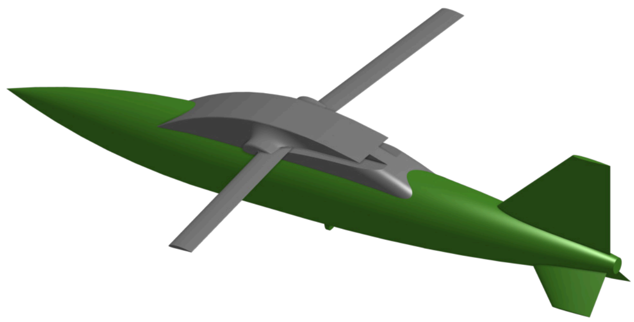

FIGURE 3.21: High Wing, Inverted Y-Tail configuration

In this version, the wing configuration and position is similar to the previous one, but instead of a standard X-tail, an inverted Y-tail is used. It will have the same properties as a conventional Y-tail configuration, just placed upside down. The reason for the flip is to accommodate for the loading of the munition onto the aircraft.

In this configuration, a complete set of primary control surfaces are included, but in an attempt to shed some weight, elevons will be re-utilized and a rudder will be added on the center fin. This will allow the glider to change direction much more efficiently and accurately depending on its target location. The extra fin, or rudder per say, reduces the amount of contribution of the tail towards the dihedral effect and is a much less complicated configuration when compared to other configurations such as the X- or V-tail.

3.11.3 High Oblique-Style Wing, X-Tail

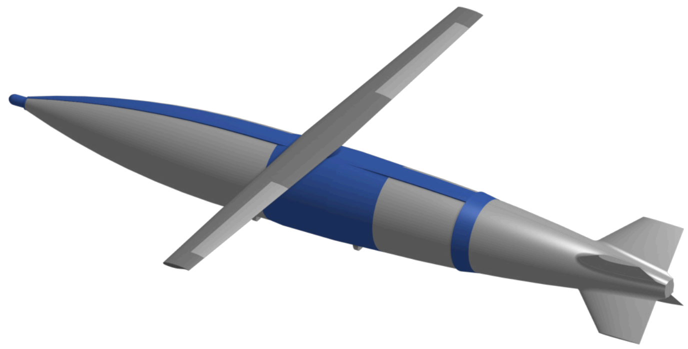

FIGURE 3.22: High Oblique-style Wing, X-Tail configuration

In this version, the tail will be the same as the first version, with the most significant difference being the tail cone requiring some added reinforcement as it will house all avionic components because the wing is in the style of an Oblique wing. The oblique wing is special as it does not require a housing for storage and instead relies on a change in orientation from a center circular roller. Its storage is in the Oblique wing style but the munition will not be flown as an oblique wing. It will also feature elevons and must work in conjunction with the navigational systems of the glide bomb.

3.11.4 Fully Integrated Winged Explosive Munition

For this concept, it covers every eventuality in terms of aerodynamics and loss in that part is deemed unacceptable. So the entire explosives part is fully customized to the wing profile of the glide kit.

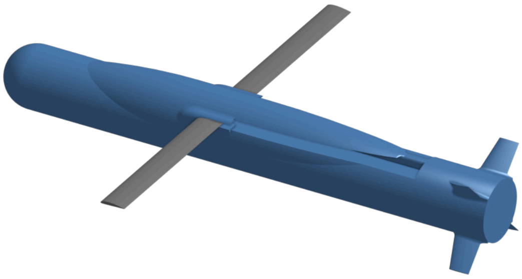

FIGURE 3.23: Fully Integrated Winged Explosive Munition V1

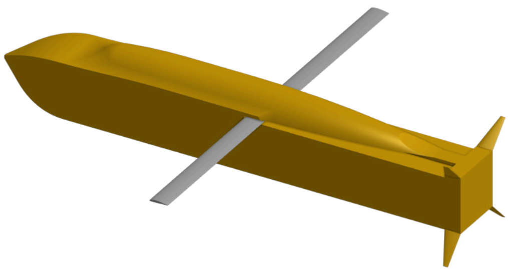

FIGURE 3.24: Fully Integrated Winged Explosive Munition V2

CHAPTER 4
RESULTS AND DISCUSSIONS

4.1 Benchmark Study

Prior to starting the process of design, benchmarking needed to be carried out in order to get a picture of how we want the final result to begin to look like. This specific study included examinations and comparisons to many glide bomb kits and gliding bombs from various nations, competitors and weight classes. In total, I conducted an assessment based on investigating 11 other gliding bombs and glide bomb kits, all of which are listed at the end of Chapter 2. Also observed, were the type/brand of bomb that is owned by the Indonesian Air Force and their suitability to be given a Wing Kit. I also made comparisons between the owned munitions and the type(s) used in/on current gliding bombs. What was discovered is that the best base profile to design the glide Kit off of is the Mark 82 unguided bomb, which sees usage in 5 other nation's gliding bombs. Also found was that, the design of a glide bomb kit was a much more economical option, rather than to make an all new gliding bomb from scratch. It would offer the best price-to-performance in terms of range and probability to hit its target more accurately. As a reference point, two glide bomb kits have been chosen as a standard benchmark, first being the American and Australian-collaboration project of the JDAM-ER, and the Russian UMPK kit, which utilizes the Mark 82 and FAB-500 bomb, respectively. Both types of Unguided bombs are owned by the Indonesian Air Force and are highly destructive. The comparison is shown in Table 4.1 . These two have been chosen for their impressive performance characteristics and were key subjects in the compilation of this project.

2 concepts have been produced and both will be compared. The final choice

Name	UMPK (Fig 2.17)	JDAM-ER (Fig 2.13)
Country of origin	Russia	United States and Australia
In operation?	Yes	Yes
Bomb name	FAB-500	Mark 82
Payload mass	500 kg	227 kg
Length	2.47 m	2.21 m
Wingspan	2.32 m	1.767 m
Guidance system	Integrated INS/GPS	Integrated INS/GLONASS/GPS
Gliding range	70 km	72.4 km

TABLE 4.1: JDAM-ER and UMPK Comparison table

of which concept is more ideal will be based on its gliding performance, aerodynamic analysis and stability. The two concepts will have some similarities where they will share/utilize the same COTS components, using the same bomb, aircraft list it will travel on, structure thickness and mission profile. Other areas mentioned here will differ from each other.

The 2 concepts will be designated as **AA1** and **AA2**.

4.2 Mission Profile

The glide bomb's mission is simple, deliver destruction from a distance. The mission profile of the proposed glide bomb kit has been determined after a thorough benchmarking assessment, along with a comparison with the Russian UMPK and American and Australian JDAM-ER. The comparisons and assessments helped in shaping the needs of the glide bomb and its mission profile. As shown in Figure 4.2, we can see what a typical mission of the munition would look like, and its significance with being dubbed a Fire-and-forget and/or Stand-Off Weapon.

Although the main purpose of the glide Kit is to aid in enhancing the range capabilities of a dumb bomb, a plan may be drawn up for it to be used to transport aid, such as medical supplies and food, to areas of conflict by replacing the warhead with an empty shell that is tough and is able to be opened and used to store supplies. This mission is limited to the amount of supplies that can be carried, which altogether would weigh the same as if the payload was a Warhead.

Altitude (Dropping)	H = 35000 ft / 10700 m (ASL)	
Wingspan	2 m	
V∞	450 knots or 231.5 m/s	
	AA1	AA2
Gross Mass (kg)	235.3	236.8
Chord length (m)	0.15	0.1
Aspect Ratio (AR)	13.333	20
Wing Area (m2)	0.3	0.2
CD0	0.00723	0.00801
CL/CD max	40.28	49.12
Minimum Glide Angle (degree)	1.42	1.17
Range (km)	431.65	523.91
Endurance (min)	167	202
V max (m/s)	1358.69	1580.96

FIGURE 4.1: Table of Performance Characteristics

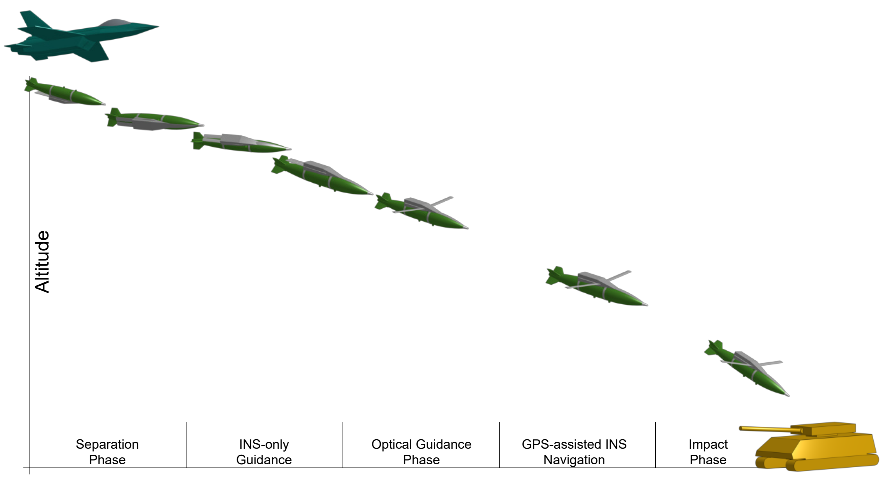

FIGURE 4.2: Mission Profile

4.3 Avionics Component Selection

4.3.1 Final Selection

When we are speaking on the component selection of a gliding bomb, it is crucial to look at what components will make up the systems that are moving and/or doing most of the heavy lifting. It is because this aircraft is, in itself, simple. As it consists of a wing kit, a standard-issue tail, and a bomb. The wing kit houses the wing and all other components that will be mentioned below, minus the bomb due to the fact that the wing kit will be attached via a clamp. The following shows the results of the component selection process and shows the ideal parts that will aid in the performance of the gliding bomb.

Part	Subpart	Part name
Guidance system	INS/GPS module	Inertial Labs INS-DM-N11
Control system	Wing actuators	Moog Electro-Mechanical Actuators
Targeting system	Optical Seeker module	Wescam MX-Series EO/IR Sensor
Power source	Power supply system	Tadiran Batteries TLM-1550ESM
Communications	Data link system	Harris Corp. MIDS-LVT
Payload	Explosive munition	General Dynamics Mark 82

TABLE 4.2: Table of Chosen components

4.3.2 Commercial-Off-The-Shelf components

One important part of this conceptual study is to use as many Commercially available and Off-The-Shelf components, or COTS, as possible. This is due to the extremely secretive nature of customized components, built for the sole purpose of rival munitions. Luckily, some manufacturers disclose/make public the fact that their products are used in rivaling gliding munition systems. They also, openly, share the specification information as well as alert others that their product is a COTS component and is open to public sale.

Subpart	Manufacturer	Product Designation
INS/GPS module	Inertial Labs	INS-DM-N11
Wing actuators	Moog Inc.	Electro-Mechanical Actuators
Optical seeker module	L3Harris	Wescam MX-Series EO/IR Sensor
Power supply system	Tadiran Batteries	TLM-1550ESM
Data linkage system	Harris Corp.	MIDS-LVT
Bomb	General Dynamics	Mark 82

TABLE 4.3: Table of chosen COTS components

4.3.3 Bomb selection

As mentioned in the previous subchapter, the Mark 82 bomb by General Dynamics 3.7 has been chosen for its reliable track record and compatibility to many aircraft that are both openly operated in many air forces around the world. This compatibility makes the final product available for many other armed forces who are looking to strengthen their armory with a gliding bomb.

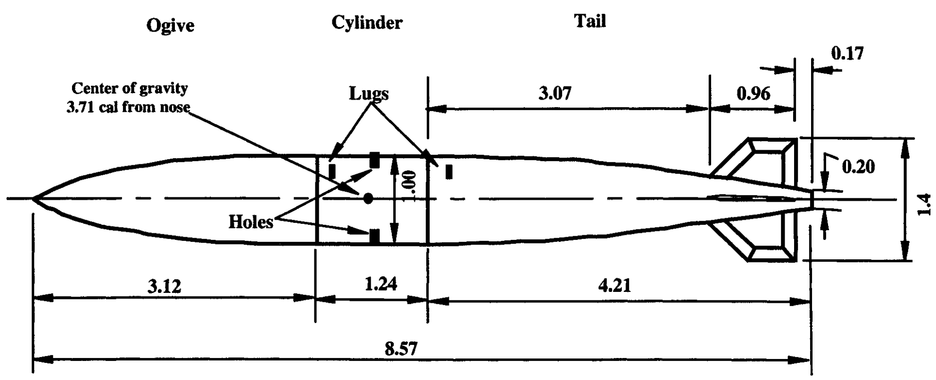

FIGURE 4.3: Mark 82 dimensions in Inches [50]

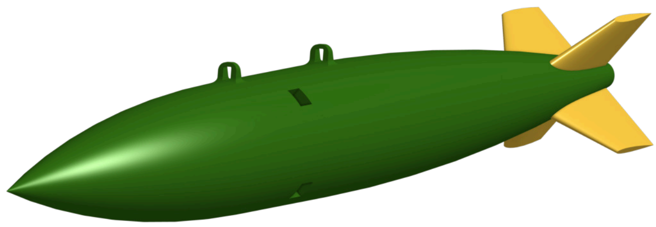

FIGURE 4.4: Mark 82 remodeled on Onshape

4.4 V-n Diagram

The V-n diagram, otherwise known as the structural envelope, is the graphical representation that relates to the specific load factors to the airspeed at which the aircraft has been designed to operate. The diagram is typically created by the loads and group of structures and is present for two purposes. First, it provides a definition on the aircraft's operating limits while also providing crucial data on the structure itself. Finally, it provides information on critical operation boundaries for operators/users. This gives the users important information on the aircraft's limits and performance characteristics. The diagram also shows key constraints on factors, such as airspeed. One such constraint may be the maximum operating velocity when control surfaces are fully deployed/deflecting (V_A). Another constraint may be the speed of dive (V_D), which should not exceed a maximum number when in operation. This diagram also plays an important role in ensuring the integrity of the structure of the aircraft as well as to ensure that its mission is completed successfully.

Prior to making one, it is necessary to collect certain specific parameters that will be used for the calculations. These numbers are obtainable from analysis on software such as XFLR5, and the list of such parameters are listed below in

Table 4.4

Parameters	AA1	AA2
Gross weight	235.3 kg	236.8 kg
Wing area	$0.3\,m^2$	$0.2\,m^2$
Air density	$1.225\,kg\,m^{-3}$	$1.225\,kg\,m^{-3}$
$C_{L_{max}}$	1.557 37	1.518 59
$C_{L_{min}}$	-0.697 95	-0.806 29
C_{L_α}	$0.093\,81\ deg^{-1}$	$0.097\,40\ deg^{-1}$
Stall speed	174.58 kts	217.23 kts
c_{mgc}	0.15 m	0.10 m
Cruising speed	450 kts	450 kts
Gust velocity	50 ft/s	50 ft/s

TABLE 4.4: Table of Parameters

Once we obtain the needed data, we can formulate the V-n diagram. The result of which is acquired after imputing the numbers from Table 4.5 into the Spreadsheet provided by Abbott Aerospace. This makes it easier to produce the diagram more accurately. Since we are working with two concepts, we have two separate V-n Diagrams below in Figures 4.5 and 4.6.

Parameters	AA1	AA2
Positive Load Factor	+3.80	-3.80
Negative Load Factor	-1.52	-1.52
Minimum Cruising Speed ($V_{C_{min}}$)	418.25kts	514.31kts
Diving Speed (V_D)	>585.55kts	>720.03kts
Maneuvering Speed ($+V_A$)	+340.32kts	+423.46kts
Negative Maneuvering Speed ($-V_A$)	-340.32kts	-423.46kts
Positive Gust Load Factor	+2.214	+2.214
Negative Gust Load Factor	-0.214	-0.214

TABLE 4.5: V-n Diagram Results

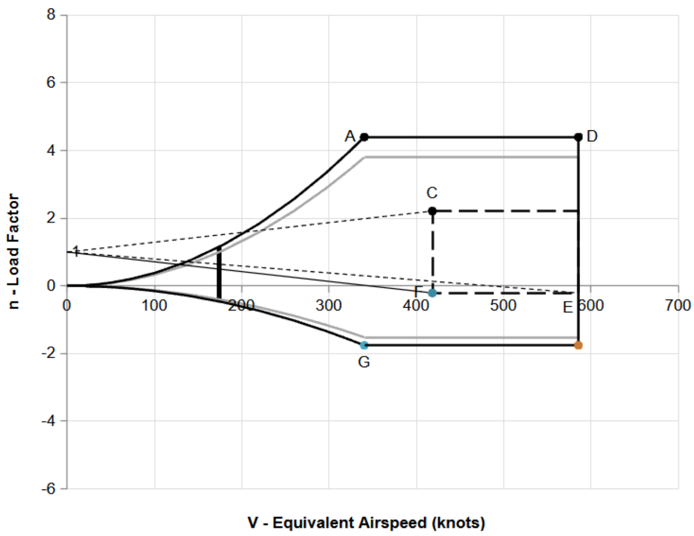

FIGURE 4.5: Vn Diagram of AA1 Concept

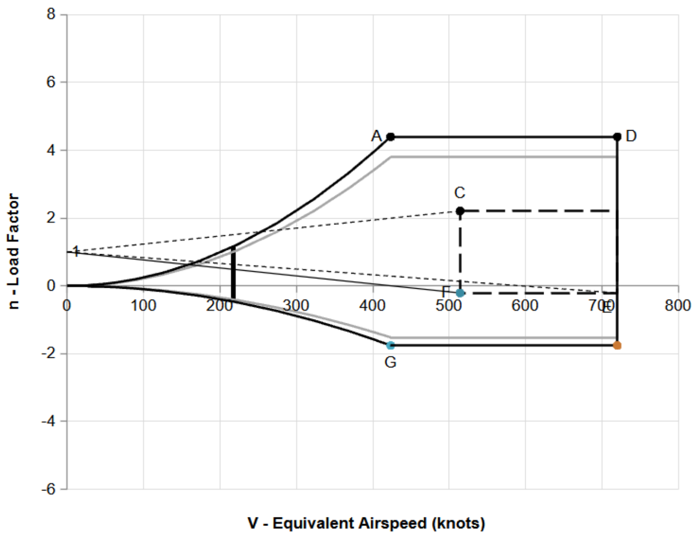

FIGURE 4.6: Vn Diagram of AA2 Concept

4.5 Aerodynamic Analysis

4.5.1 Configuration Selection

From the very beginning, the design of the wing kit has been limited due to the desire to produce a wing kit that is highly effective, yet cheap to produce.

So, the first limitation is to use presently-owned munitions rather than make a new one with better aerodynamic integration. The second limitation was in the configuration and location of the wing. Since the bomb is a very streamline device, the wing has to have a small chord length and we are stuck with a high wing configuration, due to packaging constraints of the wing kit on the bomb itself.

The only variety that can be made is by using different types of tails and even a radical concept for wing storage. The three possible options were using an X-tail, inverted Y-tail and an Oblique wing. The three configurations can be seen in figures 3.20 3.21 and 3.22. However, due to results from stability analysis and as an attempt to reduce complexity within the design, the **X-tail** is utilized and paired with the **High wing** configuration.

4.5.2 Body

After much deliberation as well as analysis on rival gliding bomb kits and components sizing, it was found that a box-shape body was found to be the most suitable option for the wing kit. It is compact, not too large, able to fit all components and wings without much drag generating. The body structure of both AA1 and AA2 can be seen in Figures 4.7 and 4.8. Those Figures show the main structural configuration of the Wing Kit that would be attached onto the munition.

4.5.3 Airfoil

Since this project is a gliding aircraft, the main requirement of the airfoil is to possess a high value of $\frac{C_L}{C_D}$. Some airfoils that have been used, analyzed, and compared include:

- Clark Y
- Sokolov
- Eppler 393
- NACA4412
- and, NACA4415

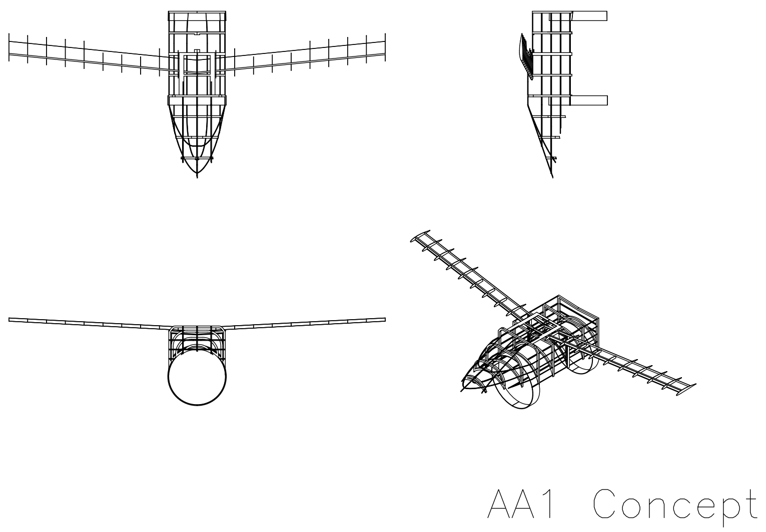

FIGURE 4.7: AA1 Wing Kit Body design

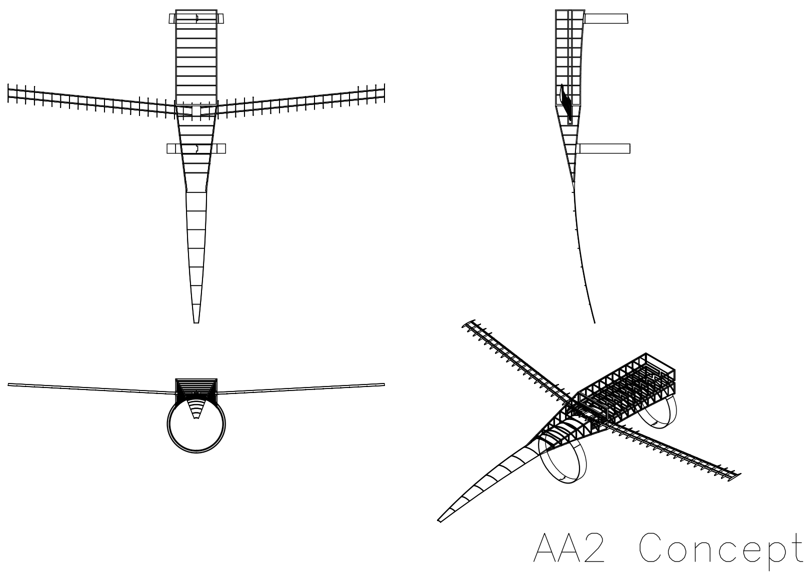

FIGURE 4.8: AA2 Wing Kit Body design

Each airfoil has been analyzed for its aerodynamic performance and those results have been generated using XFOIL at the conditions:

- Reynolds number = 10^6, and
- Mach number = 0.0

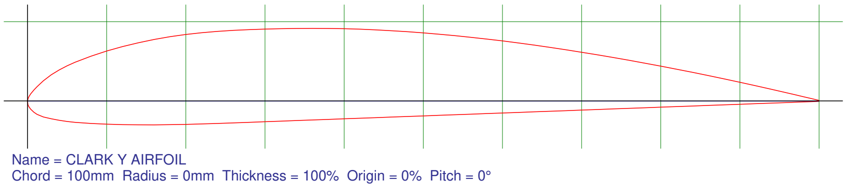

FIGURE 4.9: Clark Y Airfoil [51]

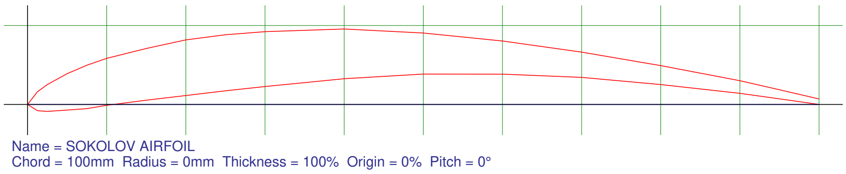

FIGURE 4.10: Sokolov Airfoil [54]

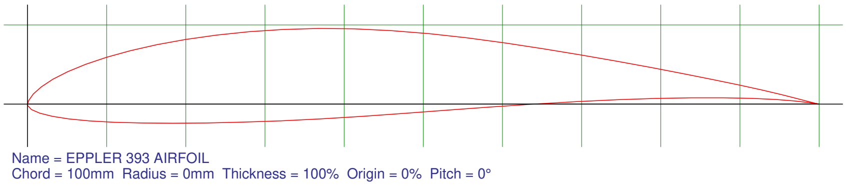

FIGURE 4.11: Eppler 393 Airfoil [52]

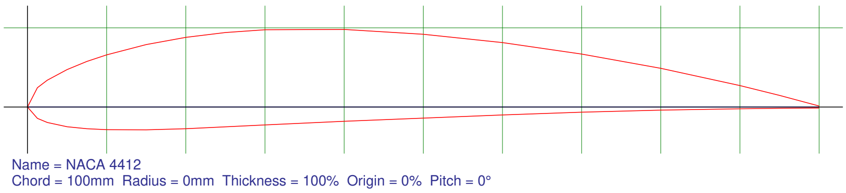

FIGURE 4.12: NACA 4412 Airfoil **4412**

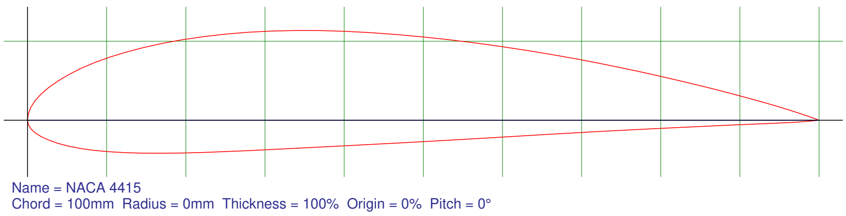

FIGURE 4.13: NACA 4415 Airfoil **4415**

In order to choose the best fitting airfoil, we must look at glider aircraft in general and look into what airfoils are used in their wings. From the results, two airfoils stood out, that being the Clark Y and Sokolov. Afterwards, the main factor of glider appropriate airfoils were look into, which was the high degree of

$\frac{C_L}{C_D}$. Several other airfoil, not particularly mentioned of in glider use, came up and those were the Eppler 393, NACA4412 and NACA4415. As a result, we now have the 5 airfoils, previously mentioned above.

Airfoil	NACA 4412	NACA 4415	Sokolov	Eppler 393	Clark Y
$C_{L_{\text{max}}}$	1.45	1.45	1.51	1.41	1.39
$C_{D_{\text{max}}}$	0.072	0.070	0.077	0.069	0.068
$(C_L/C_D)_{\text{max}}$	20.16	20.60	19.54	20.38	20.34
$(C_L/C_D)_{\text{max}}$ rank	4th	1st	5th	2nd	3rd
Laterally stable?	Yes	Yes	No	No	Yes
Longitudinally stable?	Yes	Yes	Yes	Yes	Yes
Overall rank	3rd	2nd	5th	4th	1st

TABLE 4.6: Airfoil comparison table in planned configuration

Afterwards, each airfoil was analyzed in the planned configuration of the wing and tail. The results of which are show in Table 4.6 were compared and the airfoil with the best characteristics was chosen. After analysis, the **Clark Y** airfoil was found to be the best choice for the gliding aircraft's wing. This can be seen in the data shown for the airfoil on both versions AA1 and AA2, as seen on Figure 4.14.

This comparison has resulted in the best airfoil for the gliding aircraft and has aided in the decision making process to make it much more smooth and streamlined.

4.5.4 Wing

The gliding bomb's wing has been designed on the basis of a benchmarking study against rival designs of glide bombs. The decision to go for a taper ratio of 1 from Table 4.7. was done for the ease of storage inside the wing body kit itself. The wing has also been given a dihedral angle of $3\deg$ in order to aid in stability. Another factor added to aid in stabilizing the glider is by the addition of a sweep on the wing. The wingtip has been swept back as much as 0.1 meters. or about as much as the chord.

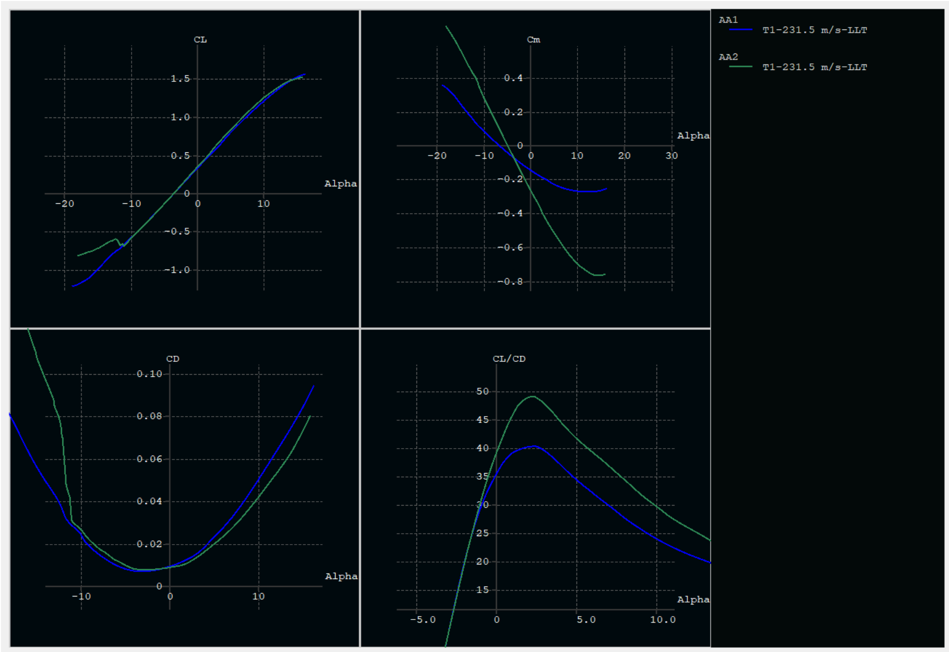

FIGURE 4.14: Aerodynamic data of Clark Y-winged aircraft

Parameters	AA1	AA2
Wing area	$0.3\,m^2$	$0.2\,m^2$
Aspect ratio	13.34	20
Wing span	2 m	2 m
Taper ratio	1	1
Chord length	0.15 m	0.1 m
Wing incidence angle	0 deg	0 deg
Dihedral angle	3 deg	3 deg
Geometric washout	0 deg	0 deg

TABLE 4.7: Wing Parameters

4.5.5 Tail

As previously mentioned, the tail section had numerous options in terms of configuration. A X-tail, an inverted Y-tail, a V-tail and even a Ring tail were drawn up. But the two configurations that were most feasible were the X-tail and inverted Y-tail. The X-tail being the more favored option as the standard unguided Mark 82 had already come with a X-tail and that would keep the bomb at its already factory-stable condition. However, its use would only be feasible if the configuration would be found to work in unison with the wing and would result in a stable gliding flight. The inverted Y-tail is the total outside design. Unlike the traditional tri-fin configuration, a single fin would be much larger than the other 2 and act as an empennage that resembles more to an aircraft vertical stabilizer. The reason why it would be inverted is due to the mounting constraints of the aircraft carrying the bomb. The tall single stabilizer would hit the aircraft's wing and damage it. The inverted tail would avoid this issue of the bomb mounting and allow the flight to fly smoothly.

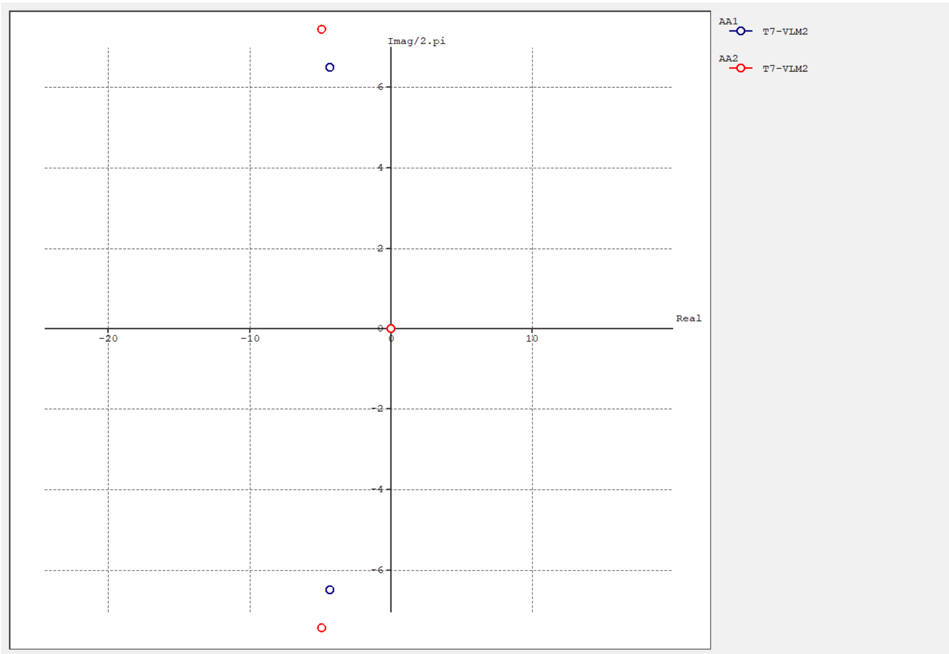

FIGURE 4.15: Lateral Stability Analysis results

To determine whether or not the configuration is stable or not, it is important to remember that the general rule for stability analysis results is that the configuration in question is deemed stable if all its points on the plot above, which consists of the resulting eigenvalues' real value on the X-axis and it's imaginary value on the Y-axis, are on the left-hand side, or in other words, possess a negative real value. The further to the left the plot is, the better it's stability. Both concepts, at their clean configurations, are stable as proven by their plots seen on Figures 4.15 and 4.16, as well as from their eigenvalues that can be seen in Appendix B.

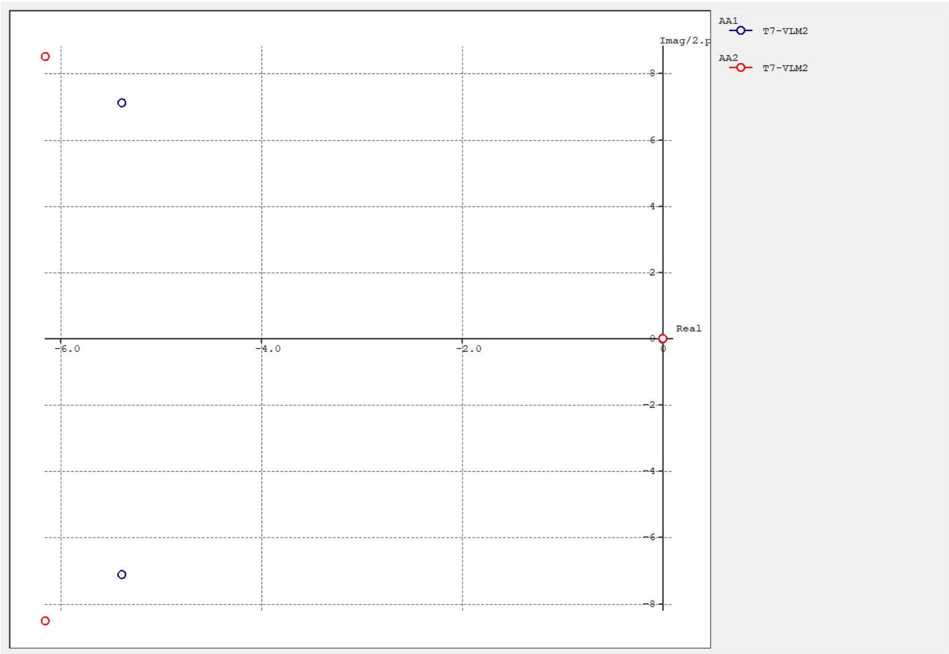

FIGURE 4.16: Longitudinal Stability Analysis results

From there we are able to see all four natural modes for the longitudinal as well as the lateral mode on the graphs. With the longitudinal mode featuring 2 symmetric phugoid modes as well as 2 symmetric short period modes. While the lateral mode features 2 Dutch roll modes, 1 spiral mode and 1 roll damping mode.

The results of the eigenvalues for the phugoid of AA1 and AA2 respectively, came to $-0.00024+0.05421i$ at a frequency of $0.009\,\mathrm{Hz}$ and damping of 0.004, and $-0.000016+0.04721i$ at a frequency of $0.008\,\mathrm{Hz}$ and damping of 0.003. Where as the results of the Dutch roll eigenvalues for AA1 and AA2 respectively, resulted to $-4.52528+40.6990i$ at a frequency of $6.517\,\mathrm{Hz}$ and damping of 0.111, and $-5.18703+46.64610i$ at a frequency of $7.470\,\mathrm{Hz}$ and damping of 0.111.

4.6 Structure Design: Kit Body/Fuselage

Since this is a precision guidance kit that is attached to an unguided munition, it will require space to store the components and wings when loaded onto the aircraft. So it was crucial in the design process, to keep in mind the size and design of the wing kit body and its structure. By organizing the avionics, we are able to potentially avoid potential conflicts in space between equipment, wing and structure. As a result, the final design has ensured the integrity of both avionics and body.

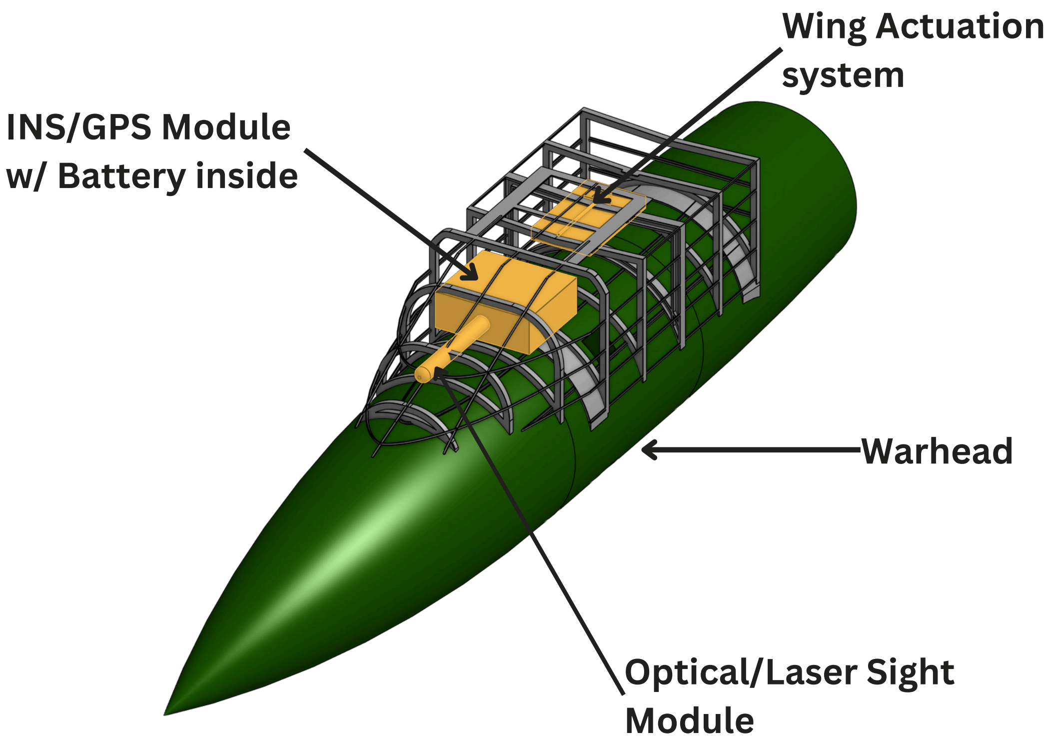

FIGURE 4.17: Line up of Avionic Components for AA1 concept

Figures 4.17 and 4.18 shows the placement of all equipment within the body structure.

It can be seen that there is space within the tail structure but is left unused. This was purposefully done in order to augment the weight of the gliding munition.

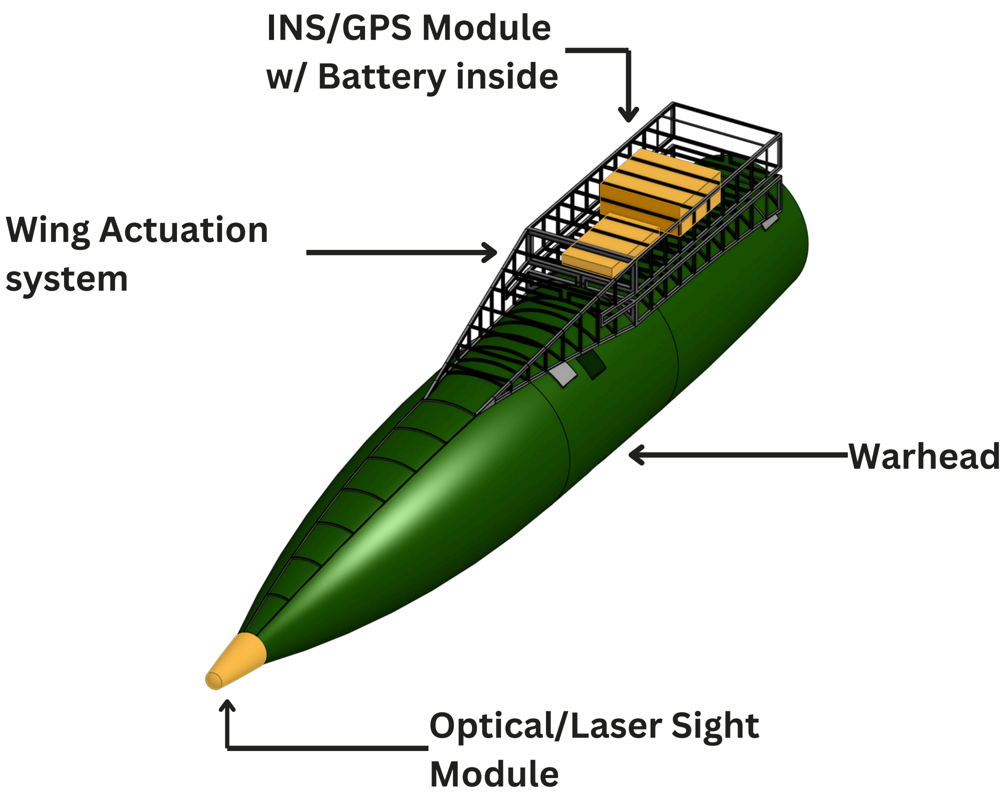

FIGURE 4.18: Line up of Avionic Components for AA2 concept

Once all components have been properly installed, the next phase is to obtain data for the external shape of the wing kit itself. This is an important step in order to minimize aerodynamic efficiency loss and to also reduce potential drag that would greatly affect the performance of the glider.

Prior to sketching, starting with initial sizing is necessary in order to get the design dimensions of the frame. After obtaining the results, we can begin sketching out the frame design using Onshape CAD software. The size of each frame is shown in Table 4.8.

Type	Width	Thickness	Depth
I-beam (Fig 4.19)	0.015 m	0.003 m	0.015 m
C-beam (Fig 4.20)	0.01 m	0.002 m	0.01 m

TABLE 4.8: Frame cross-section dimensions

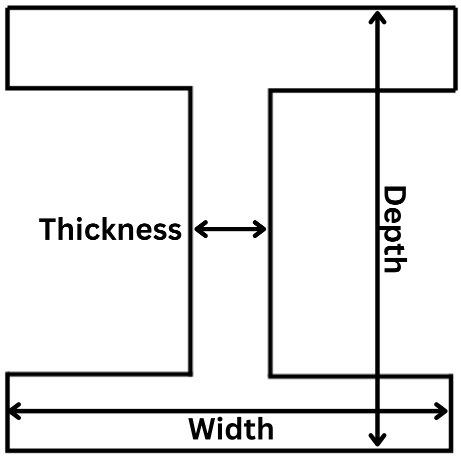

FIGURE 4.19: I-beam cross section

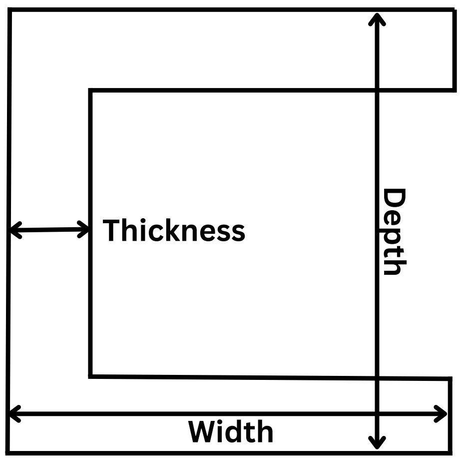

FIGURE 4.20: C-beam cross section

4.7 Structure Design: Wing

Following the design of the body, we move onto the wings, the most important part of the glider as it is where the lift is generated. As it is such a critical component, extreme precision and meticulous planning is required to design the wing and to have it meet design and performance requirements.

Firstly, the wing's setup. A high Wing configuration has been chosen for this project as it is the most popular choice for gliders and gliding bombs, and with good reason for it. The high wing configuration offers several advantages, such as the facilitating of eased loading of payload, as it will be installed above the warhead (when in glide). It also offers greater gliding control as its center of gravity is located lower than the wing. It also allows for an increased dihedral effect(C_{l_β}). This allows the glider to be more laterally stable and is due to the increased contribution of the fuselage towards the dihedral effect of the wing ($C_{l_{\beta W}}$). The glider will also be less prone to stall as its stall speed will be much lower due to the high wing and would also produce more lift compared to other configurations, which is ideal for gliding aircraft. The wing would also induce drag that produces an upwards nose pitching moment, which destabilizes the aircraft longitudinally and is due to the higher wing drag line relative to the center of gravity ($M_{D_{cg}} > 0$). [49]

The ideal wing airfoil has been found to be the (Clark Y airfoil or Sokolov airfoil) for its high Lift-to-Drag ratio and constant use in Civilian gliding aircraft. The wingspan, taken as 2 meters was chosen due to the length being the average span on many other glide bomb kits

The wing, designed on Onshape, has its dimensions, shape and airfoil analyzed for stability and drag on both XFLR5. After a suitable location for the wing has been found, the wing's structure gets designed.

We first have to conduct initial sizing research on the ideal size of the spars for the wing. Ideally, we would like it to be as light as possible, but also be able to sustain forces of drag and the stresses and strains of gliding flight. Once initial sizing has been completed and data obtained and verified, we can now focus on the sketching of said structure on Onshape. Here, calculations and concepts are put from pen to paper, per say. The Table 4.9 below shows information on the sizing of the spar as well as the thickness of the ribs of the wing.

As for the shape of the spar, we shall utilize the I-beam shape as it is a much more slim-lined shape compared to using full rectangular spars. It is also ideal as it is able to withstand a wide range of loads. Structurally speaking, the convenience and usefulness of the I-beam can be explained using basic structural engineering terms and Equations. One form of stress and its Equation below in Equation 4.1 for bending moment explains why the I-beam is advantageous to many who use it.

$$\sigma = \frac{My}{I} \tag{4.1}$$

With σ representing the bending stress, M being the applied moment on the beam, y the Distance from the neutral axis to the point where the stress is being calculated, and I is the inertial moment of the beam's cross section around the neutral point.

For about the same amount of material used by the I-beam, it has a higher moment of Inertia (I) compared to other shapes, other choices being rectangular or circular. This is due to the material being able to be spread much more distantly from the neutral axis, thus increasing inertia and resulting in the reduction of bending stress (σ) for the same amount of bending moment (M). This proves the credibility of the I-beam and makes it effective in resisting bending pressures [55].

The following Table 4.9 shows the wing structures dimensions and will be used as the basic reference for the entirety of the design process.

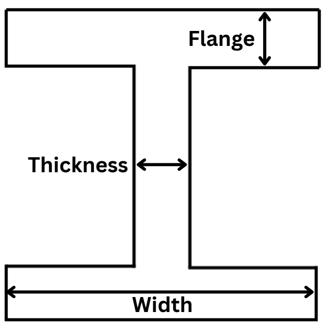

FIGURE 4.21: Wing Spar Structure Shape

The thickness of the structural elements of the wing have been calculated by doing the steps mentioned in the [45] book. From calculations, the exact value

Parameters	Value
Root Thickness	0.508 mm
Root Flange	0.508 mm
Root Width	200 mm
Tip Thickness	0.508 mm
Tip Flange	0.508 mm
Tip Width	200 mm
Rib Thickness	0.508 mm

TABLE 4.9: Wing Structure Parameters

for the thickness of the ribs and spar worked out to be below the recommended minimum of 0.02 inches, or $0.508mm$. Hence why, to avoid any structural penalties, the minimum value is taken as the value mentioned in Table 4.9.

4.8 Structure Design: Tail/Fin

4.8.1 V1: Standard X-Tail

The last and certainly not least step in the design process shifts its focus on the design of the empennage, or tail section. This part is apparently crucial as it is the area of the glider that provides the stability (and control). The first step was to draw inspiration from what competitors were doing and start from there. The most popular option for an empennage was to utilize an X-tail configuration. This is the standard issue tail section that comes with the Mark 82 munition, with some slight adjustments. The structure of the

4.8.2 V2: JDAM Tail

The tail section is the last area of the aircraft that we will be focusing on. But that does not mean that it is the least important. The function of the tail, or empennage, is to provide stability and control to the entire aircraft. For the purpose of increased performance, the tail section will utilize another piece of equipment that is in the arsenal of the Indonesian Air Force. Currently, the Indonesian Air Force is in possession of around 102 JDAM kits [56]. Where these kits will be installed to the tail ends of Mark 82 bombs. These are the same kits utilized by the JDAM ER, just minus the wing kit. What makes the JDAM kit special is that all 4 of its fins, in an X-tail configuration, are movable and adjust the course of the bomb's drop. So in the spirit of warfare technology collaboration, the Wing kit would fit perfectly with the JDAM kit at its rear.

4.8.3 V3: JDAM-Style X-tail and system (re-engineered system)

In order to aid in directional control, the tail is made so all of its 4 fins are able to move mid air as some sort of rudder/elevator system. To prioritize better integration with the navigational systems, the tail must be made in-house and from the ground up in order for it to suit the needs and systems that are used in the wing kit. This tail would adjust headings, glide angles, and rolling movements when necessary.

4.8.4 V4: Inverted Y-tail

For increased stability, a customized tail will be needed to allow the aircraft to glide much more smoothly and precisely. An inverted Y-tail shape would allow this as the main vertical stabilizer would be much larger and taller than the other 2 fins. This higher empennage would allow for better longitudinal stability and would bring about enhanced directional augmentation as it has 1 straight structure rather than 2 that would be in a V configuration (upper half of an X-tail setup). The reason for it being inverted is for the saving of space when the munition is being loaded onto the fighter aircraft. This would keep the taller empennage away from the jet's wing and would not cause any potential damage to the fighter or pilot.

4.9 Structural Assembly and Analysis

After completing every design phase under the sun, the project has finally reached its end, assembly. Here, we will need to combine all structures with components, systems and subsystems. This phase symbolizes the end of the design and engineering work and transforms isolated parts and components into an integrated structure.

4.9.1 AA1 Gliding Shark

Figures 4.22 and 4.23 show the external and structural layouts of the AA1 concept. They provide a complete perspective of the assembled structure.

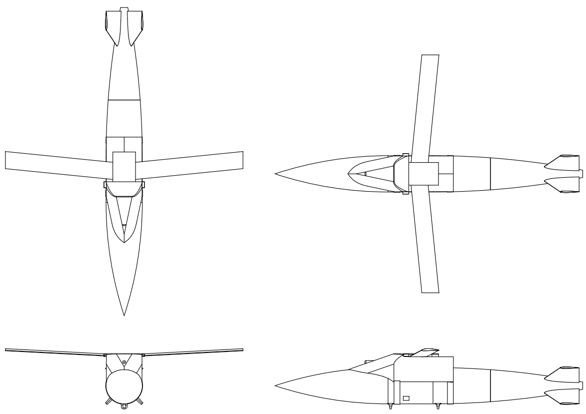

FIGURE 4.22: AA1 Sketch

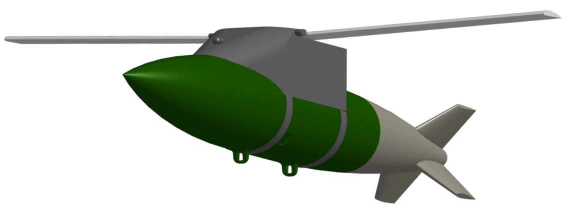

FIGURE 4.23: AA1 Gliding Shark

4.9.2 AA2 Sky Shark

Figures 4.24 and 4.25 show the external and structural layouts of the AA2 concept. They provide a complete perspective of the assembled structure.

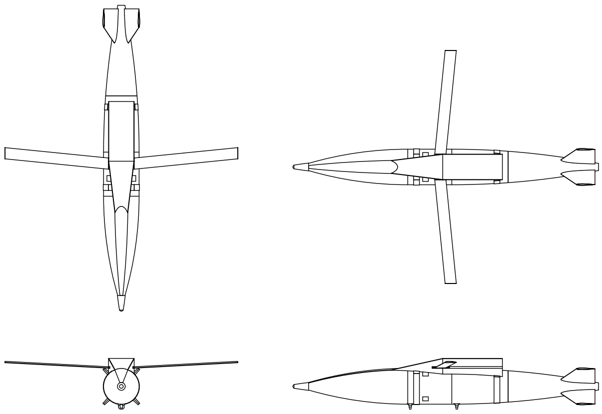

FIGURE 4.24: AA2 Sketch

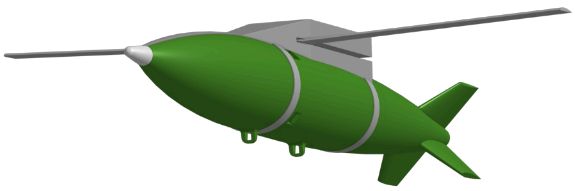

FIGURE 4.25: AA2 Sky Shark

4.10 Final Decided Version

Based on stability, performance and packaging, the **AA1 Gliding Shark** version of the two concepts have been chosen as the final design of this conceptual report.

4.10.1 Performance Characteristics and Specifications

As previously mentioned and seen in Figure 4.26, AA1 features a Wing with a Chord length of 0.15 meters, spanning a length of 2 meters at a $3/deg$ dihedral angle and a sweep of 0.1 meters.

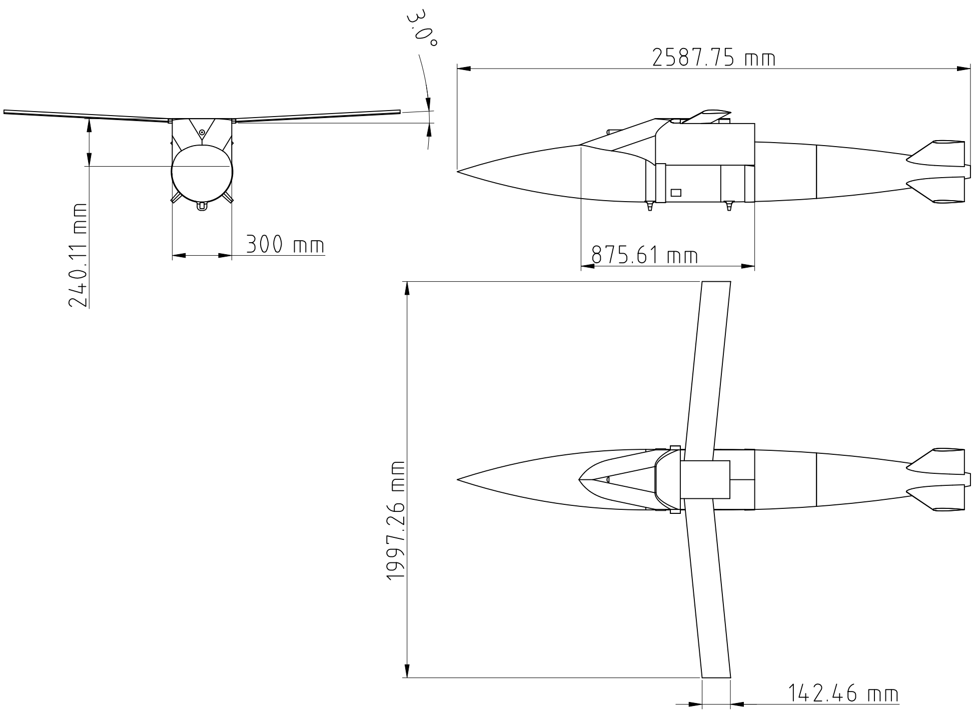

FIGURE 4.26: AA1 3-View Sketch

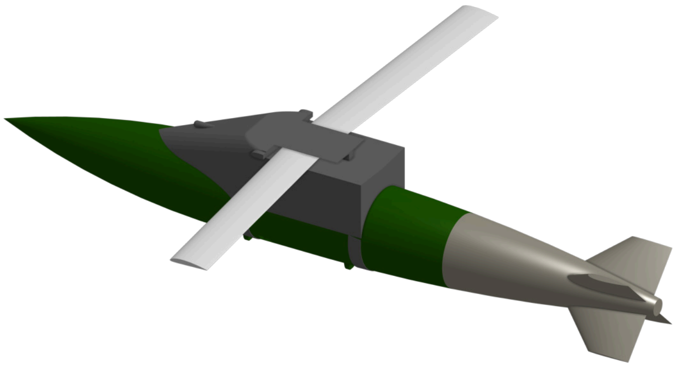

FIGURE 4.27: AA1 Dynamic View

Its structural layout can be seen in either Figure 4.7 or Figures 4.28 and 4.30 below. As mentioned, they feature a cage-like design with a blend of I-beam and C-beam structures whose dimensions can be seen in Figure 4.8. Similarly, the wing structure has been modeled through calculations from [45] and the shape and dimensions of the rib and spar structural elements can be seen in Figures 4.21 and Table 4.9.

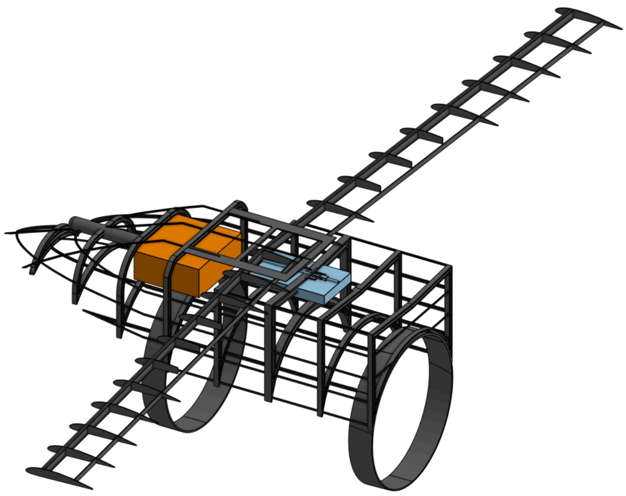

FIGURE 4.28: AA1 Structure Dynamic View

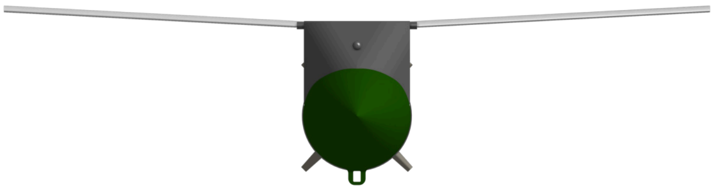

FIGURE 4.29: AA1 Front View

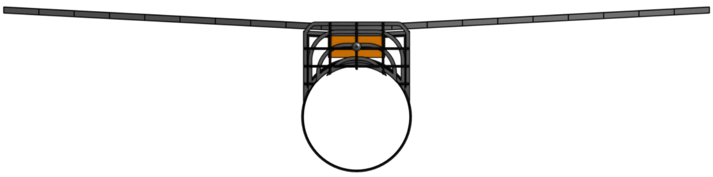

FIGURE 4.30: AA1 Structure Front View

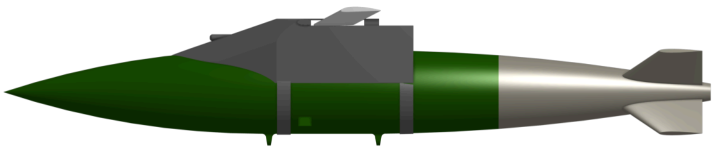

FIGURE 4.31: AA1 Side View

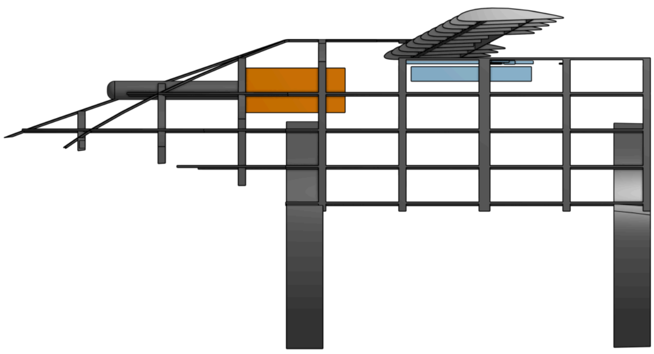

FIGURE 4.32: AA1 Structure Side View

Modeled after Figure 2.21 from [28], Figure 4.33 shows the performance characteristics of the AA1 gliding bomb which includes its Rate of Descent (RD), Horizontal velocity (V_h) and glide Path angle (γ_d)(Denoted as Gamma d in the table)

Plane Name	AA1
Polar Name	T1-231.5-m/s-LLT
Freestream Velocity	231.5 m/s
Weight	2266.11 N
Mass	235.3 kg

alpha (deg)	CL	CD	Cm	CL/CD	CD/CL	Gamma d (deg)	RD (m/s)	Vh (m/s)
0	0.333	0.009	-0.157	35.454	0.028	1.616	6.527	192.377
1	0.425	0.011	-0.179	39.153	0.026	1.463	5.911	170.438
2	0.515	0.013	-0.199	40.243	0.025	1.423	5.751	154.760
3	0.603	0.015	-0.218	39.564	0.025	1.448	5.849	143.048
4	0.702	0.019	-0.239	37.038	0.027	1.547	6.248	132.559
5	0.799	0.023	-0.259	34.422	0.029	1.664	6.723	124.227
6	0.887	0.028	-0.275	32.087	0.031	1.785	7.211	117.899
7	0.973	0.033	-0.288	29.896	0.033	1.916	7.739	112.573
8	1.054	0.038	-0.298	27.645	0.036	2.072	8.369	108.164
9	1.135	0.044	-0.308	25.702	0.039	2.228	9.000	104.260
10	1.211	0.051	-0.315	23.945	0.042	2.391	9.660	100.927
11	1.284	0.057	-0.320	22.464	0.045	2.549	10.295	97.995
12	1.353	0.064	-0.324	21.203	0.047	2.700	10.906	95.480
13	1.417	0.070	-0.326	20.105	0.050	2.848	11.501	93.283
14	1.475	0.077	-0.325	19.037	0.053	3.007	12.143	91.446
15	1.522	0.085	-0.321	17.926	0.056	3.193	12.894	90.005
16	1.555	0.093	-0.312	16.678	0.060	3.431	13.856	89.060

FIGURE 4.33: AA1 Performance Characteristics

Below, in Figure 4.34, is a Hodograph of AA1, similar to Figure 2.22 and using the same assumption of $\cos\gamma_d = 1$

Other performance characteristics such as Maximum speed, Range, $\frac{C_L}{C_D}_{\max}$, Stall speed (V_S), $C_{L_{\max}}$, $C_{L_{\min}}$, Diving speed (V_D) and Load factors can be found

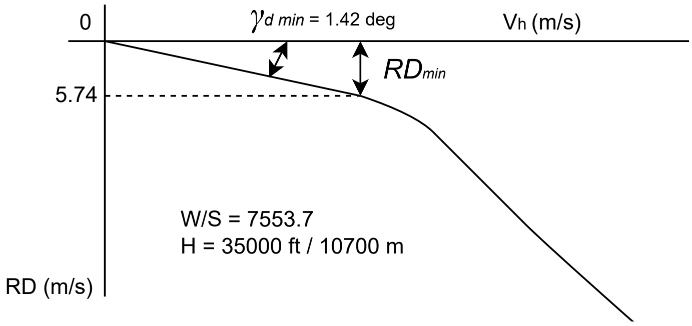

FIGURE 4.34: AA1 Hodograph of Gliding Performance with the assumption of $\cos\gamma_d = 1$

in Figure 4.1 and Tables 4.4 and 4.5 respectively. With the V-n diagram for AA1 located at Figure 4.5. The analysis for the Lateral and Longitudinal Stability of AA1 can be found in Figures 4.15 and 4.16, respectively. With AA1 being represented by the **Blue** circles. For the logs of the stability analysis on XFLR5, it can be found in Appendix B.

Listed below in Tables 4.10 and 4.11 are the list of materials as well as weights/masses of the components that make up the AA1 glide bomb. The kit utilizes the dense and strong nature of Aluminum 2024-T6 for the structural components and uses Carbon fiber composites as the skin of the kit because of its high tensile and shear strength which would aid in protecting the avionic components from the elements around the air as it glides towards it target. Data on materials and their characteristics were obtained from [57].

Material	$\rho(\mathrm{kg\,m^{-3}})$	$\tau(\mathrm{MPa})$	$\sigma_{\mathrm{max}}(\mathrm{MPa})$	$\sigma_{\mathrm{Y}}(\mathrm{MPa})$
Al 2024-T6	2780	283	427	345
Carbon Fiber	2000	590	4140	3380

TABLE 4.10: AA1 materials list with characteristic data by [57]

Component name	Mass
Mk 82 bomb	227 kg
Avionic components	2.353 kg
Kit structure	1.34 kg
Kit skin/shell	1.48 kg
Wings	3.1 kg
Total	235.273 kg

TABLE 4.11: AA1 mass components.

CHAPTER 5
SUMMARY, CONCLUSION, RECOMMENDATION

5.1 Summary

The summary of this thesis, based on what has been written and analyzed, is as follows:

- All collected data for the benchmarking study and comparisons have been carried out independently and is based on available data on the internet.
- The mission profile was developed to meet its performance requirements.
- From benchmarking, the bomb model that was to be utilized had been chosen and the preliminary design stage had begun. The results of which were several configurations and ideas, all made on the Onshape CAD software.
- Analysis was then carried out, mainly on the aerodynamic coefficients of the different concepts and configurations before finalizing.
- The process moved to structural design phase, where Onshape CAD software was used to draw up as well as add materials to said design to obtain estimations on the total gross weight of the glide bomb.
- With weights now imputed, the chosen configuration can now be analyzed in order to ensure that it is statically and also dynamically stable via the use of XFLR5 analysis software.
- After obtaining the complete data, the V-n diagram was constructed to provide the essential details about the structural and operational restrictions of the glider.
- As the V-n diagram was being produced, performance calculations were done which provided the gliding bomb's range, endurance and maximum airspeed.

5.2 Conclusion

The main goal of this thesis is to design a concept of a gliding bomb. This study has successfully enabled an already available (in the Indonesian Air Force's arsenal) dumb bomb to be used in a much more efficient and strategic manner by having it travel long distances on its own, rather than being carried directly over its target by aircraft. The glide bomb concept being showcased here has the capability to travel distances in excess of $300km$, or 431.65 kilometers to be precise. The bomb, when in symmetric flight, is both statically and dynamically stable, which in itself is impressive considering that there is no stability augmentation being put into play to make the flight stable in the first place. All avionic components used are not customized specification, but rather commercially available components that are sold as parts openly to numerous parties around the world.

5.3 Recommendations

Although this study is purely conceptual, there is much room for improvement. Some I can recommend include:

- Further research on the avionic systems and subsystems specifications for increased weight reduction and better performance characteristics.
- Utilize a more scientific method to size the kit in proportion to the bomb to reduce unnecessary drag or excessive unused space inside the kit.
- Increased focus on glider controllability during its flight to reduce the chances of going off course due to perturbations.
- Structural analysis can be carried out to ensure the strength of the kits' structure and its capability to withstand G-forces.
- Further investigation into the navigational system to enhance the guidance capabilities of the gliding bomb.
- Analyze the Circular Error Probable, or CEP for a better understanding of the bomb's accuracy to hit it's target.
- Cost analysis to give a base figure of potential costs to develop and manufacture this design.

- Optimization in areas such as weight distribution, sizing, control and navigation for optimum performance.

Bibliography

[1] "Indonesia Air Force," Wikipedia. (), [Online]. Available: https://upload.wikimedia.org/wikipedia/commons/4/46/Marsekal_TNI_Fadjar_Prasetyo%2C_S.E.%2C_M.P.P.%2C_CSFA.%2C_dengan_Crew_Dinamic_Show_Team.jpg (visited on 12/30/2024).

[2] "KAI T-50 Golden Eagle," Wikipedia. (), [Online]. Available: https://en.wikipedia.org/wiki/KAI_T-50_Golden_Eagle (visited on 12/30/2024).

[3] "A400M," Wikipedia. (), [Online]. Available: https://upload.wikimedia.org/wikipedia/commons/f/f3/Royal_Air_Force_Airbus_A400M_ZM400_in_flight_over_Bristol_%2845158515%29.jpg (visited on 12/30/2024).

[4] "Glide Bomb definition," Merriam-Webster.com Dictionary. (), [Online]. Available: https://www.merriam-webster.com/dictionary/glide-bomb (visited on 11/30/2024).

[5] A. Sayl and F. Erden, "The History of Guided Bombs, Guidance Kits, Wing Kits, and Wing Deployment Mechanisms," 2024.

[6] T. Saxon, "*Kehl* : The German use of guided weapons against naval targets 194344," *Defence Studies*, vol. 3, no. 1, pp. 1–16, Mar. 2003, ISSN: 1470-2436, 1743-9698. DOI: 10.1080/14702430308405049. [Online]. Available: https://www.tandfonline.com/doi/full/10.1080/14702430308405049 (visited on 12/02/2024).

[7] D. Blackweider, "The Long Road to Desert Storm and Beyond: The development of precision Guided Bombs," Air University United States AIr Force, Maxwell Air Force Base, Alabama, May 1992, 68 pp.

[8] "Henschel Hs.293." (), [Online]. Available: http://www.walterwerke.co.uk/missiles/hs293.htm (visited on 12/03/2024).

[9] Samantha Franco. “Fritz X: The Worlds First Precision-Guided Missile Took Out the Italian Navys Flagship.” (Feb. 14, 2023), [Online]. Available: https://www.warhistoryonline.com/weapons/fritz-x.html (visited on 12/03/2024).

[10] Bob Bergin. “Bombing Burmas Bridges.” (Apr. 2019), [Online]. Available: https://warfarehistorynetwork.com/article/bombing-burmas-bridges/ (visited on 12/03/2024).

[11] Andreas Parsch. “Martin Marietta AGM-62 Walleye,” 2002. (), [Online]. Available: https://www.designation-systems.net/dusrm/m-62.html (visited on 12/03/2024).

[12] Edgar B, *AGM-65 Maverick*, 2021. [Online]. Available: https://www.artstation.com/artwork/g82qKx (visited on 12/03/2024).

[13] theonlyone223, *GBU-8/B HOBOS*, 2023. [Online]. Available: https://sketchfab.com/3d-models/gbu-8b-hobos-3c2d400c8acb4cb085c8e1d01aac327c (visited on 12/03/2024).

[14] P. DELeon, “The Laser-Guided Bomb: Case History of a Development,”

[15] S. Affan Ahmed, M. Mohsin, and S. M. Zubair Ali, “Survey and technological analysis of laser and its defense applications,” *Defence Technology*, vol. 17, no. 2, pp. 583–592, Apr. 2021, ISSN: 22149147. DOI: 10.1016/j.dt.2020.02.012. [Online]. Available: https://linkinghub.elsevier.com/retrieve/pii/S2214914719312231 (visited on 12/02/2024).

[16] Andreas Parsch. “Texas Instruments Paveway I & Pave Storm (GBU-1/B, GBU-2/B, GBU-3/B, GBU-5/B, GBU-6/B, GBU-7/B, GBU-10/B, GBU-11/B, GBU-12/B).” (2008), [Online]. Available: https://www.designation-systems.net/dusrm/app5/paveway-1.html (visited on 12/03/2024).

[17] “JDAM JDAM-ER.” (Nov. 1, 2024), [Online]. Available: https://www.armyrecognition.com/military-products/army/missiles/bombs/jdam-joint-direct-attack-munition-gps-inertial-precision-strike-munition-data?highlight=WyJqZGFtIl0= (visited on 12/03/2024).

[18] jeyhun1985, *Paveway IV LGB (FBX)*, 2021. [Online]. Available: https://sketchfab.com/3d-models/paveway-iv-lgb-fbx-f5dfad1120854681a5475ff41c8d8c3b (visited on 12/03/2024).

[19] "HGK-82." (), [Online]. Available: https://www.aselsan.com/en/defence/product/2882/hgk82 (visited on 12/03/2024).

[20] "JDAM Matures Parts 1 and 2,"

[21] NurW. "LIG Nex1 : RTAF adalah Pelanggan Baru Bom Berpandu GPS KGGB." (Jun. 23, 2022), [Online]. Available: https://defense-studies.blogspot.com/2022/09/lig-nex1-rtaf-adalah-pelanggan-baru-bom.html (visited on 12/03/2024).

[22] "KGK-84." (), [Online]. Available: https://www.aselsan.com/en/defence/product/2865/kgk84 (visited on 12/03/2024).

[23] "Al Tariq formerly known as Umbani." (), [Online]. Available: http://www.deneldynamics.co.za/products/missiles/stand-off-weapons/al-tariq- (visited on 12/03/2024).

[24] Piotr Butowski. "The Truth About Russias Mysterious Winged Glide Bombs." (Jul. 19, 2023), [Online]. Available: https://www.twz.com/the-truth-about-russias-mysterious-winged-glide-bombs (visited on 12/03/2024).

[25] "Trends in World Military Expenditure, 2023,"

[26] "Force Balance Coordinates," NASA. (), [Online]. Available: https://www.grc.nasa.gov/www/k-12/airplane/tunbalaxes.html (visited on 12/29/2024).

[27] A. T. A. Shidiqi, "A Conceptual Design of Flexible Mission MALE: Aerodynamics and Stability,"

[28] G. J. J. Ruijgrok, *Elements of Airplane Performance*, Second edition. Delft: VSSG, ISBN: 978-90-6562-232-7.

[29] M. V. Cook, *Flight Dynamics Principles* (Elsevier Aerospace Engineering Series), 2nd ed. Amsterdam Boston: Elsevier/Butterworth-Heinemann, 2007, ISBN: 978-0-7506-6927-6.

[30] "Simplified Aircraft Motion." (), [Online]. Available: https://www1.grc.nasa.gov/beginners-guide-to-aeronautics/simplified-aircraft-motion/ (visited on 12/03/2024).

[31] Kayhan Kurul, "Structural Design of Part of Aircraft Control System," Brno University of Technology, 47 pp. [Online]. Available: https://www.researchgate.net/publication/342106041_Structural_Design_of_Part_of_Aircraft_Control_System_Bachelor_Thesis (visited on 12/03/2024).

[32] C. Cutler. "The 3 Types Of Static And Dynamic Aircraft Stability." (Mar. 26, 2015), [Online]. Available: https://www.boldmethod.com/learn-to-fly/aerodynamics/3-types-of-static-and-dynamic-stability-in-aircraft/ (visited on 10/27/2024).

[33] T. H. G. Megson, *Aircraft Structures for Engineering Students* (Elsevier Aerospace Engineering Series), 4th ed. Oxford ; Burlington, MA: Butterworth-Heinemann, 2007, 804 pp., ISBN: 978-0-7506-6739-5.

[34] "TUDelft 3.1.4 Main Takeaways on Aircraft Structural Elements." (), [Online]. Available: https://ocw.tudelft.nl/course-readings/3-1-4-main-takeaways-on-aircraft-structural-elements/ (visited on 12/13/2024).

[35] Oleg Lisitsin. "From Ailerons to Flaps: The Main Stages of Design of an Aircraft Wing." (Aug. 18, 2020), [Online]. Available: https://engre.co/blogs/articles/from-ailerons-to-flaps-the-main-stages-of-design-of-an-aircraft-wing/ (visited on 12/03/2024).

[36] "In Picture: Yasin advanced precision-guided smart bomb." (Nov. 1, 2023), [Online]. Available: https://iranpress.com/in-picture-yasin-advanced-precision-guided-smart-bomb (visited on 12/03/2024).

[37] Dr Carlo Kopp and Dr Martin Andrew. "PLA Guided Bombs." (Apr. 2012), [Online]. Available: https://www.ausairpower.net/APA-PLA-GBU.html#mozTocId132067 (visited on 12/03/2024).

[38] Tamir Eshel. "Rafael's SPICE Guided Weapon." (May 6, 2003), [Online]. Available: https://defense-update.com/20030506_rafaels-spice-guided-weapon.html (visited on 12/03/2024).

[39] "AGM-154 JSOW Can Turn Into Cruise Missile: This Might Be Washington's Plan to Avoid Escalation and Whatnot." (Sep. 22, 2024), [Online]. Available: https://en.defence-ua.com/analysis/agm_154_jsow_can_turn_into_cruise_missile_this_might_be_washingtons_plan_to_avoid_escalation_and_whatnot-11943.html (visited on 12/03/2024).

[40] "South African UAB and CD family "Raptor" for the operators "Mirage" and "Gripenov": Argentina "in transit"." (Mar. 31, 2017), [Online]. Available: http://www.walterwerke.co.uk/missiles/hs293.htm (visited on 12/03/2024).

[41] David Donald. "German-Israeli Smart Bomb Project Unveiled." (Jul. 11, 2011), [Online]. Available: https://www.ainonline.com/aviation-news/defense/2011-07-11/german-israeli-smart-bomb-project-unveiled (visited on 12/03/2024).

[42] Harry McNeil. "Indias new homegrown GAURAV glide bomb hits the mark in test." (Aug. 14, 2024), [Online]. Available: https://www.airforce-technology.com/news/indias-new-homegrown-gaurav-glide-bomb-hits-the-mark-in-test/ (visited on 12/03/2024).

[43] J. C. Gaubatz and R. J. Hansman, "Design and Development of Stability and Control Systems for Small, Deployable Aircraft,"

[44] "AA-SM-518." (Jul. 13, 2016), [Online]. Available: https://www.abbottaerospace.com/downloads/aa-sm-518/ (visited on 12/03/2024).

[45] S. Gudmundsson, *General Aviation Aircraft Design: Applied Methods and Procedures*, Second edition. Oxford Cambridge: Butterworth-Heinemann, an imprint of Elsevier, 2022, 1 p., ISBN: 978-0-12-818465-3.

[46] "Mark 82." (), [Online]. Available: https://en.wikipedia.org/wiki/File:Mk-82_Bomb.jpg (visited on 12/03/2024).

[47] "FAB-500 M-62." (), [Online]. Available: https://roe.ru/eng/catalog/aerospace-systems/air-bombs/fab-500-m-62/.

[48] "Bomb P-250L." (), [Online]. Available: https://saribahari.id/id/produk/bomb-p-250l.

[49] M. H. Sadraey, *Aircraft Design: A Systems Engineering Approach* (Aerospace Series). Chichestet, West Sussex: Wiley, 2013, 778 pp., ISBN: 978-1-119-95340-1.

[50] A. Dupuis, "Aerodynamic characteristic and analysis of a MK82 bomb configuration from free-flight tests," in *AIAA Atmospheric Flight Mechanics Conference and Exhibit*, Montreal,Canada: American Institute of Aeronautics and Astronautics, Aug. 6, 2001. DOI: 10.2514/6.2001-4325. [Online]. Available: https://arc.aiaa.org/doi/10.2514/6.2001-4325 (visited on 10/20/2024).

[51] "Clark Y." (), [Online]. Available: http://airfoiltools.com/plotter/index (visited on 12/03/2024).

[52] "Eppler 393." (), [Online]. Available: http://airfoiltools.com/plotter/index (visited on 12/03/2024).

[53] "NACA 65-410." (), [Online]. Available: http://airfoiltools.com/plotter/index (visited on 12/03/2024).

[54] "Sokolov." (), [Online]. Available: http://airfoiltools.com/plotter/index (visited on 12/03/2024).

[55] Paul E. Best, *Analysis And Comparison of I-Beam And Solid Wing Spars*. [Online]. Available: http://westcoastpiet.pietenpols.org/images/Construction/I%20Beam%20Analysis.pdf (visited on 12/10/2024).

[56] "JDAM Kits TNI AU Telah Tiba," DEFENSE STUDIES. (Aug. 27, 2020), [Online]. Available: https://defense-studies.blogspot.com/2020/08/jdam-kits-tni-au-telah-tiba.html (visited on 11/30/2024).

[57] "MatWeb." (), [Online]. Available: https://www.matweb.com/ (visited on 12/30/2024).

Appendices

Appendix A: Glide Bomb comparison

Designation		AA1 Gliding Shark	AA2 Sky Shark
Country of Origin		Indonesia	Indonesia
Manufacturer		AA	AA
Length (m)		2.21	2.21
Diameter (m)		0.273	0.273
Wingspan (m)		2	2
Chord	Root chord (m)	0.15	0.1
	Tip chord (m)	0.15	0.1
Aspect Ratio (AR)		13.33333333	20
Wing area (m^2)		0.3	0.2
Wing loading (Total Weight/Wing Area)(kg/m^2)		756.6666667	1135
Payload name		Mark 82	Mark 82
Payload mass (kg)		227	227
Guidance system		Integrated INS/GLONASS/GPS	Integrated INS/GLONASS/GPS
Range (km)		300+ (Maximum)	300+ (Maximum)
Compatible Aircraft		F-16, T-50 and Hawk 201	F-16, T-50 and Hawk 200

Designation		UMPK (FAB-500)	JDAM-ER	Yasin
Country of Origin		Russia	United States	Iran
Manufacturer		Bazalt Design Bureau	Boeing/McDonnell Douglas	Iranian Defence Industry
Length (m)		2.47	2.21	N/A
Diameter (m)		0.4	0.273	N/A
Wingspan (m)		2.32	1.767	N/A
Chord	Root chord (m)	0.275	0.15	N/A
	Tip chord (m)	0.275	0.15	N/A
Aspect Ratio (AR)		8.436363636	11.78	N/A
Wing area (m^2)		0.638	0.26505	N/A
Wing loading (Total Weight/Wing Area)(kg/m^2)		783.6990596	856.4421807	N/A
Payload name		FAB 500	Mark 82	250 kg General Purpose Bomb
Payload mass (kg)		500	227	227
Guidance system		Integrated INS/GPS	Integrated INS/GLONASS/GPS	Integrated INS/GPS
Range (km)		60-70	70-80	N/A
Compatible Aircraft		Su-27, Su-30, and Su-35	F-15, F-16, F-18, F-22, F-35 among others	MiG-29 and UAVs

Designation		LS PGB	KGGB	KGK
Country of Origin		China	South Korea	Turkiye
Manufacturer		LOTDC	LiG Nex1	TUBITAK-SAGE
Length (m)		3.5	2.21	2.21
Diameter (m)		0.377	0.273	0.273
Wingspan (m)		2.5	2.625	2.8
Chord	Root chord (m)	0.225	0.2	0.16
	Tip chord (m)	0.225	0.2	0.16
Aspect Ratio (AR)		11.11111111	13.125	17.5
Wing area (m^2)		0.5625	0.525	0.448
Wing loading (Total Weight/Wing Area)(kg/m^2)		888.8888889	432.3809524	506.6964286
Payload name		250 kg General Purpose Bomb	Mark 82	Mark 82
Payload mass (kg)		500	227	227
Guidance system		Integrated INS/GPS	Integrated INS/GPS	Integrated INS/GPS
Range (km)		40-65	76.5-103	37-111
Compatible Aircraft		J-10, J-16, JF-17, and MiG-29	F-5, F-15, F-16, T-50 and KF-21	F-4 and F-16

Designation		SPICE	Umbani/Al Tariq	AGM-154 JSOW
Country of Origin		Israel	South Africa	United States
Manufacturer		Rafael Advanced Defence Systems	Denel Dynamics	Raytheon
Length (m)		3.035	2.21	4.1
Diameter (m)		0.357	0.273	0.33
Wingspan (m)		N/A	2.28	3.2
Chord	Root chord (m)	N/A	0.13	0.275
	Tip chord (m)	N/A	0.13	0.275
Aspect Ratio (AR)		N/A	17.53846154	11.63636364
Wing area (m^2)		N/A	0.2964	0.88
Wing loading (Total Weight/Wing Area)(kg/m^2)		N/A	765.8569501	564.7727273
Payload name		Mark 83/84	Mark 82	AGM-154 JSOW
Payload mass (kg)		450-900	227	497
Guidance system		Integrated INS/GPS	Integrated INS/GLONASS	Integrated INS/GPS
Range (km)		N/A	N/A	22-130
Compatible Aircraft		F-15, F-16, Su-30 and JAS 39	BAE Hawk 100, JAS 39, and Mirage F1	F-15, F-16, F-18, F-22, F-35 among others

Designation		HOPE	HOSBO
Country of Origin		Germany	Germany
Manufacturer		Diehl BGT Defence	Diehl BGT Defence
Length (m)		5	3.5
Diameter (m)		0.4	0.4
Wingspan (m)		4.32	2.5
Chord	Root chord (m)	0.45	0.45
	Tip chord (m)	0.2	0.2
Aspect Ratio (AR)		13.29230769	7.692307692
Wing area (m^2)		1.404	0.8125
Wing loading (Total Weight/Wing Area)(kg/m^2)		997.1509972	1116.307692
Payload name		HOPE	HOSBO
Payload mass (kg)		1400	907
Guidance system		Integrated INS/GPS with electro optical video	Integrated INS/GPS with electro optical video
Range (km)		160	160
Compatible Aircraft		Eurofighter Typhoon, Panavia Tornado	Eurofighter Typhoon, Panavia Tornado

Appendix B: XFLR5 Stability Output

```
xflr5 v6.61
30.12.2024  13:42:01

Launching Analysis

Launching the 3D Panel Analysis....
AA1
Type 7 - Stability polar

Wings as thin surfaces
Using ring vortices - VLM2
Using Neumann boundary conditions for wings

Density   =       1.225kg/m3
Viscosity =     1.5e-05m²/s

Reference Area   =     0.29959m²
Reference length =      1.9973m

Counted  858 panel elements


   Solving the problem...

      Calculation for control position  0.00
   Mass=     231.000 kg

   ___Center of Gravity Position - Body axis____
    CoG_x=      1.1782 m
    CoG_y=     -0.0000 m
    CoG_z=      0.0067 m

   ___Inertia - Body Axis - CoG Origin____
    Ibxx=       1.385 kg.m²
    Ibyy=       6.348 kg.m²
    Ibzz=       6.993 kg.m²
    Ibxz=     0.03046 kg.m²

      Creating the unit RHS vectors...
      Creating the influence matrix...
      Performing LU Matrix decomposition...
      Solving the LU system...
      Time for linear system solve: 0.084 s
      Searching for zero-moment angle... Alpha=-0.88529°
      Creating source strengths...
      Calculating doublet strength...
      Calculating speed to balance the weight...VInf = 255.19950 m/s

      ___Inertia - Stability Axis - CoG Origin____
      Isxx=       1.388
      Isyy=       6.348
      Iszz=       6.991
      Isxz=      0.1171

      Calculating the stability derivatives
         Creating the RHS translation vectors
         LU solving for RHS - longitudinal
         Calculating forces and derivatives - lateral
         Creating the RHS rotation vectors
         LU solving for RHS - lateral
         Calculating forces and derivatives - lateral

      No active control - skipping control derivatives
```

```
      Longitudinal derivatives
      Xu=     -1.0667         Cxu=   -0.022779
      Xw=      7.1436         Cxa=     0.15255
      Zu=     -17.763         Czu= -8.2468e-05
      Zw=     -275.41         CLa=      5.8812
      Zq=     -72.392         CLq=      20.612
      Mu=    -0.16113         Cmu=    -0.02294
      Mw=     -50.087         Cma=     -7.1306
      Mq=     -60.846         Cmq=      -115.5
      Neutral Point position=   1.36004 m


      Lateral derivatives
      Yv=     -40.522         CYb=    -0.86532
      Yp=     -10.751         CYp=     -0.2299
      Yr=      51.947         CYr=      1.1108
      Lv=     -7.0408         Clb=    -0.07528
      Lp=     -64.912         Clp=    -0.69499
      Lr=      7.2451         Clr=     0.07757
      Nv=      46.175         Cnb=     0.49369
      Np=      3.9196         Cnp=    0.041966
      Nr=     -60.084         Cnr=    -0.64329

      _____State matrices__________
       Longitudinal state matrix
            -0.0046177          0.0309247                  0
-9.81
            -0.0768977           -1.19224            254.886
0
            -0.0253846           -7.89057           -9.58539
0
                     0                  0                  1
0
       Lateral state matrix
             -0.175419         -0.0465415           -254.975
9.81
               -4.5233           -46.8002             4.5026
0
               6.52943          -0.223122           -8.51941
0
                     0                  1                  0
0



      ___Longitudinal modes____

      Eigenvalue:     -5.389+   -44.65i   |      -5.389+    44.65i   |
-0.002295+ -0.05283i   |   -0.002295+  0.05283i

________________________________________________________________________________
_____________________
      Eigenvector:         1+        0i   |           1+        0i   |
1+        0i   |           1+        0i
                        1512+     5795i   |        1512+    -5795i   |
-0.003563+1.006e-06i   |   -0.003563+-1.006e-06i
                       990.2+   -360.3i   |       990.2+    360.3i   |
0.0002851+7.432e-07i   |  0.0002851+-7.432e-07i
                       5.317+    22.82i   |       5.317+   -22.82i   |
-0.000248+ 0.005385i   |   -0.000248+-0.005385i
```

```
      ___Lateral modes____

      Eigenvalue:     -46.88+        0i   |      -4.309+   -40.64i   |
-4.309+    40.64i   |   -0.001145+        0i

________________________________________________________________________________
_____________________
      Eigenvector:         1+        0i   |          1+        0i   |
1+        0i   |           1+        0i
                       51.81+        0i   |   -0.06313+ -0.04349i   |
-0.06313+  0.04349i   |    -0.02285+        0i
                      0.1312+        0i   |    0.01627+   0.1593i   |
0.01627+  -0.1593i   |      0.7671+        0i
                      -1.105+        0i   |   0.001221+-0.001424i   |
0.001221+ 0.001424i   |       19.96+        0i

      Calculating aerodynamic coefficients in the far field plane
        Calculating point   -0.89°....
      Computing On-Body Speeds...
      Computing Plane for alpha=  -0.89°
       Calculating aerodynamic coefficients...
         Calculating wing...Main Wing
         Calculating wing...Elevator
         Calculating wing...Fin

   Phillips formulae:
       Phugoid eigenvalue:      -0.00024+  0.05421i
               frequency:  0.009 Hz
               damping:    0.004
       Dutch-Roll eigenvalue:   -4.52528+ 40.69900i
               frequency:  6.517 Hz
               damping:    0.111


     ______Finished operating point calculation for control position
0.00________




Panel Analysis completed successfully

Analysis ended Mon Dec 30 13:42:02 2024
Elapsed: 0.166 s
```

```
xflr5 v6.61
30.12.2024  13:42:38

Launching Analysis

Launching the 3D Panel Analysis....
AA2
Type 7 - Stability polar

Wings as thin surfaces
Using ring vortices - VLM2
Using Neumann boundary conditions for wings

Density   =       1.225kg/m3
Viscosity =     1.5e-05m²/s

Reference Area   =     0.19973m²
Reference length =      1.9973m

Counted  858 panel elements


   Solving the problem...

      Calculation for control position  0.00
   Mass=     231.000 kg

   ___Center of Gravity Position - Body axis____
    CoG_x=      1.1804 m
    CoG_y=      0.0000 m
    CoG_z=      0.0049 m

   ___Inertia - Body Axis - CoG Origin____
    Ibxx=       1.221 kg.m²
    Ibyy=       6.207 kg.m²
    Ibzz=       7.017 kg.m²
    Ibxz=     0.09391 kg.m²

      Creating the unit RHS vectors...
      Creating the influence matrix...
      Performing LU Matrix decomposition...
      Solving the LU system...
      Time for linear system solve: 0.088 s
      Searching for zero-moment angle... Alpha=-0.69552°
      Creating source strengths...
      Calculating doublet strength...
      Calculating speed to balance the weight...VInf = 293.26967 m/s

      ___Inertia - Stability Axis - CoG Origin____
      Isxx=       1.224
      Isyy=       6.207
      Iszz=       7.014
      Isxz=      0.1642

      Calculating the stability derivatives
         Creating the RHS translation vectors
         LU solving for RHS - longitudinal
         Calculating forces and derivatives - lateral
         Creating the RHS rotation vectors
         LU solving for RHS - lateral
         Calculating forces and derivatives - lateral

      No active control - skipping control derivatives
```

```
      Longitudinal derivatives
      Xu=    -0.94356        Cxu=     -0.0263
      Xw=      7.1165        Cxa=     0.19836
      Zu=     -15.456        Czu= -5.7287e-05
      Zw=     -236.83        CLa=      6.6012
      Zq=      -77.95        CLq=      43.455
      Mu=   -0.089859        Cmu=   -0.025047
      Mw=      -60.99        Cma=         -17
      Mq=     -70.012        Cmq=      -390.3
      Neutral Point position=   1.43797 m


      Lateral derivatives
      Yv=     -46.299        CYb=     -1.2905
      Yp=     -9.7113        CYp=    -0.27106
      Yr=      59.434        CYr=      1.6589
      Lv=     -6.0547        Clb=   -0.084499
      Lp=     -55.846        Clp=    -0.78045
      Lr=      6.5233        Clr=    0.091163
      Nv=      52.925        Cnb=     0.73861
      Np=      4.1703        Cnp=     0.05828
      Nr=     -68.827        Cnr=    -0.96187

      _____State matrices__________
       Longitudinal state matrix
           -0.00408469          0.0308073                  0
-9.81
            -0.0669098           -1.02522            292.932
0
            -0.0144777           -9.82642             -11.28
0
                     0                  0                  1
0
       Lateral state matrix
             -0.200427         -0.0420404           -293.012
9.81
              -3.94742           -45.6997            4.02626
0
               7.45324          -0.475554           -9.71871
0
                     0                  1                  0
0


      ___Longitudinal modes____

      Eigenvalue:     -6.153+   -53.41i   |      -6.153+    53.41i   |
-0.00204+ -0.04666i   |    -0.00204+  0.04666i
________________________________________________________________________________
_____________________
      Eigenvector:        1+        0i   |           1+        0i   |
1+        0i   |          1+        0i
                        6927+1.879e+04i   |        6927+-1.879e+04i   |
-0.001729+ 7.37e-07i   |   -0.001729+-7.37e-07i
                        3304+    -1592i   |        3304+     1592i   |
0.0002224+2.779e-07i   |  0.0002224+-2.779e-07i
                       22.38+    64.45i   |       22.38+   -64.45i   |
-0.0002139+ 0.004756i   |   -0.0002139+-0.004756i
```

```
      ___Lateral modes____

      Eigenvalue:     -45.83+        0i   |      -4.893+   -46.57i   |
-4.893+    46.57i   |   -0.0008157+        0i

________________________________________________________________________________
_____________________
      Eigenvector:         1+        0i   |           1+        0i   |
1+        0i   |           1+        0i
                       25.79+        0i   |     -0.0491+ -0.04035i   |
-0.0491+  0.04035i   |    -0.01873+        0i
                      0.1332+        0i   |     0.01605+   0.1589i   |
0.01605+  -0.1589i   |      0.7679+        0i
                     -0.5627+        0i   |   0.0009667+-0.0009529i   |
0.0009667+0.0009529i   |       22.96+        0i

      Calculating aerodynamic coefficients in the far field plane
        Calculating point   -0.70°....
      Computing On-Body Speeds...
      Computing Plane for alpha=  -0.70°
       Calculating aerodynamic coefficients...
         Calculating wing...Main Wing
         Calculating wing...Elevator
         Calculating wing...Fin

   Phillips formulae:
       Phugoid eigenvalue:      -0.00016+  0.04721i
               frequency:  0.008 Hz
               damping:    0.003
       Dutch-Roll eigenvalue:   -5.18703+ 46.64610i
               frequency:  7.470 Hz
               damping:    0.111


     ______Finished operating point calculation for control position
0.00________




Panel Analysis completed successfully

Analysis ended Mon Dec 30 13:42:38 2024
Elapsed: 0.176 s
```

Turnitin Report

bimo_thesis_manuscript_2024_compressed (1).pdf

ORIGINALITY REPORT

8%	7%	2%	4%
SIMILARITY INDEX	INTERNET SOURCES	PUBLICATIONS	STUDENT PAPERS

PRIMARY SOURCES

1	Submitted to University of Glasgow Student Paper	1%
2	www.designation-systems.net Internet Source	1%
3	vdoc.pub Internet Source	1%
4	repository.ipmi.ac.id Internet Source	<1%
5	Submitted to Sim University Student Paper	<1%
6	roe.ru Internet Source	<1%
7	www.sunnews.co.kr Internet Source	<1%
8	sourceforge.net Internet Source	<1%
9	www.armyrecognition.com Internet Source	<1%

10	Submitted to University of Hertfordshire Student Paper	<1 %
11	Submitted to Kingston University Student Paper	<1 %
12	etheses.whiterose.ac.uk Internet Source	<1 %
13	Festas, João Filipe Vieira. "Landing Gear Design for Forest Firefighting Drone And Introduction of Novel Extinguishing Method", Universidade do Porto (Portugal), 2024 Publication	<1 %
14	ir.uitm.edu.my Internet Source	<1 %
15	Submitted to International School of Zug and Luzern - Riverside Campus Student Paper	<1 %
16	repositorio.usm.cl Internet Source	<1 %
17	etd.aau.edu.et Internet Source	<1 %
18	Submitted to Engineers Australia Student Paper	<1 %
19	nanopdf.com Internet Source	<1 %
	strakscontemporary.com	

20	Internet Source		<1 %
21	websites.umich.edu Internet Source		<1 %
22	Submitted to Sheffield Hallam University Student Paper		<1 %
23	vac.co-aol.com Internet Source		<1 %
24	Submitted to University of Balamand Student Paper		<1 %
25	Submitted to University of Sheffield Student Paper		<1 %
26	Submitted to University of Stellenbosch, South Africa Student Paper		<1 %
27	Submitted to American University of Bahrain Student Paper		<1 %
28	Bandu N. Pamadi. "Performance, Stability, Dynamics, and Control of Airplanes, Second Edition", American Institute of Aeronautics and Astronautics (AIAA), 2004 Publication		<1 %
29	Jitendra R. Raol, Jatinder Singh. "Flight Mechanics Modeling and Analysis", CRC Press, 2023 Publication		<1 %

30	sketchfab.com Internet Source	<1 %
31	Submitted to City University Student Paper	<1 %
32	Erwin Mooij. "Chapter 8 Terminal Area Energy Management", Springer Science and Business Media LLC, 2024 Publication	<1 %
33	Submitted to Universiti Putra Malaysia Student Paper	<1 %
34	aviationfile.com Internet Source	<1 %
35	Alain Dupuis. "Aerodynamic characteristic and analysis of a MK82 bomb configuration from free-flight tests", AIAA Atmospheric Flight Mechanics Conference and Exhibit, 2001 Publication	<1 %
36	Guo-chao FAN, Chun-sheng HU, Xue-en ZHENG, Cheng-dong XU. "A Semantic Management Method of Simulation Models in GNSS Distributed Simulation Environment", IEICE Transactions on Information and Systems, 2019 Publication	<1 %
37	Mohammad H. Sadraey. "Aircraft Performance - An Engineering Approach",	<1 %

CRC Press, 2023
Publication

38	Submitted to North West University Student Paper	<1 %
39	Submitted to TU Delft Student Paper	<1 %
40	Submitted to University of Teesside Student Paper	<1 %
41	repository.sgu.ac.id Internet Source	<1 %
42	Submitted to Emirates Aviation College, Aerospace & Academic Studies Student Paper	<1 %
43	Submitted to Fakultat fur Maschinenwesen der Technischen Universitat Munchen Student Paper	<1 %
44	Fumiya Iida, Russ Tedrake. "Minimalistic control of a compass gait robot in rough terrain", 2009 IEEE International Conference on Robotics and Automation, 2009 Publication	<1 %
45	Marron, Russell Wade. "Multifunctional Photonic Crystals via Interference Lithography", Drexel University, 2023 Publication	<1 %
46	Submitted to University of Surrey Student Paper	

<1 %

47	authors.library.caltech.edu Internet Source	<1 %
48	eprints.utm.my Internet Source	<1 %
49	scholar.sun.ac.za Internet Source	<1 %
50	it.unionpedia.org Internet Source	<1 %
51	www.ferra.com.au Internet Source	<1 %
52	www.ros.hw.ac.uk Internet Source	<1 %
53	Submitted to Cranfield University Student Paper	<1 %
54	Mario Asselin. "An Introduction to Aircraft Performance", American Institute of Aeronautics and Astronautics (AIAA), 1997 Publication	<1 %
55	do Vale, Pedro Domingos Moreira da Rocha Campos. "Aircraft Wing Structure Benchmark: Cantilever vs. Braced Wing Configurations", Universidade do Minho (Portugal), 2024 Publication	<1 %

56	escholarship.org Internet Source	<1 %
57	mediatum.ub.tum.de Internet Source	<1 %
58	www.utupub.fi Internet Source	<1 %
59	Espíndola, Francisco Nuno Maurício. "Design of a Long-Range Wing for the UAS30 Platform", Universidade da Beira Interior (Portugal), 2024 Publication	<1 %
60	docslib.org Internet Source	<1 %
61	eprints.covenantuniversity.edu.ng Internet Source	<1 %
62	etd.lib.metu.edu.tr Internet Source	<1 %
63	pure.tue.nl Internet Source	<1 %
64	upcommons.upc.edu Internet Source	<1 %
65	www.govinfo.gov Internet Source	<1 %
66	www.sec.gov Internet Source	<1 %

67	wwww.nodexlgraphgallery.org Internet Source	<1%
68	Fiedler, Mariel. "Third Generation Holocaust Survivors: a Healing and Community-Building Curriculum", California State University, Long Beach, 2020 Publication	<1%
69	Miller, Noah S.. "Deep Integration of a Flight Vehicle Dynamic Model in a Vector Tracking Software Defined Receiver", Auburn University, 2024 Publication	<1%
70	Robert Walmsley, Rishad Ahmed, Christian Klumpner, Beeond M. Saleh. "An Optimisation Tool for Hybrid-Electric Aircraft Propulsion Systems", 2023 IEEE International Electric Machines & Drives Conference (IEMDC), 2023 Publication	<1%
71	asiatimes.com Internet Source	<1%
72	d-nb.info Internet Source	<1%
73	defence24.pl Internet Source	<1%
74	J.M. Sánchez-Lozano, J.C. Correa-Rubio, M. Fernández-Martínez. "A double fuzzy multi-	<1%

criteria analysis to evaluate international high-performance aircrafts for defense purposes", Engineering Applications of Artificial Intelligence, 2022

Publication

75	N H Mansor, R Abdul-Rahman. "Cubic Spline-Based Genetic Algorithm Optimization for Millimeter and Microwave Integrated Circuits", IOP Conference Series: Materials Science and Engineering, 2020 Publication	<1 %

Exclude quotes	On	Exclude matches	Off
Exclude bibliography	On		

Curriculum Vitae

	Basic Information
Name	Muhammad Bimo Adjie Athallah
Place of Birth	Surabaya, East Java, Indonesia
Date of Birth	May 24th, 2003
Address	Puri Taman Asri, Blok B-24, Pagesangan, Surabaya, Indonesia
Year	**Education**
2021 - present	International University Liaison Indonesia (IULI)
2018 - 2021	SPINS Interactional School (Senior High School)
2015 - 2018	SPINS Interactional School (Junior High School)
2009 - 2015	SPINS Interactional School (Elementary School)
Year	**Courses**
2020	German Language Courses (A1-B2) Class
Year	**Seminars & Workshops**
2023	Basic Aicraft Maintenance Training
2022	Terradrone Small UAV piloting course
Year	**Work Experiences**
2022-23	Vice-head of IULI Aviation Engineering Student Association
2023-24	Head of IULI Aviation Engineering Student Association
2023	Member PN Indo Jakarta branch, Organizational Division
2023	ABB FIA Formula E World Championship, Jakarta ePrix round Volunteer